Catalytic Upgrading of Biomass Fermentation Products and Bio-methane to Energy Dense Hydrocarbon Fuels

by

Shaima Nahreen

A dissertation submitted to the Graduate Faculty of
Auburn University
in partial fulfillment of the
requirements for the Degree of
Doctor of Philosophy

Auburn, Alabama
May 10, 2015

Keywords: transportation fuel, catalysis, biomass, deoxygenation, extraction

Approved by

Ram B. Gupta, Co-chair, Professor of Chemical Engineering
Sushil Adhikari, Co-chair, Associate Professor of Biosystems Engineering
Yoon Y. Lee, Professor of Chemical Engineering
Jin Wang, Associate Professor of Chemical Engineering

Abstract

Since the last few decades of 20th century, studies on renewable and alternative energy sources have drawn much attention both in academic and industrial research. The public and private sectors felt the obvious need of discovering alternative energy sources other than petroleum crude due to its limited supply compared to the increasing demand with fast pace of modern civilization and industrialization worldwide. New policies and acts are being enabled to encourage the research and application of renewable and alternative energy and fuels. In transportation sector, to use the alternative and renewable energy sources without massive change of the established infrastructure, only biomass and bio-resources can be chemically converted or upgraded to liquid transportation fuel which can be used as drop-in fuel or fuel blend in conventional automobile engines. Biomass conversion to liquid oil can be done in several ways like biochemical conversion i.e. fermentation, thermo-chemical conversion i.e. pyrolysis etc. In this study biomass fermentation products such as alcohol ketone and carboxylic acid mixtures and also bio-methane or shale gas are catalytically upgraded in a thermochemical conversion process to produce energy dense higher hydrocarbon molecules that can be used as liquid fuel or energy sources.

Acetone-butanol-ethanol (ABE) mixture, containing 62.9 wt% n-butanol, 29.3 wt.% acetone and 7.8 wt.% ethanol, can be produced from biomass through the well-established ABE fermentation process using genetically-modified Clostridium acetobutylicum. In Chapter 2, the catalytic dehydration reactions of ABE mixture are studied to deoxygenate the mixture. Feed of ABE mixture was preheated and pumped

through a catalytic packed bed tubular reactor in a continuous process at pressures of 3-6 bars. Experiments were run at different operating temperatures and feed flow rates to investigate the effect on the dehydration products, which are mixtures of three phases: (1) a gas phase consisting of light hydrocarbons and carbon dioxide, (2) an organic liquid phase consisting of heavy hydrocarbons, and (3) an aqueous phase with dissolved oxygenated hydrocarbons. The conversion was examined on two different catalysts: an alumina (γ-Al_2O_3) and a zeolite (ZSM-5). The dehydration products from the ABE mixture were mostly unsaturated hydrocarbon chains in the range of C_2-C_{16}. Based on the higher heating values (HHV) of the liquid products and infra-red spectra of the gas products, it can be concluded that the products from the ABE feedstock were different than those from the individual components, which suggests a cross reactivity of the components during the reaction. HHV of the liquid product increased with a decrease in the feed flow rate, and γ-Al_2O_3 catalyst was found to perform better than ZSM-5 for getting a good conversion of ABE in terms of liquid product energy content at a moderate reaction time. The gaseous product contained mostly 1-butene and its isomers and some other lighter unsaturated hydrocarbon gases. This gas stream was used as the extractant in Chapter 3 to study the separation of ABE components from dilute aqueous solution having the same concentration of the fermentation broth. Chemically pure 1-butene gas was liquefied in a pressure vessel where direct liquid-liquid extraction takes place and mole based distribution coefficient of 1.71 was attained for n-butanol single component extraction. For acetone, ethanol and butyric acid extraction separately from aqueous solvent the distribution coefficients were lower. To compare the separation efficiency a two-step approach of adsorption on activated charcoal followed by liquid-solid extraction using 1-butene and percent recovery of each of the components, mole and mass based distribution coefficients were calculated and it was observed that other than for n-butanol, the distribution coefficients for other components increased compared to that of

the direct liquid-liquid extraction process. For extraction of ABE as a mixture, a preferential extraction of n-butanol was observed over the other components in the mixture due to its least polar characteristic among the components and thus higher solubility in the organic phase.

Another significant and common product in biomass fermentation processes using Clostridium genus biocatalysts is butyrates or butyric acid. For example, it is produced as a by-product with acetone-n-butanol-ethanol (ABE) mixture in the well-known ABE fermentation process. Using genetically modified microbial strain in an advanced fermentation method with integrated separation, a butyric acid concentration of as high as 60 g/l can be achieved. Butyric acid can be further catalytically deoxygenated to produce ketones and long-chain hydrocarbons. In Chapter 4 of this study, conversional efficiencies of two commercial acid catalysts γ-Al$_2$O$_3$ and ZrO$_2$ are examined. For *in-situ* aromatization of the deoxygenation products in a single step reactor, ZSM-5 catalyst was tested in a series bed followed by γ-Al$_2$O$_3$ and ZrO$_2$. Due to the amphoteric properties of having both lewis acid and basic sites and also stronger aprotonic acid sites due to higher concentration of oxygen in the molecule, ZrO$_2$ has much superior deoxygenation activity than γ-Al$_2$O$_3$, as former showed above 90% conversion of butyric acid to high-energy organic liquids; for example, the higher heating value (HHV) of the organic liquid product is 36 kJ/g for the deoxygenation at 400°C. The composition of the liquid product depends upon the temperature and weight-hourly-space-velocity (WHSV), and the heavy hydrocarbons can be produced in a single step though the yield decreases with increase in temperature. Almost equal amounts of n-heptanone and aromatic components are produced when a series packed bed of ZrO$_2$ and ZSM-5 is used. An optimum condition for a series bed of ZrO$_2$ and ZSM-5 catalysts has been determined to produce a mixture of energy-dense hydrocarbons and aromatics directly from butyric acid.

In Chapter 5 of this study catalytic upgrading of methane from bio resources as well as from shale gas is discussed in a direct and more energy efficient route without using oxygen. In this work, a noble transition metal, ruthenium, is chosen as the catalyst with the objective of lowering the methane activation temperature, higher stability and also to have better conversion than other transition metal catalysts which are studied. The catalyst was prepared by 1.5 wt. % or 3 wt.% ruthenium loading on ZSM-5, zeolite support and on silica support separately to compare the effect of metal loading and metal support combination on the conversion process. The operating temperature was varied from 400° to 800°C. From online GC analysis and FT-IR analysis of the product gas it was observed that a sudden rise in methane conversion took place at 700°C operating temperature on 3 wt.% Ru/ZSM-5 catalyst bed and heavy hydrocarbon molecules of C_4 to C_{10} range was produced but with a very low yield. For 1.5 wt.% Ru/ZSM-5 and 3 wt.% Ru/SiO$_2$ catalyst beds , methane conversion were found to be low even at high temperature and no significant production of higher hydrocarbon molecules were observed. A catalyst bed of 3 wt.% Ru/SiO$_2$ followed by pure ZSM-5 in series is also studied and the products are found to be comparable with that of 3 wt.% Ru/ZSM-5 catalyst bed with high methane conversion. The special framework structure in the ZSM-5 catalyst influenced the product molecular structure to produce cyclic higher hydrocarbon molecules after methane is activated on the surface with ruthenium metal catalyst and produced methyl radicals at above 700°C in a considerable amount. In this work as the catalysts are prepared in the lab, extensive catalyst characterization is done for both fresh and spent catalysts to determine the changes and stability. The probable future directions of continuation and improvement of the catalytic upgrading processes are discussed in a brief manner in Chapter 6 of this study.

Acknowledgments

I would like to thank, my advisor, Dr. Ram B. Gupta for his guidance and support through-out my Ph.D. research. As a mentor, he provided me with new and exciting research ideas and helped me overcoming obstacles while achieving the goals of my research projects. I would like to express my gratitude to the committee members: Dr. Yoon Y. Lee and Dr. Jin Wang for their valuable suggestions and comments and taking out time from their busy schedule to help with my dissertation. A special thanks to my co-advisor who has been really helpful during the entire course of time, especially at the end when he supported me in all aspects to finish and defend my research successfully Also I am grateful to my university reader, Dr. Oladiran Fasina, for taking the time to read through this dissertation meticulously and also for his valuable comments and suggestions.

I would also like to thank the department chair, Dr. Mario R. Eden, graduate program chair Dr. Virginia A. Davis and dean of engineering, Dr. Cristopher B. Roberts for their incessant support, helpful advices and inspirational words.

My heartfelt gratitude goes to the staff of chemical engineering department of Auburn University, Ms. Karen Cochran, Ms. Georgetta Dennis, Ms. Elaine Manning and Ms. Jennifer Harris, for helping me with logistics, academic formalities and financial matters. My sincere gratitude to Mr. Brian Schwieker, without whom I would not be able to design and build my experimental set ups perfectly.

My group colleagues had an immense contribution in my research work by helping me with analysis instruments, problem solving ideas and moral support. I would like to specially thank Dr. Hema Ramsurn, who not only has been a very dear friend but also a mentor to me. I was lucky to have brilliant friends as Dr. Courtney Ober, Dr. Emmanuel Nyankson, Dr. Jennifer Duggan, Pranav Vengsarkar, Dr. Rui Xu, Dr. Nourredine Abdoulmoumin, Charlotte Stewart and Richard Cullum. I would like to thank them for helping with my research work as well as by making the work environment very enjoyable for me.

Last but not the least, I would specially like to thank my parents and family back in Bangladesh, who have been very supportive and encouraged me all the way till the end of my dissertation work, without their persistent support, it would not be possible for me to reach here. My heartfelt gratitude also goes to my Auburn family and friends, who have played massive roles to help me survive and thrive in a place far away from home.

Table of Contents

List of Tables

List of Figures

xviii

List of Abbreviations

ABE   Acetone, n-Butanol, Ethanol

BET   Brunauer, Emmett and Teller

FT-IR   Fourier Transform- Infra Red

GC   Gas Chromatography

GC-MS   Gas Chromatography with Mass Spectrometry

HHV   Higher Heating Value

HPLC   High Performance Liquid Chromatography

SEM   Scanning Electron Microscope

TCD   Thermal Conductivity Detector

TGA   Thermo Gravimetric Analysis

TOC   Total Organic Carbon

TPR   Temperature Programmed Reduction

UV   Ultra Violet

WHST   Weight Hourly Space Time

XRD   X-Ray Diffraction

ZSM-5   Zeolite Socony Mobil-5

Chapter 1

Introduction

1.1 Need for alternative energy

ABE (acetone-n-butanol-ethanol) fermentation process is a well-established process for producing n-butanol from biomass. Production of ABE from biomass got the incentive as USA put on a prohibition on usage of amyl acetate as a solvent in car lacquers. As a result, demand of butyl acetate or butanol increased abruptly as an alternative solvent during years 1930 to 1950. Fermentation of molasses substrates was popular during the rise of ABE industry. A good number of ABE fermentation industries were established worldwide in USA, Japan, South Africa, USSR and China during that period of 20th century. During World War II, shortage of acetone also induced the spread out of ABE production at industrial scale. But later during 1960s petrochemical industry flourished and competitive solvents were being produced in refineries which put the ABE fermentation industries in a challenge of economic viability. Also the increasing price of feedstock made the ABE a less attractive option compared to the petrochemical products. As a consequence all the ABE plants ceased operations by the end of 1980s.

From last 2 decades the price fluctuation of petroleum crude oil and the fast depletion rate of proven reserve of fossil fuel resources are raising much concern worldwide. According to energy statistics of US Energy Information Administration (EIA) USA has the largest share (21.5%) in total liquid oil consumption of the world. In that share 71% is

being consumed in the huge transportation sector of USA which is an amount of 220 billion gallons per year.

U.S. Oil Use By Sector

Electricity 1%
Residential 7%
Industrial 23%
Transportation 69%

Data are for 2005.
Source: Energy Information Administration, *Annual Energy Outlook 2005*
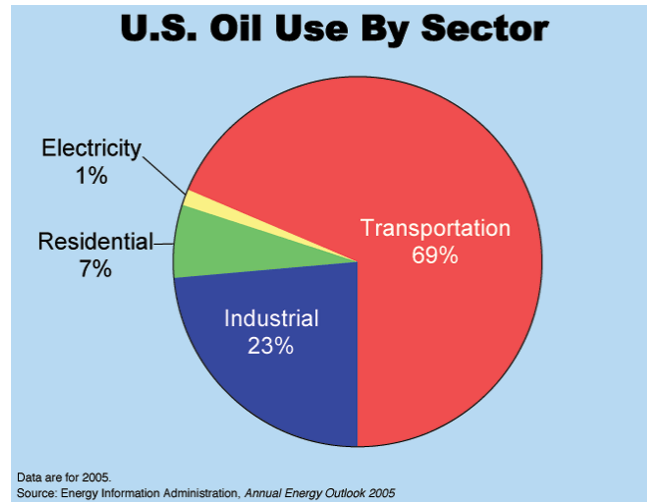
Figure 1.1: Distribution of oil consumption in different sectors of USA

As fossil fuel reserve is depleting at a faster rate than exploration of new reserves and with increasing consumption of liquid oil with the advancement of modern civilization worldwide, finding out alternative and renewable sources for producing liquid oil has become essential. Among all the other renewable energy sources like solar, wind, hydro, geothermal and biomass, only biomass can produce liquid fuels which can be used in transportation vehicle engines. The search for renewable source for production of liquid fuel has started way back in 1970s, when Brazil started successful industrial production of bioethanol. Sugarcane has being used as the feedstock mostly in Brazil. Later during 1990s growing interest in bioethanol production as liquid fuel alternative in automotive engines have become conspicuous in USA. The climate change effect caused by the major green house gas (GHG) CO_2 was another alarming issue which also inspired theresearch of production of renewable liquid fuels. Biofuel also produces CO_2 in the fermentation and combustion process, but this CO_2 comes from the 'free carbon cycle' that was already exposed to the environment in another form. The CO_2 emission from

the usage of fossil fuel comes from a 'locked carbon cycle' which increases the amount of GHG from the baseline and are told to be responsible for the unpredictable climate change problems.

1.2 Comparison of bioethanol and biobutanol as alternative liquid fuel

The concept of using bioethanol as a transportation fuel seemed to be really promising and government has taken several steps to boost up this industry. The Biomass Research and Development Act of 2000 enforced by the US Department of Agriculture (USDA) created a Biomass R&D technical advisory committee to provide a national vision for bioenergy and bio based products. This committee set a very challenging goal of supplying 20% of nation's transportation fuel requirement and 25% of chemical requirement from only Biomass source by 2030 [1]. The US government also allotted a good amount of funding on biofuel research and establishment of biofuel industry. With all these initiatives and motivations from the government and from social and environmental responsibilities researchers and entrepreneurs came forward for the production of liquid transportation fuel from biomass. Bioetahnol, though has been considered to be the most probable alternative for liquid fuel, but due to its high oxygen content (34.7 %, low energy content, low boiling and flash point and and corrosive properties make transportation and storage difficult. Due to these shortcomings ethanol could not directly substitute gasoline or diesel in automotive engines rather it has been used as fuel blend. On the other hand, biobutanol has higher energy density which is comparable to that of gasoline and it has several fuel properties that make it very attractive option as a substitute for gasoline or diesel. Some of them are as follows

- can be made from natural sugar or starch including waste materials.

3

- has 92% of the energy content of gasoline (110,000 Btu's per gallon for n-butanol vs. 115,000 Btu per gallon for gasoline). Ethanol contains about 84,000 Btu per gallon.

- mixes well with gasoline or ethanol.

- can be used in place of gasoline with no engine or fuel system changes.

- makes usable hydrogen as a byproduct.

- N-butanol is six times less "evaporative" than ethanol and 13.5 times less evaporative than gasoline, making it safer to use as an oxygenate.

- N-butanol is not hygroscopic where ethanol attracts water.

- N-butanol can be shipped through existing fuel pipelines where ethanol must be transported via rail, barge or truck.

- N-butanol can be used as a replacement for gasoline gallon for gallon e.g. 100%, or any other percentage. Ethanol can only be used as an additive to gasoline up to about 85% and then only after significant modifications to the engine. Worldwide 10% ethanol blends predominate.

Table 1.1: Comparison of fuel properties

	Petrol	Ethanol	Butanol
Formula	C_4- C_{12} hydrocarbons	CH_3CH_2OH	$CH_3(CH_2)_3OH$
Boiling Point (°C)	32-210	78	118
Heating value (MJ/kg)	32.5	21.2	29.2
Air Fuel ratio	14.6	3.0	11.2
Research Octane Number (RON)	91-99	129	96

Above all the advantages of biobutanol over bioethanol, there are some drawbacks as well. Using current ABE technology the total energy yield of n-butanol is about half of that of ethanol using corn or switch grass as feedstock. Again due to high price of feedstock low yield can be a big challenge in case of economic feasibility assessment [2]. Now with upcoming improved fermentation methodologies and genetically modified bacteria and yeast strains, yield of n-butanol and over all ABE production rate is increasing [3],[4],[5],[6] .

1.3 Production process of biobutanol: historical background and current research

N-butanol was first produced by anaerobic bacteria fermentation in 1861 by the famous scientist Louis Pasteur. In the beginning of 20th century interest about producing n-butanol grew largely due to its application in synthetic rubber production. During World War I shortage of acetone as a solvent induced the ABE fermentation process where a good amount of n-butanol was being produced along with acetone. Chaim Weiamann, a researcher in Manchester University issued a British patent on the ABE fermentation process using Clostridium *acetobutylicum* microbial strain and maize mash in addition to potato as feed stock.   Prohibition of using some specific solvents as car lacquers, butyl acetone came to replace that, which also caused a boom in the ABE fermentation industry.

During 1930s the development of other microbial strains from molasses substrate expanded the industrial production of ABE worldwide in USA, Japan, South Africa and USSR and ABE fermentation was the most well established process for production of acetone and butanol till the end of World War II demand of acetone grew higher and higher during that period. During 1960s, with the rise of petrochemical industry, competitive production of other solvents from the petroleum fractions at lower cost challenged the economic feasibility of the ABE process. Also the food vs feed stock

issue posed a problem when feed stock price started going higher and the ABE fermentation process industries started to close their facilities.

Again in 1980s when the petroleum crude oil price started rising rapidly worldwide, the research on alternative fuel sources triggered largely. Since 1990s, research on biobutanol production again started getting attention in research labs of government organizations (USDA, DOE) and also in universities. The major issues of ABE production process, which the researchers are trying to find solutions for are as follows:

- the toxicity effect of n-butanol and other salts on the microbial strain in the fermentation broth [3]

- increasing the production level of ABE in the fermentation broth by producing genetically modified microbial strain [7]

-improving the production process by introducing continuous flow bioreactors, fed batch technique other new technologies [5],[8],[4]

- *in- situ* separation of ABE to decrease the toxicity and thus increase production [9]

If all the above mentioned are well taken care of; acetone, n-butanol and ethanol production by the BAE process will undoubtedly be the most feasible solution to produce biobutanol which can solve the liquid fuel crisis at a great extent.

The biomass to fuel production pathway via fermentation can be represented with following block diagram:
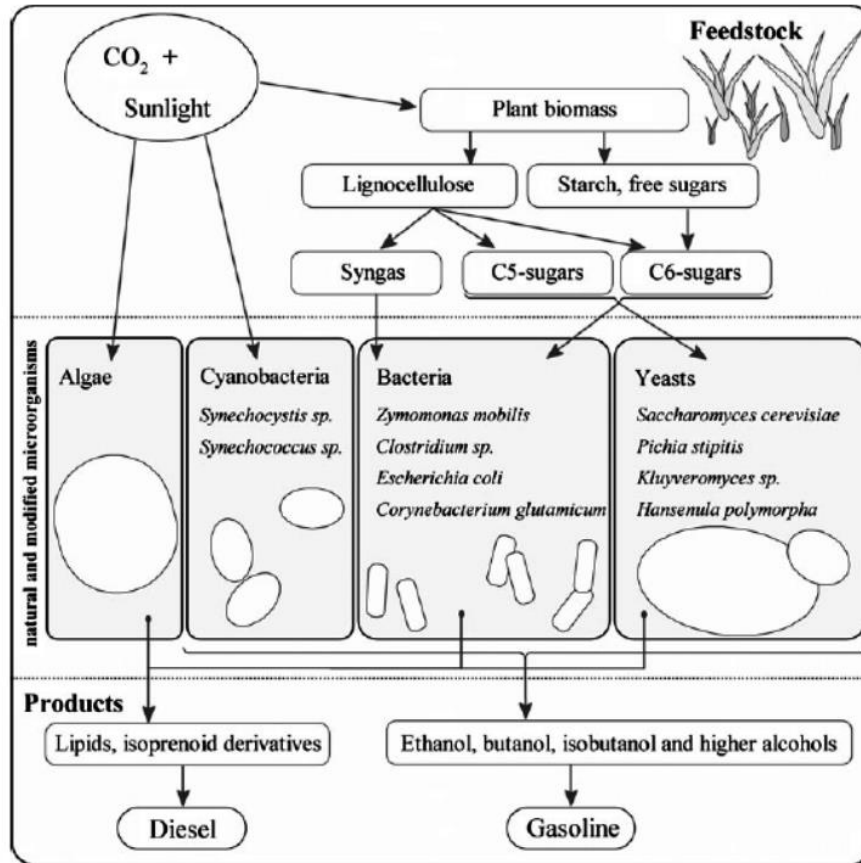
Figure 1.2: Liquid transportation fuel from biomass : production pathway via fermentation [10]

In the ABE fermentation process the fermentation mechanism can be shown by the following flow chart
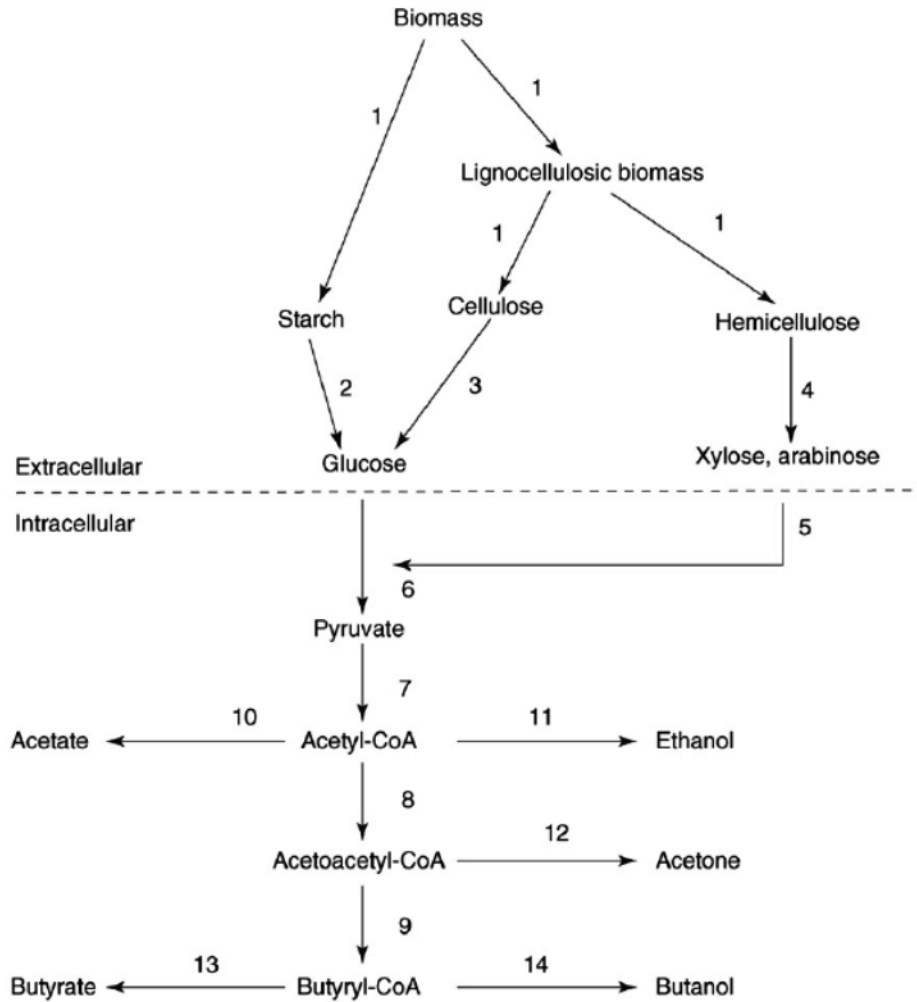
Figure 1.3: fermentation pathway for production of ABE from biomass [3]

Different kind of biomass has been used as fermentation feed stock. Corn stover and switchgrass are some of them. Also different kinds of genetically modified microbial strain are being experimented for increasing the yield and productivity of ABE in the fermentation process so that the economic feasibility issue can be resolved.

Table 1.2: Yield and selectivity results from ABE fermentation using different feedstock and microbial strain[11]:

Substrate	Hydrolysis method	Strain used	Yield (g/g)/ Productivity (g/l h)	Total ABE (g/l)	References
Wheat straw	H_2SO_4 + enzyme	*C. beijerinckii* P260	0.60/0.42	25	Qureshi et al. (2007)
Wheat straw	H_2SO_4 + enzyme	*C. beijerinckii* P260	0.41/0.31	21.42	Qureshi et al. (2008a)
Corn fiber	H_2SO_4	*C. beijerinckii* BA101	0.39/0.10	9.3	Qureshi et al. (2008c)
Palm oil mill effluent + sago starch	Enzyme	*C. saccharoperbutylacetonicum* N1-4	0.40/0.10	14.38	Hipolito et al. (2008)
Dried distillers' grains and soluble (DDGS)	Ammonium fiber expansion + enzyme	*C. beijerinckii* BA101	0.34/0.14	10.4	Ezeji and Blaschek (2008)
Rice bran and defatted rice bran	HCl + enzyme	*C. beijerinckii* NCIMB 8052	0.31/0.26	16.42	Lee et al. (2009)
Barley straw	H_2SO_4 + enzyme	*C. beijerinckii* P260	0.43/0.39	26.64	Qureshi et al. (2010a)
Corn stover	H_2SO_4 + enzyme	*C. beijerinckii* P260	0.44/0.31	26.27	Qureshi et al. (2010b)
Switchgrass	H_2SO_4 + enzyme	*C. beijerinckii* P260	0.39/0.17	14.61	Qureshi et al. (2010b)
Wheat bran	H_2SO_4	*C. beijerinckii* ATCC 55025	0.32/0.16	11.8	Liu et al. (2010)
SO_2–ethanol–water (SEW) spent liquor	SO_2–ethanol–water	*C. acetobutylicum* DSM 792	0.20/0.09	8.79	Survase et al. (2011a)
Sugar maple wood	Hot water extraction + sulfuric acid	*C. acetobutylicum* ATCC 824	0.22/0.15	11.0	Sun and Liu (2011)
Rice straw	H_2SO_4 + enzyme	*C.acetobutylicum* MTCC 481	1.04[a]/0.017	3.0	Ranjan and Moholkar (2011)
Cassava baggase	Enzyme	*C. acetobutylicum* JB200	0.39/0.62	33.87	Lu et al. (2011)
Maize stalk juice	–	*C. beijerinckii* NCIMB 8052	0.27[a]/0.30	11.5	Wang and Blaschek (2011)

[a] Only butanol yield and productivity

From table 1.2, it can be seen that the highest amount of total ABE produced is 33.87 g/L which is still quite low. With continuous separation of the fermentation products from the broth can decrease toxicity and product inhibition resulting in higher yield up to 50 to 60 g /L   total ABE production.

1.4 Separation of acetone, n-butanol, ethanol (ABE) mixture form fermentation broth

One of the main challenges of n-butanol production by ABE fermentation process is the separation of ABE mixture from the very dilute aqueous solution produced in fermentation process. Several separation processes such as distillation, gas stripping,

liquid-liquid extraction, adsorption, pervaporation etc. have been studied for ABE separation to some extent. The major issues involved in these processes in application in ABE separation from dilute fermentation broth are the energy requirement for the separation process and also the low separation product yield. The ABE concentration in the fermentation product is very low [10]. Therefore, to increase the concentration for separation purpose a large amount of aqueous solution has been handled to get a small yield of ABE mixture which requires larger system or vessels involving higher cost. The energy requirement in the separation process contributes the major fraction of operational cost of the entire ABE fermentation and up-gradation process [12].

The typical composition of the fermentation broth in ABE fermentation process from a lab scale recipe is as follows:

Table 1.3: Concentration of the components in ABE fermentation broth (lab recipe)

Components	Concentration (g/L)
KH_2PO_4	0.75
K_2HPO_4	0.75
$MgSO_4$	0.4
$MgSO_4.H_2O$	0.01
$FeSO_4.7H_2O$	0.01
Cysteine	0.5

There will also be 5.0 g of yeast extract, 2.0 g of asparagine. H_2O, 2.2 g of $(NH_4)_2SO_4$ and 60.0 g of sugar (glucose). Along with ABE, some acetic acid and butyric acid will be produced in the fermentation process as well.

In this work, model solution of ABE in water has been used as the feed instead of directly using the fermentation to understand the ABE chemistry properly and ABE has the major concentrations in the broth compared to the other components. The probable separation processes for ABE from the dilute model solution (aq.) are discussed in detail in Chapter 3 of this dissertation.

1.5 Proposed process scheme for production of liquid transportation fuel from ABE mixture:

For producing liquid transportation fuel from alternative and renewable sources, biomass is the only option as feed stock. No other form of alternative energy source can produce liquid transportation fuel eligible to be used in automotive engines. In this project, the main goal is production of liquid transportation fuel from acetone-n-butanol, ethanol mixture derived from biomass source. As alcohols and ketones possess high oxygen content which contributes in low energy density, to upgrade the ABE mixture to drop-in liquid fuel the first step will be de-oxygenation of the mixture. The de-oxygenation process can be done by catalytic dehydration reaction where oxygen will be removed in form of water. Commercial inorganic catalysts like γ-Al_2O_3 and zeolites are used for the dehydration reaction as these catalysts have strong acid sites which can aid and increase the dehydration reaction activity. The de-oxygenation /dehydration product mixture will contain unsaturated hydrocarbon chains of butene, propylene, ethylene etc. And some saturated hydrocarbon chains as well. The unsaturated hydrocarbon chains can be further processed to produce hydrocarbon ranges from different liquid fuels like gasoline (C_7 to C_{11}), diesel (C_8 to C_{21}), jet fuel (C_8 to C_{16}) etc. also value added polymers and plastics can be produced from the ABE deoxygenation product.
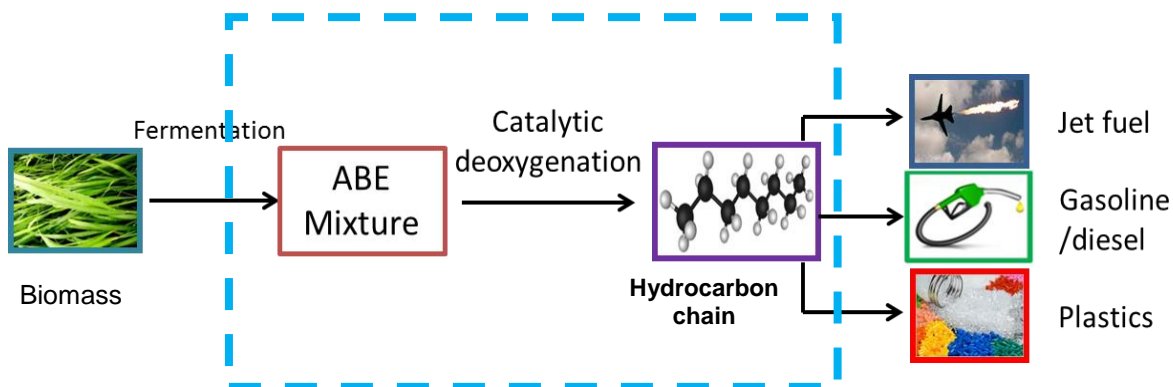
Figure 1.4: Flow diagram for producing liquid transportation fuel or polymer products from biomass via ABE up-gradation steps.

In this work, the fermentation process was not performed as ABE fermentation is already a well-established process. The fermentation product concentration has been taken from current published works [10] and a model solution of ABE in water has been prepared as the feed solution for the deoxygenation process. The proposed project area is shown in Figure 1.4 in the dashed rectangle. From the catalytic deoxygenation process a liquid organic phase and gaseous hydrocarbon phase are produced. This organic liquid phase produced in ABE deoxygenation process can directly be used as drop in fuel or as fuel blend.

Although separation of ABE from the dilute aqueous solution is not shown in this project area but it has a significant part in this study. From the ABE de-oxygenation step, a good amount of butene and its isomers are produced along with other unsaturated hydrocarbon gases; a part of this product gas stream will be used as an extractant fluid in a liquid- liquid extraction column for separation of ABE mixture from dilute water solution. The proposed integrated process scheme is shown in Figure 1.5
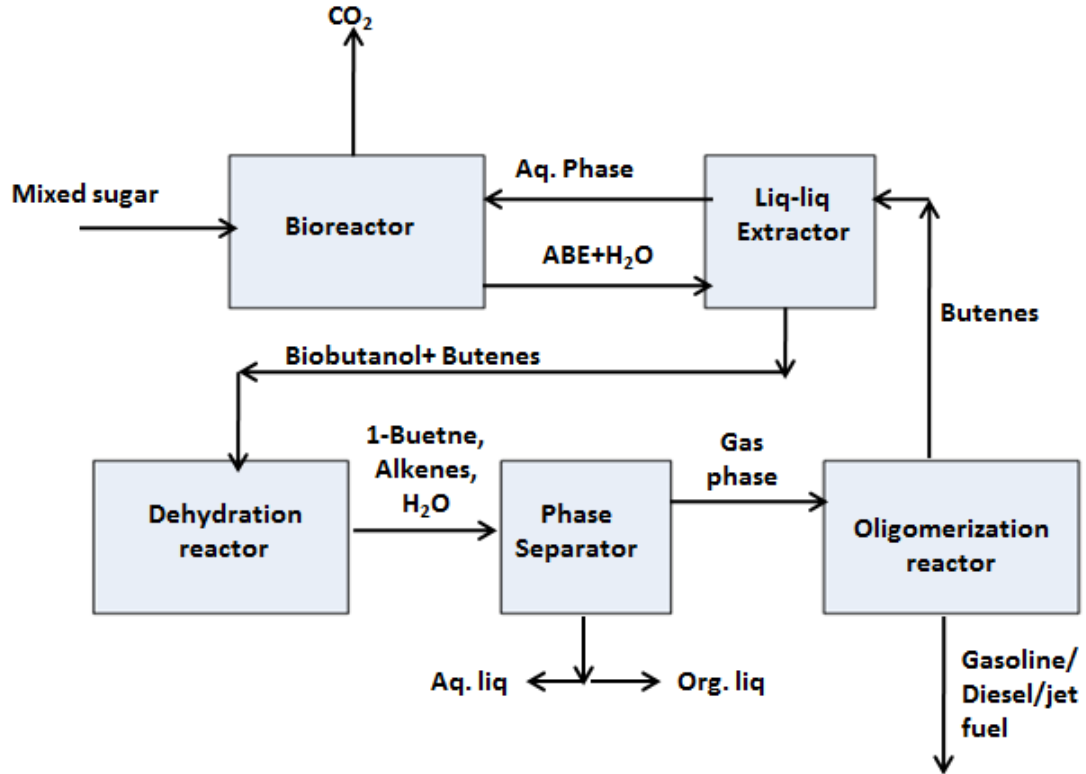
Figure 1.5: Integrated process block diagram for producing drop-in fuel including ABE separation and catalytic deoxygenation

One very significant advantage of this proposed process is that, it doesn't require the separation of acetone, n-butanol and ethanol individually to be treated as fuel. For directly using biobutanol as a fuel it has to be separated from the acetone-n-butanol-ethanol mixture produced in ABE fermentation process. This separation process is difficult and expensive as the boiling points of these three components are not very far apart. Again biobutanol has lower energy content than gasoline. So conversion of the whole mixture of ABE to liquid drop in fuel provides a privilege of saving the separation cost, minimizes the loss of hydrocarbons as all the hydrocarbon produced in the

fermentation process are being processed in different steps to produce liquid-drop in fuel.

The advantages of the proposed integrated process for production of drop in-fuel from ABE mixture are as follows:

- This is a novel process to upgrade ABE mixture into drop-in fuels
- Undertaking expensive separation processes for separating acetone , n-butanol and ethanol are not needed as conversion of ABE to drop-in fuel is being done for the whole mixture at the same ratio as they get produced in the fermentation broth
- Avoidance of the use of expensive noble-metal catalysts
- High-energy efficiency by selecting low energy intensive procedure
- Integrated reaction and separation steps
- Intermediate products are recycled and used for separation purpose
- Mild operating conditions of process
- If price falls in crude oil market the 1-buetene intermediate can be diverted to produce high value added polymers.

1.6. Production of butyric acid from biomass fermentation and catalytic deoxygenation

As renewable ethanol production from corn starch is questioned upon because of the food versus fuel issue, biofuel production from cellulosic sources and biomass based biodiesel are predicted to be contributing more to reach the mandated use enacted by the Energy Independence and Security Act, 2007 (Figure 1.6). To attain the targeted goal of 16 billion gallons of biofuel production from cellulosic feed other fermentation products than bioethanol and biobutanol need to be explored. Butyric acid can be

produced by fermentation with high yield by using Clostridium butyricum or Clostridium tyrobutyricum
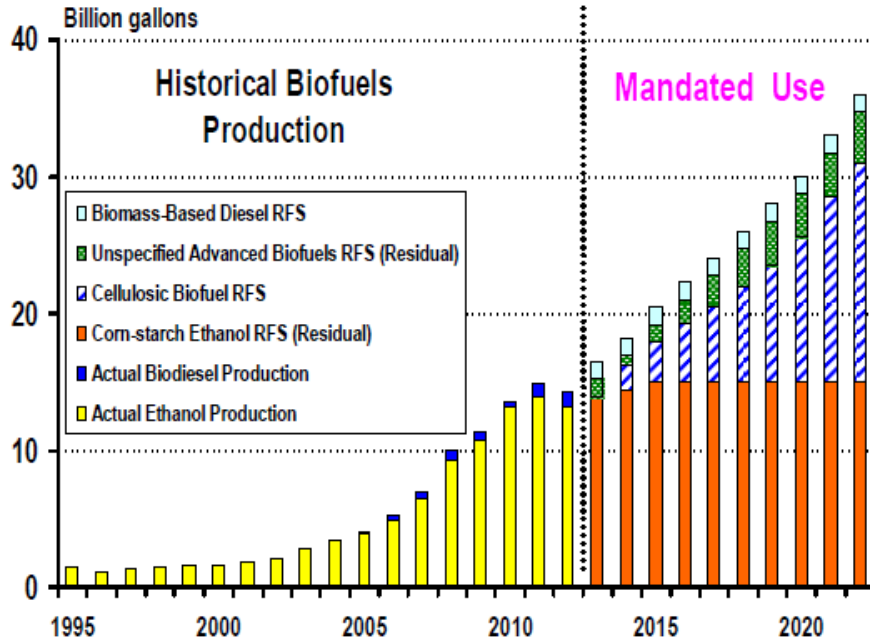
Figure 1.6: Biofuels production per annum in billion gallons: historical and projected[13]

microbial strains [14], [15] is an appropriate separation approach applied along with fermentation process. Also butyric acid can be generated as a byproduct of ABE fermentation although the yield is much lower[16]. There are several end products that can produce either butyrate or butanol from the same microbial catalysts in parallel metabolic pathways[17][18]. One of these probable pathways is shown above in Figure 1.3. Production of butyric acid by fermentation has now drawn attention along with butanol production, as butanol fermentation process has certain drawbacks specially the inhibition effect of butanol on the microbial strain limits the yield of biobutanol at a lower concentration like 20 g/L. If butyric acid is produced as the principal product in a fermentation process the yield can be as high as 60 g/L, and it can be an attractive raw

material for producing higher hydrocarbon that can be used as transportation fuel. Because of the molecular structure of butyric acid, it is difficult to break two carbon-oxygen bonds to remove oxygen and produce higher hydrocarbon chain or aromatic products. Acid catalysts can also perform a major role in deoxygenation of butyric acid but the reaction mechanism is going to be different than deoxygenation of alcohols and ketones which possess single oxygen atoms. In this work deoxygenation of butyric acid has also been studied in the process of producing liquid hydrocarbon fuel from renewable biomass sources. Upgrading of butyric acid to higher chain hydrocarbon has been looked into by chemical catalysis at 400°C to 600°C operating temperatures and moderate operating pressure of 3 to 5 bars. Single catalyst bed and a new methodology of series bed of catalysts are also introduced to influence the product composition and hydrocarbon range and selectivity.

1.7 Upgrading bio-methane to higher hydrocarbon fuels

Producing liquid hydrocarbon fuel from renewable or alternative sources is the main objective of this research work. Biomass is the only renewable source from which liquid hydrocarbon can be derived. Another possible way to produce higher hydrocarbon molecules from renewable source is to convert bio-based methane generated in natural processes to higher hydrocarbon molecules again with the help of chemical catalysis. Methane emission in the atmosphere takes place from various sources. Contribution of each source in methane emission in USA is shown in Figure 1.7. This emission of methane to atmosphere has very significant effect on climate change and decay of ozone layer because it is 21 times more potential as a green-house gas compared to carbon di-oxide. So minimizing the emission of methane or capturing this naturally generated methane in an efficient manner and using it as energy source as biogas or for

production of higher hydrocarbon can be a very cost effective solution of this perilous environmental problem.
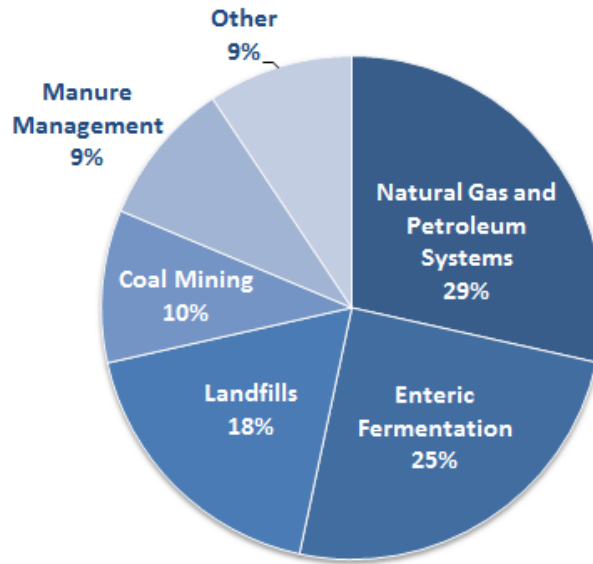
Figure 1.7: US methane emission by source [source: Inventory of US gas emissions and sinks: 1990-2012][19]

Agriculture, farm animals and landfills are the major contributing natural source of methane other than industrial or petroleum systems. Efficient technologies have already been established and continuous improvement is taking place in production facilities of renewable methane or biogas from landfills and agricultural and animal wastes[20]. In year 2009 the total methane emission from agricultural sources like crop residue burning, rice cultivation, solid waste by domesticated animals etc. was 215.9 million metric tons of CO_2 equivalent [19]. Bio-methane can also be captured from waste water treatment plants as pulp in paper industries.

Other than bio based or renewable resources of methane, huge amount of methane gas reserve is discovered in USA, Canada, China and a few more countries trapped in shale formations underground. In year 2000 contribution of shale gas in total natural

production of USA was only 1% but in 2010 it increased to 20% and according to the prediction of Energy Information Administration by year 2035 contribution of shale gas in total dry natural gas production will be above 45% [21].

U.S. dry natural gas production
trillion cubic feet   billion cubic feet per day
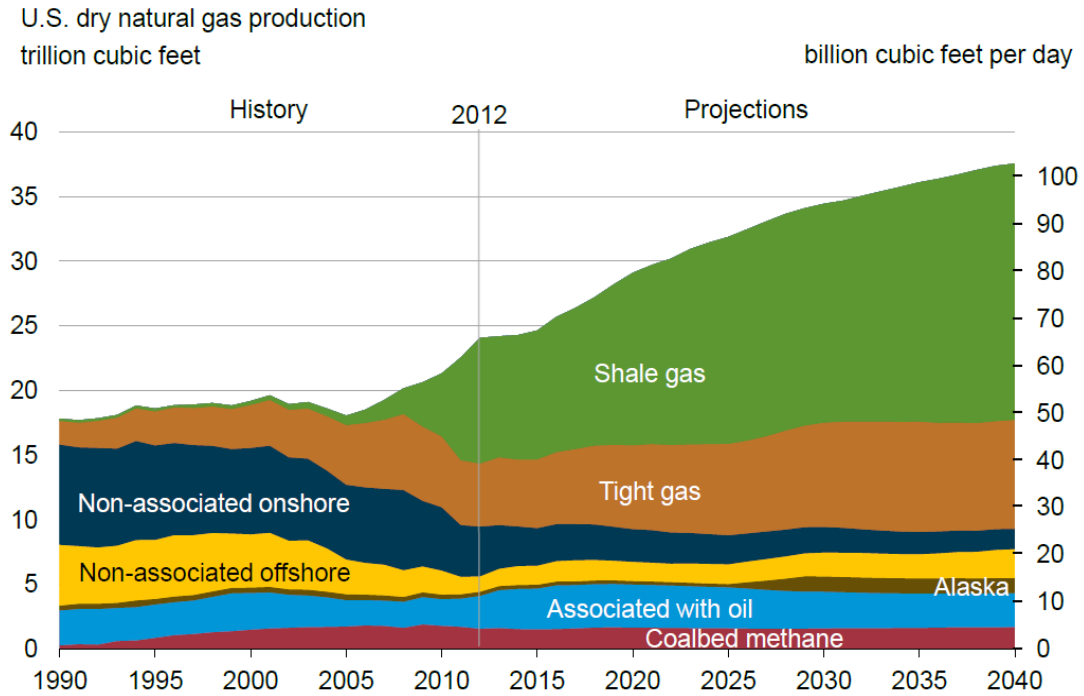
Source: EIA, Annual Energy Outlook 2014 Early Release

Figure 1.8: Prediction of total natural gas production in USA from various petroleum sources[21]

In Figure 1.8 the significant change is natural gas production is USA is shown since year 2010 due to the contribution of reserve shale gas. According to the report at year 2012 USA was the largest producer of dry natural gas in the world. In near future it can be expected that there will be a huge surplus of natural gas as the established oil and gas companies are developing efficient and safe fractionation process for shale gas applications. Though shale is not from a renewable source by definition but it can contribute as an alternative energy resource for power generation, domestic and

industrial heating and cooling and also in transportation sector. Though as a transportation fuel gaseous methane or compressed natural gas is being used but not in a large scale. Usage of natural gas in the transportation sector is less than 1% of total natural gas consumption in USA. It is still not popular in transportation sector due to the infrastructure and technological obstacles as establishment of natural refueling station all over the country, transportation of natural gas due to its low density and also current automobile engines have to be redesigned to accommodate this fuel source efficiently. To have efficient use of this discovered huge resource in the transportation sector, a potential solution will be the conversion of methane to higher hydrocarbon or liquid hydrocarbon which can be used as fuel or fuel blend in conventional automobile engines.

In this work upgrading process of methane to higher hydrocarbon molecules has been studied in a very specific chemical conversion route. A direct conversion of gaseous methane on a bifunctional metal catalyst on a support material like silica and zeolite is carried out without any presence of oxygen unlike conventional gas to liquid (GTL) processes like Fischer-Tropsch synthesis[22] where methane is converted to higher hydrocarbon via production of synthesis gas that is CO and H_2. In this work the proposed direct conversion of methane avoids the route of oxidation and the probable products are C_4 to C_{10} hydrocarbon and hydrogen and this route is shown in Figure 1.9. Direct conversion of methane has been studied on different transition metal catalysts [23][24] but in this work ruthenium metal catalyst on different material combination has been studied and the catalyst performance are also optimized by varying operating temperature and catalyst stability is also studied by performance with time.
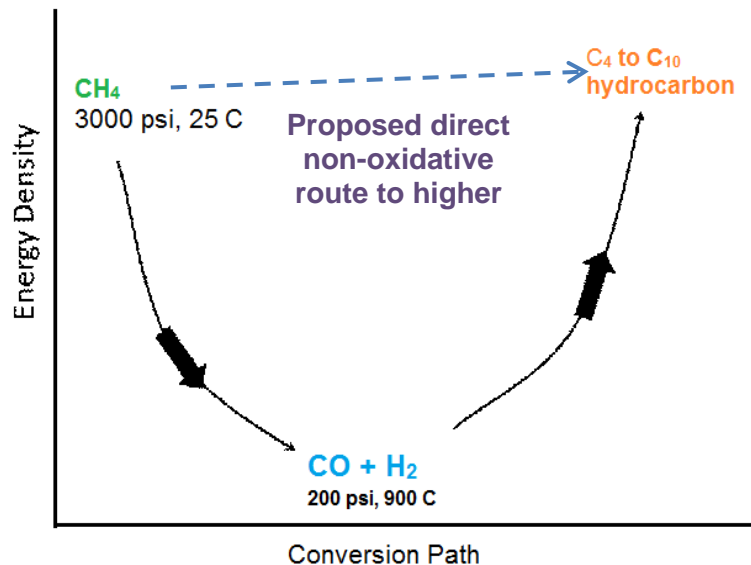
Figure 1.9: Proposed direct non-oxidative conversion path of methane to higher hydrocarbon molecules

In all the above mentioned processes of upgrading biomass fermentation products and bio-methane or shale gas the most vital part is catalysis. Finding out the most suitable catalyst for the upgrading processes to produce higher hydrocarbons and optimizing the catalyst performance with operating parameters like temperature and pressure are a major part of this research. Catalyst characterization is also done using several analysis techniques and measurements. For upgrading of methane the catalysts are prepared from scratch by impregnation, calcination and reduction in the laboratory and characterization is done for each type of catalysts. Mechanisms of the chemical reactions with catalysis are tried to be predicted from the product quality and composition.

References

[1] R. D Perlack, L. L Wright, A. F Turhollow, R. L Graham, B. J Stokes, and D. C Erbach, "Biomass as Feedstock for a Bioenergy and Bioproducts Industry : The Technical Feasibility of a Billion-Ton Annual Supply," *Agriculture*, vol. 1, no. April, 2005.

[2] P. H. Pfromm, V. Amanor-Boadu, R. Nelson, P. Vadlani, and R. Madl, "Bio-butanol vs. bio-ethanol: A technical and economic assessment for corn and switchgrass fermented by yeast or Clostridium acetobutylicum," *Biomass and Bioenergy*, vol. 34, no. 4, pp. 515–524, Apr. 2010.

[3] T. C. Ezeji, N. Qureshi, and H. P. Blaschek, "Bioproduction of butanol from biomass: from genes to bioreactors.," *Curr. Opin. Biotechnol.*, vol. 18, no. 3, pp. 220–227, Jun. 2007.

[4] T. C. Ezeji, N. Qureshi, and H. P. Blaschek, "Acetone butanol ethanol (ABE) production from concentrated substrate: reduction in substrate inhibition by fed-batch technique and product inhibition by gas stripping.," *Appl. Microbiol. Biotechnol.*, vol. 63, no. 6, pp. 653–658, Feb. 2004.

[5] T. Ezeji, N. Qureshi, and H. P. Blaschek, "Production of acetone–butanol–ethanol (ABE) in a continuous flow bioreactor using degermed corn and Clostridium beijerinckii," *Process Biochem.*, vol. 42, no. 1, pp. 34–39, Jan. 2007.

[6] T. Ezeji, N. Qureshi, and H. P. Blaschek, "Butanol Production From Agricultural Residues : Impact of Degradation Products on Clostridium beijerinckii Growth and Butanol Fermentation," vol. 97, no. 6, pp. 1460–1469, 2007.

[7] O. Mutschlechner, H. Swoboda, and J. R. Gapes, "Continuous two-stage ABE-fermentation using Clostridium beijerinckii NRRL B592 operating with a growth rate in the first stage vessel close to its maximal value.," *J. Mol. Microbiol. Biotechnol.*, vol. 2, no. 1, pp. 101–105, Jan. 2000.

[8] N. Qureshi and H. P. Blaschek, "Production of acetone butanol ethanol (ABE) by a hyper-producing mutant strain of Clostridium beijerinckii BA101 and recovery by pervaporation.," *Biotechnol. Prog.*, vol. 15, no. 4, pp. 594–602, 1999.

[9] S. R. Roffler, H. W. Blanch, and C. R. Wilke, "In situ extractive fermentation of acetone and butanol.," *Biotechnol. Bioeng.*, vol. 31, no. 2, pp. 135–43, Feb. 1988.

[10] C. Weber, A. Farwick, F. Benisch, D. Brat, H. Dietz, T. Subtil, and E. Boles, "Trends and challenges in the microbial production of lignocellulosic bioalcohol fuels.," *Appl. Microbiol. Biotechnol.*, vol. 87, no. 4, pp. 1303–1315, Jul. 2010.

[11] G. Jurgens, S. Survase, O. Berezina, E. Sklavounos, J. Linnekoski, A. Kurkijärvi, M. Väkevä, A. van Heiningen, and T. Granström, "Butanol production from lignocellulosics.," *Biotechnol. Lett.*, vol. 34, no. 8, pp. 1415–34, Aug. 2012.

[12] N. Qureshi and S. Hughes, "Energy-efficient recovery of butanol from model solutions and fermentation broth by adsorption," *Bioprocess Biosyst Eng*, vol. 27, pp. 215–222, 2005.

[13] R. Schnepf and B. D. Yacobucci, "Renewable Fuel Standard (RFS): Overview and Issues," *CRS Rep. Congr.*, 2013.

[14] M. Dwidar, J.-Y. Park, R. J. Mitchell, and B.-I. Sang, "The future of butyric acid in industry.," *ScientificWorldJournal.*, vol. 2012, pp. 1–9, Jan. 2012.

[15] S. Liu, K. M. Bischoff, T. D. Leathers, N. Qureshi, J. O. Rich, and S. R. Hughes, "Butyric acid from anaerobic fermentation of lignocellulosic biomass hydrolysates by Clostridium tyrobutyricum strain RPT-4213.," *Bioresour. Technol.*, vol. 143, pp. 322–9, Sep. 2013.

[16] L. K. Bowles and W. L. Ellefson, "Effects of butanol on Clostridium acetobutylicum.," *Appl. Environ. Microbiol.*, vol. 50, no. 5, pp. 1165–70, Nov. 1985.

[17] D. E. Ramey, "Production of butyric acid and butanol from biomass," *Final Report DOE*, 2004. [Online]. Available: http://www.afdc.energy.gov/pdfs/843183.pdf. [Accessed: 20-Apr-2014].

[18] X. Gao, H. Zhao, G. Zhang, K. He, and Y. Jin, "Genome shuffling of Clostridium acetobutylicum CICC 8012 for improved production of acetone-butanol-ethanol (ABE)," *Curr. Microbiol.*, vol. 65, pp. 128–132, 2012.

[19] U S Energy Information Administration, "Emissions of Greenhouse Gases in the United States 2009," no. March, 2011.

[20] a S. G. F. Communities, "Turning waste into vehicle fuel: renewable natural gas (rng)."

[21] U. S. E. I. Administration, "Annual Energy Outlook 2014," *Doe/Eia*, vol. 0383, pp. 1–269, 2014.

[22] J. H. Lunsford, "Catalytic conversion of methane to more useful chemicals and fuels: a challenge for the 21st century," *Catal. Today*, vol. 63, no. 2–4, pp. 165–174, Dec. 2000.

[23] M. M. Koranne, D. W. Goodman, and G. W. Zajac, "Direct conversion of methane to higher hydrocarbons via an oxygen free, low-temperature route," *Catal. Letters*, vol. 30, pp. 219–234, 1994.

[24] S. Majhi, P. Mohanty, H. Wang, and K. K. Pant, "Direct conversion of natural gas to higher hydrocarbons: A review," *J. Energy Chem.*, vol. 22, no. 4, pp. 543–554, Jul. 2013.

Chapter 2

Conversion of the Acetone, N-Butanol, Ethanol (ABE) Mixture to Hydrocarbons by Catalytic Deoxygenation

2.1 Introduction

The current energy crisis stemming from the depletion of fossil fuels has prompted interest in producing alternative fuels that are compatible with the petroleum liquids. To produce drop-in fuels for transportation and power generation, conversion of biomass is an attractive option. Commercial production of ethanol as a fuel blend has already been well recognized. Compared to ethanol, 1-butanol has about 20% higher energy content per mass, a lower vapor pressure, is less corrosive, has a lower aqueous solubility and is compatible with the existing petroleum infrastructure [1]. The most established process of producing 1-butanol form a renewable source of biomass is the 'Acetone-n-Butanol-Ethanol' (ABE) fermentation [1], where sugars can be fermented using bacteria of Genus 'Clostridium' [2], [3]. Recent genetic improvement in the bacterium can give product concentrations of 8.2 g/l acetone, 17.6 g/l 1-butanol and 2.2 g/l ethanol [4]. Here the mass ratio of acetone:1-butanol:ethanol is obtained as 3.7:8:1 which is different than the traditional Clostridium *acetobutylicum* giving 3:6:1 [5]. Two main challenges of the ABE process are low yield and contamination by aerobic and acid producing anaerobic bacteria [6]. The low yield is being addressed by continuous separation of ABE from the bioreactor [7] and the toxicity tolerance is being addressed by the genetic improvement in the microorganism [8], [9],[10].

ABE mixture can become a compatible fuel if it is transformed into a drop-in fuel for replacement of gasoline, diesel or jet fuel. However, to date, not much work has been done on the conversion of the ABE mixture. Recently, the US Navy has studied catalytic conversion of 1-butene, a dehydration product of 1-butanol [11], [12]. Though the dehydration of ABE mixture has not been studied, individual work on the catalytic dehydration of n-butanol, acetone and ethanol has been reported [13],[14]. The dehydration of pure n-butanol mostly produces 1-butene, isobutene, and some ethers depending on the reaction temperature. The dehydration of pure acetone produces a wide range of compounds, the gas phase consisting of CO_2 and C1 to C4 hydrocarbons and the liquid phase consisting of C5 to C6 aliphatics and aromatics hydrocarbons. The products can vary with the temperature and catalyst used. The dehydration of pure ethanol usually produces ethylene and some ethers [15] depending on temperature and the catalyst used. In general, the use of commercial γ-Al2O3 as a dehydration catalyst is quite common for alcohols with the product varying from olefins to ethers depending on the process temperature and strength of the acid sites [16], [17]. For example, using γ-Al2O3 below 300 °C produces more ethers than olefins, and with an increase in the temperature, olefins production supersedes that of ethers [14] . The removal of oxygen from the ABE mixture is the main goal of performing catalytic dehydration, hence it is desirable to produce as little oxygenated hydrocarbons as possible which is usually achieved at the high temperatures[18],[14]. Other catalysts such as iron, manganese and cobalt oxides are also sometimes utilized for catalytic dehydration of alcohols but they are not as widely used as γ-Al2O3 [19], [20]. Zeolites with varying SiO2 to Al2O3 ratios are also being used for catalytic dehydration [21][22]. For example, dehydration of acetone has been done using HZSM-5 and zeolite-β catalysts to produce olefins and aromatics [18], [23]. Using a packed bed of HZSM-5 with space velocity of 4 h-1, complete acetone conversion with 71% towards

mono-aromatics has been achieved [18]. Using a zeolite-β catalyst, markedly enhanced selectivity to isobutene was observed [23]. On the other hand, γ-Al$_2$O$_3$ catalyzed conversion of acetone can produce allenes (e.g., propa-di-ene) at 300 to 700˚C. Conversion of acetone and n-butanol to C$_1$ to C$_{10}$ hydrocarbons has been studied on HZSM-5 type zeolites with a varying SiO$_2$/Al$_2$O$_3$ ratio, where the production of gaseous olefins and nonaromatic liquid hydrocarbons were found to decrease with an increase in the temperature and space time, while the amount of aromatic hydrocarbons and gaseous paraffins increased [22]. The γ-Al$_2$O$_3$ catalyzed dehydration of ethanol above 135˚C produces mostly produce ethylene, while at lower temperatures produces mostly ethyl ether [24],[25].

While, individual catalytic dehydration of n-butanol, acetone and ethanol has been studied but no work has been reported on the dehydration of the mixture as produced from the ABE fermentation process.This work examines the dehydration of ABE mixture. In this work, the mixture of acetone, n-butanol and ethanol has been taken in a mass ratio of 3.7:8:1, which implies a composition of 29.3, 62.9, and 7.8 wt.%, respectively, a typical composition obtained from genetically modified clostridium bacteria [4]. The main objective of this work was to dehydrate the ABE mixture to long chain hydrocarbons. Experiments are carried out to determine suitable reaction conditions to effectively remove the oxygen in order to produce high-energy content hydrocarbon liquids which can be directly used as drop in fuel or to produce unsaturated hydrocarbons gases which can be further oligomerized to produce the liquids [26], [27], [28]. Catalytic dehydration of ABE mixture is examined over two different catalysts: γ-Al$_2$O$_3$ and ZSM-5. The effect of reaction temperature and weight hourly space velocity on quality and quantity of the dehydration products is examined. In addition, the products

from dehydration of the individual ABE components are compared to the products from the ABE mixture to observe the cross reactivity of the components, if any.
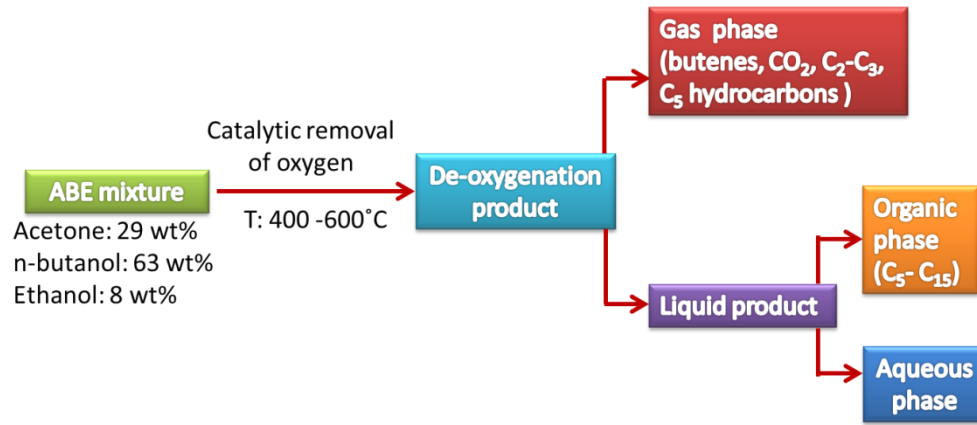
Figure 2.1: ABE catalytic de-oxygenation process scheme

2.2 Objectives

The objective of this work was to remove oxygen from ABE mixture by catalytic dehydration process to produce unsaturated higher hydrocarbon products.

- Comparison of the product characteristics from the de-oxygenation of individual components with the ABE mixture.

- Determining the effect of temperature and feed flow rate on conversion and removal of oxygen.

- Comparison of the performance of two different catalysts on the de-oxygenation process.

2.3 Experimental Section

2.3.1 Materials

ACS grade n-butanol (99.4%), acetone (99.9%), ethanol (99.98%) were used in this study. ABE mixture is prepared as a mixture of n-butanol (62.9 wt.%) , acetone (29.3 wt.%) and ethanol (7.8 wt.%). Catalysts γ-Al_2O_3 as cylindrical pellets (0.32 mm dia, 220 m^2/g surface area and 0.62 mL/g pore volume) (Figure 2.2a) and ZSM-5 as powder (23:1 SiO_2:Al_2O_3 molar ratio, 425 m^2/g surface area and 0.118 mL/g pore volume)(figure 2.2b) are used as received from Alfa Aesar (Ward Hill, MA). Silica sand (0.853 to 2.00 mm dia) is used as the filler material. Anhydrous calcium sulfate are used as desiccant for gases.

(a) (b)

Figure 2.2: (a) Cylindrical pellets of γ-Al2O3 catalyst (b) Powdered ZSM-5 ,Zeolite catalyst

2.3.2 Apparatus and procedure

A schematic of the apparatus is shown in Figure 2.3 and the experimental setup in the lab is shown in Figure 2.4. The feed liquid was pumped to the reactor using a high pressure positive displacement pump in which flow rate was controlled and pressure was adjusted to overcome the pressure drop across the catalysts bed. A stainless steel tubular reactor (High Pressure Equipment Company, Erie, PA) with 0.8 cm internal diameter (i.d.) and 20.4 mL internal volume was placed inside an electric furnace. The

feed was pumped through a coiled tubing inside the furnace to preheated before entering the reactor. Fluid temperature in the reactor was monitored by a thermocouple (Omega). The reactor was packed with either 10.5 g of γ-Al_2O_3 cylindrical pellets, or 2.9 g of ZSM-5 mixed with 7.1 g of silica sand. The product outlet line from the reactor was a 1/16" 316 stainless steel tubing which was first air cooled and then water cooled using a copper heat exchanger. After passing through the heat exchanger, the product, a gas/liquid mixture, is fed to a 'phase separator' consisting of a 30 ml Jerguson gage with sight glass. The mixture entered at the middle of the separator and the separated gas exited from the top. A volumetric gas flow meter (Cole Parmer, Vernon Hills, IL) of maximum capacity 500 mL/min calibrated with respect to air was connected to the top outlet of the phase separator. At the outlet of the flow meter, a pressure gauge of maximum capacity of 60 psig was placed to measure the pressure. The gas product then passed through a tubular steel vessel packed with anhydrous calcium sulfate to remove the moisture before entering gas chromatograph.
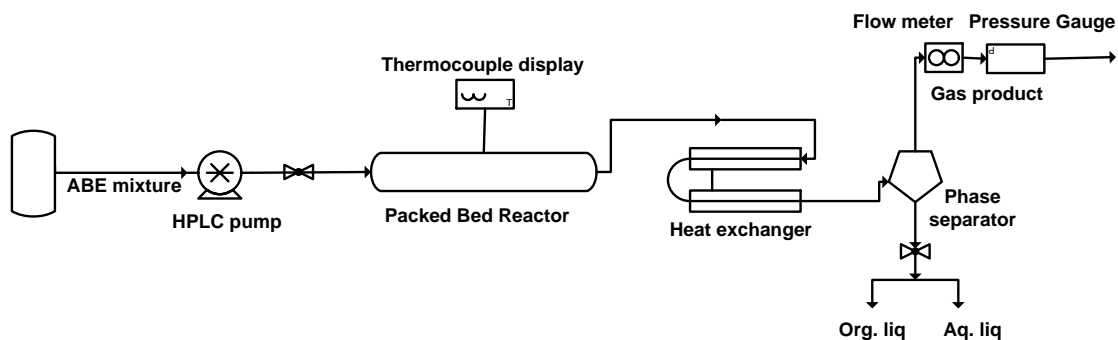
Figure 2.3: Process flow diagram of the catalytic dehydration

Figure 2.4: Experimental setup in lab for ABE catalytic de-oxygenation process

A control valve, at the bottom outlet of the phase separator, is opened to collect the liquid product gathered in a given duration. After every two experimental runs, nitrogen gas is passed through the reactor at 400°C to remove any chemical residue.

Two operating parameters, reaction temperature and feed flow rate, are varied to examine the dehydration kinetics for both the catalysts.

2.3.3 Product characterization

2.3.3.1 GC chromatography A SRI 8610C gas chromatograph (GC) with a thermal conductivity detector (TCD) was used to determine the composition of the gas product. A capillary Supel-Q PLOT column (Supelco, Sigma-Aldrich, St. Louis, MO) with 'divinylbenzine polymer' as the stationary phase and 27 m in length and 0.32 mm i.d. was used for the gas chromatographic analysis. This column was selected as it can separate CO_2 and C_1-C_5 hydrocarbons. The column oven was maintained at 70°C. Helium was used as the carrier gas. Sample injection to the GC was done online by means of a six-port injection valve attached through a 10 µL sample loop.

2.3.3.2 Fourier Transform Infrared (FTIR) spectroscopy

The IR analysis of the gas mixture was done using a Nicolet IR100 FTIR instrument and Spectra Tech Econo gas cell of 50 mm path length and NaCl windows. Product gas was collected by connecting the top outlet tubing from the phase separator to a 1-liter flex film gas sampling bag (SKC, Inc., PA). A gas tight syringe of 5 ml capacity (SGE, Austin, TX) was used to transfer gas from the sample bag to the gas cell. The cell was flushed with gas several times to ensure that no air or previous gases were left inside. The background taken for subtraction was the IR spectrum of the empty cell containing pure nitrogen. The IR analysis was done especially to detect the type of bonds in the gaseous products which couldn't be detected in the GC analysis. For example, in the GC analysis, 1-butane and other butene could not be distinguished as all the C_4 hydrocarbons have almost the same retention time in the column. But in the IR analysis, distinctive peaks are observed due to the C=C bond.

2.3.3.3 Calorific value analysis

The calorific value of the liquid feed and dehydration products were analyzed by an IKA C 200 calorimeter. As the feed and product were both very combustible and volatile, they were first soaked in cotton and then combusted in a bomb calorimeter on a stainless steel crucible pressurized with oxygen at 34 bars. The HHV of the cotton was subtracted from to obtain the HHV of the sample only.

2.3.3.4 Total Organic Carbon (TOC) analysis

The organic carbon content of the liquid product was measured using a TOC analyzer (TOC-Vcsn, Shimadzu).

2.3.3.5 Gas Chromatography-Mass Spectrometry (GC-MS) analysis

The liquid product mixture was also analyzed by a GCT Premier Gas Chromatography mass spectrometry (Waters, Milford, MA). The GC-MS was equipped with a DB-5 column from Agilent technologies to separate the hydrocarbon components. It also contained a flame ionization detector (FID) and could separate and detect from very low hydrocarbons from C_2 to C_{20}.

2.4 Reactions Involved

Major reactions involved in the dehydration process are briefly described below.

Dehydration of n-butanol

$$C_4H_9OH \xrightarrow{\gamma-Al_2O_3} H_2C = CH - CH_2 - CH_3 + H_2O$$
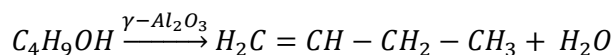
This is the dominant reaction above 400°C, where almost 99% conversion of 1-butanol is achieved to 1-butene and its isomers [17]. With an increase in space velocity, skeletal isomerization of 1-butene increases cis- and trans-butene products [29]. At a lower temperature, incomplete deoxygenation results in the formation of ethers,

$$2C_4H_9OH \xrightarrow{\gamma-Al_2O_3} C_4 H_9 - O - C_4 H_9 + H_2O$$
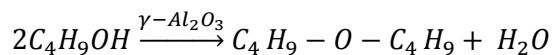
This is the dominant reaction in 200-350°C range. With increase in the temperature, selectivity towards 1-butene increases over dibutyl ether, and ether production becomes minimal above 400 °C [14]. At the high temperatures such bimolecular reactions are generally slower than the monomolecular reactions leading to the production of alkenes [30].

Dehydration of acetone

$$(CH_3 - CO - CH_3) \xrightarrow{\gamma-Al_2O_3} CO_2 + light\ alkanes\ and\ alkenes\ upto\ C_4 (gas\ phase)$$
$$+ Mixture\ of\ Aromatics\ and\ cyclic\ organic\ compounds (C_5$$
$$- C_{12})\ (liq\ Phase)$$
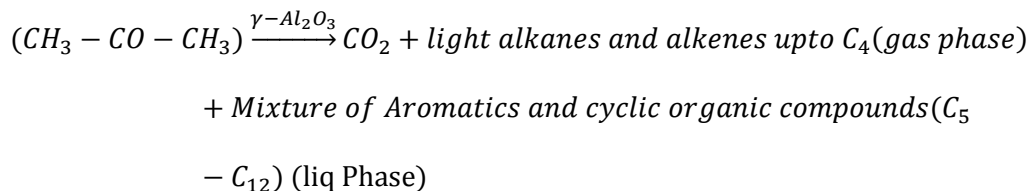
The above reaction products are based on experimental results as no specific reaction mechanism was found for γ-Al$_2$O$_3$ catalyzed dehydration of acetone in the literature.

$$(CH_3 - CO - CH_3) \xrightarrow{ZSM-5} CO_2 + C_2\ to\ C_6\ aliphatics$$
$$+ Mixture\ of\ Aromatics\ and\ cyclic\ organic\ compounds\ (C_5 - C_{12})$$
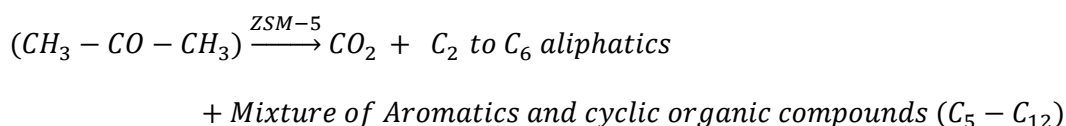
ZSM-5 catalyzed dehydration produces both aliphatic and aromatic hydrocarbon along with carbon dioxide. In a study using ZSM-5 catalyzed dehydration of acetone at 400°C, the reaction products were found to contain meta and para xylene, benzene, toluene and furan as well in the liquid phase [18].

Dehydration of Ethanol

$$CH_3 - CH_2 - OH \xrightarrow{\gamma-Al_2O_3} CH_2 = CH_2 + H_2O$$

$$CH_3 - CH_2 - OH \xrightarrow{\gamma-Al_2O_3} C_2H_5 - O - C_2H_5 + H_2O$$
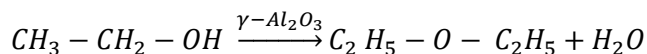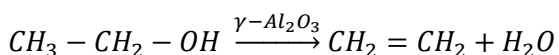
Here, ethanol reacts with alumina to form surface alkoxides which decompose to yield ethylene and diethyl ether [31]. The ether formation is favored below 135 °C and the ethylene formation is suppressed at a high concentration of surface ethoxide and surface hydroxyl groups. However, at higher temperatures, ethylene is the only product found regardless of the surface concentrations of the above mentioned groups [24]. Similar reaction mechanisms are followed for 1-butanol dehydration on γ-Al$_2$O$_3$ catalyst except that the produced 1-butene may undergo isomerization or bond shifting.
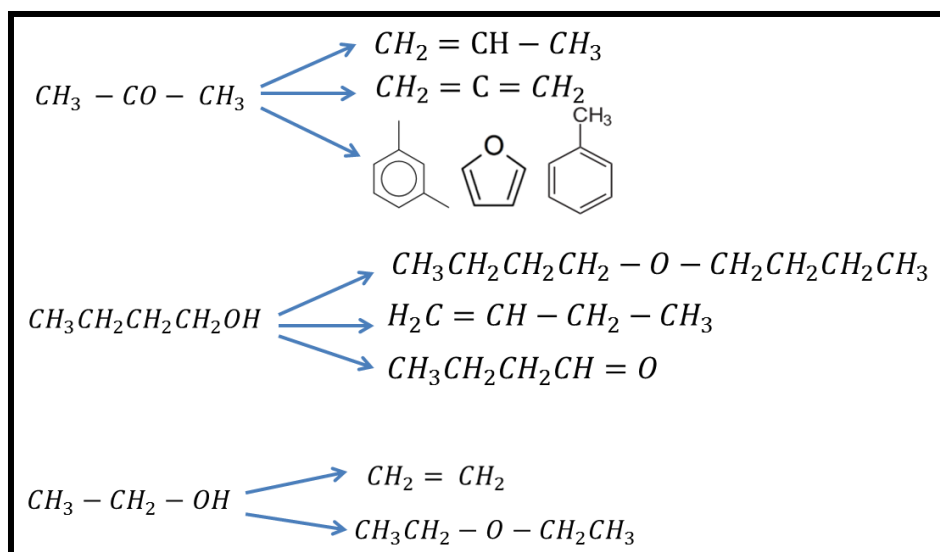
Figure 2.5: Probable reaction products from ABE individual component catalytic Deoxygenation

In ABE mixture dehydration, these products cross react giving additional hydrocarbons and that is how longer chain hydrocarbons are formed containing high heating value in only one step of conversion.

2.5. Results and Discussion

The dehydration products of the ABE mixture consist of a wide range of hydrocarbons as well as CO_2 and H_2O. In the gaseous product, a range of C_2 to C_5 hydrocarbons were found by GC analysis, mostly comprised of 1-butene and its isomers (>60%) as shown in Table 2. The liquid product separated into two phases: organic liquid and aqueous liquid. The organic liquid contained a wide range of products including cyclopentane, cyclohexane, furan, decene, benzene and other unsaturated and saturated hydrocarbons, aromatics and oxygenated hydrocarbons. The aqueous liquid contained mainly water and some oxygenated hydrocarbons at low levels. The composition of the

products varied depending upon the catalyst and reaction time, which is linked to the feed flow rate, as shown in Table 2.
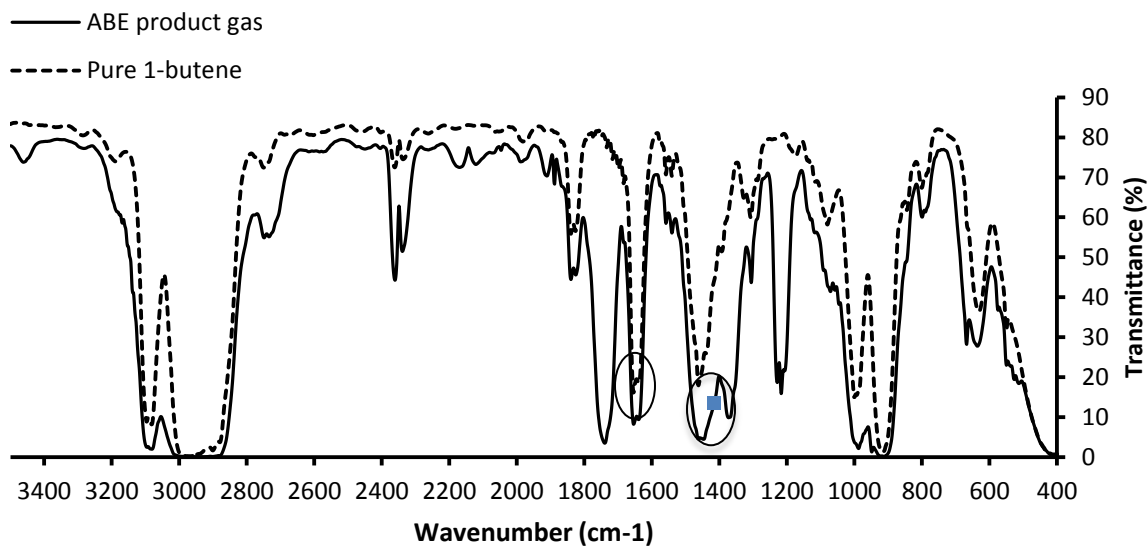
Figure 2.6: Comparison of IR spectra of pure 1-butene gas with ABE dehydration product gas obtained using γ-Al2O3 catalyst at 400 ˚C (0.08 g/min feed flow rate)

From Figure 2.6 it can be seen that the ABE product gas has carbon-carbon double bond peaks at wavenumbers 1655 cm^{-1} and 1445 cm^{-1} similar to those for pure 1-butene

2.5.1 Comparison of dehydration products of individual components and the mixture
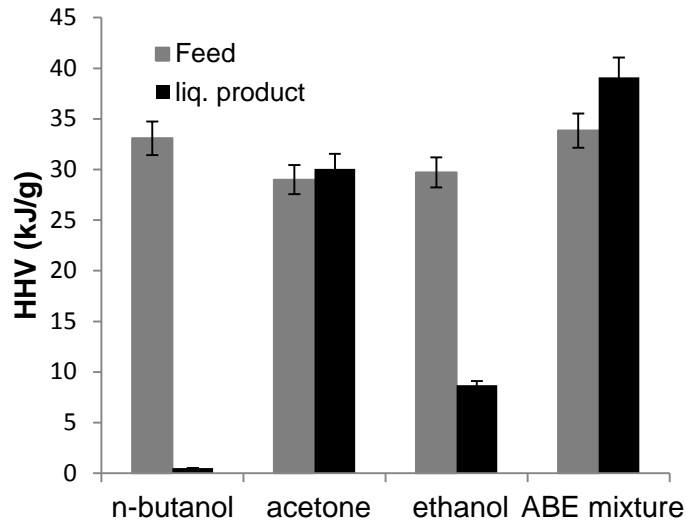
Figure 2.7(a): Comparison of HHV of liquid feeds and organic liquid products from dehydration using γ-Al2O3 catalyst at 400 ˚C
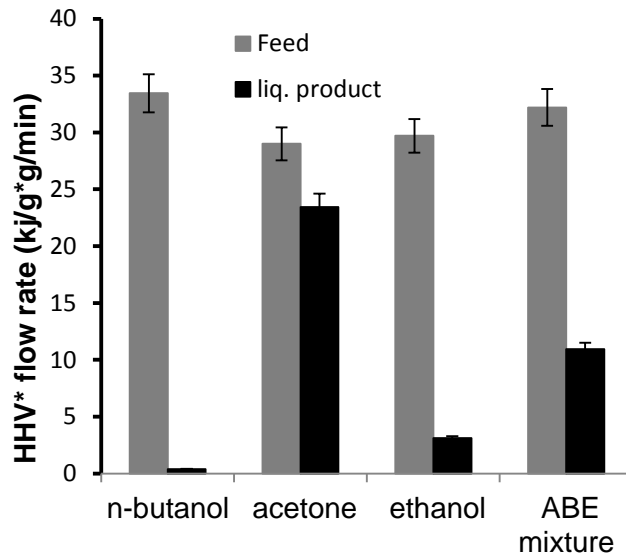
Figure 2.7(b): Comparison of energy flow in feeds and organic liquid products from dehydration using γ-Al2O3 catalyst at 400 ˚C

N-butanol, acetone, ethanol and ABE mixture were fed to the packed bed reactor separately at 1.0 ml/min flow rate (at the pump conditions). In general, the dehydration on γ-Al_2O_3 at 400 °C produces gas phase, organic phase, and aqueous phase products. Dehydration of n-butanol and ethanol give only an aqueous phase and gas phase. Dehydration of acetone at 400 °C produces only an organic liquid phase and gas phase. The ABE mixture gives all three, gas, organic and aqueous phases. The HHVs of the feeds and products for ABE were compared to the feed and product HHVs for the individual components (Figure 2.7). In the case of n-butanol and ethanol the HHV of the organic liquid product decreased compared to the HHV of feed (Figure 2.7a), indicating that most of the organic carbons were converted to light hydrocarbons going into the gaseous product stream. In the case of acetone, the HHV of the organic liquid product didn't change much from that of the feed, due to a very low conversion at these operating conditions. For ABE mixture, the organic phase of the liquid product showed a higher HHV than that of the feed. In Figure 2.7(b) the energy flow going in with the feed liquid and part of energy flow out as the organic liquid are compared for pure components and for the ABE mixture. The organic liquid product from the dehydration of the ABE mixture has higher HHV than any of the pure component dehydration products but as the mass production rate of that is low the total energy flow (HHV * mass flow rate) in kJ/min is also low.

The product HHV from the ABE mixture is comparable to that of jet fuel (42-43 kJ/g). This also implies that the liquid dehydration product of ABE mixture is not the exact summation of the dehydration products of its individual components as none of the product HHVs were close to that from ABE mixture. This observation is also supported by IR spectra of the products from individual components to that from ABE (Figure 2.8).

In the case of ABE gas product some new bonds are formed showing unique peaks in the IR spectra which absent from any of the gas products from the single components.

Ethanol product

Acetone product gas

n-Butanol product gas

ABE product gas

a.u.

Wavenumber (cm^{-1})
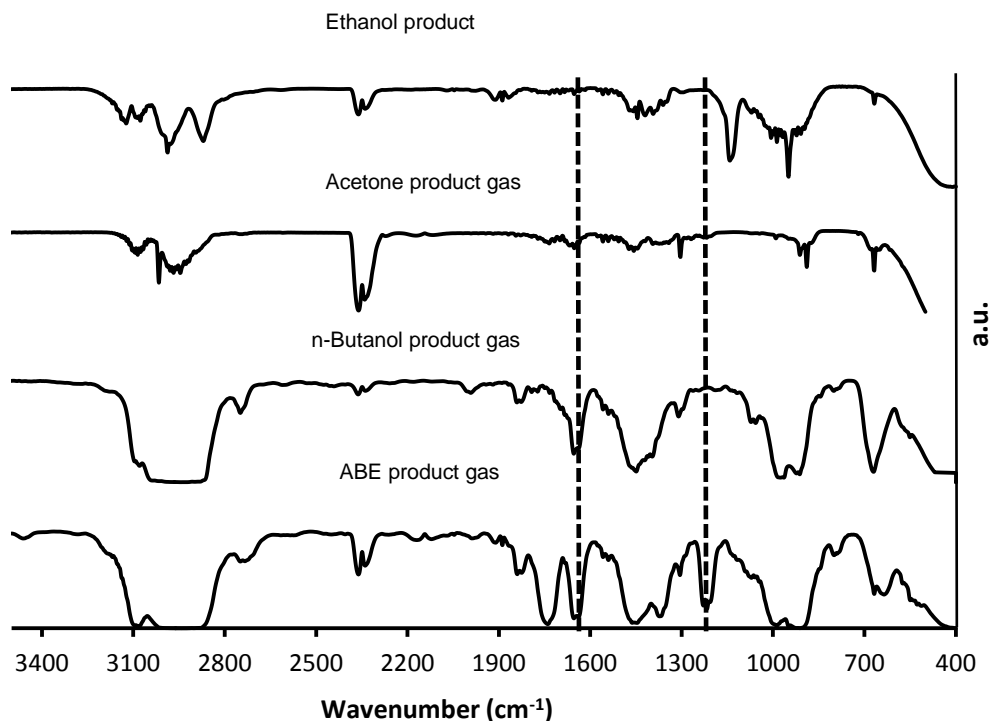
Figure 2.8: IR spectra of gaseous products from ABE mixture and its components

for dehydration on γ-Al2O3 catalyst at 400 ˚C

Here, the two new peaks are at 1205 and 1740 cm^{-1} which represent the formation of some new oxygenated hydrocarbon compounds due to the interaction of the component molecules of ABE mixture.

By estimating the O/C ratio from the HHV, the O/C ratio of the organic liquid product ABE mixture on γ-Al$_2$O$_3$ catalyst at 400 ˚C was found as low as 0.03, as compared to the feed O/C ratio of 0.25 The correlation [32] used for calculating the mass ratio O/C ratio is as follows.

$$y = 14.371x^2 - 35.542x + 40.106 \qquad (1)$$

$R^2 = 0.9996$

where, y is HHV of sample in kJ/g, and x is the O/C mass ratio in the sample.
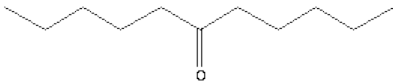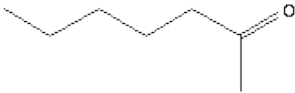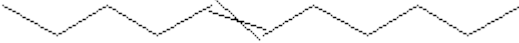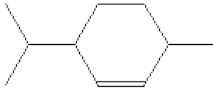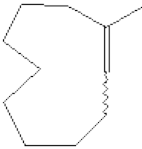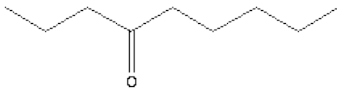
Table 2.1(a): O/C mass ratio of feed and liquid products of catalytic dehydration on γ-Al$_2$O$_3$ at 400˚C
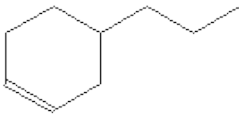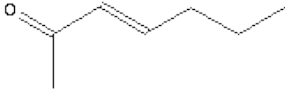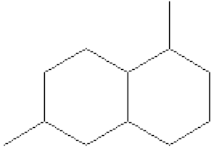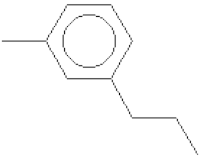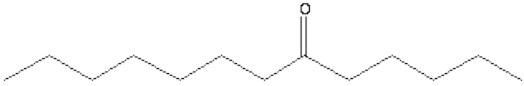
Components	Feed(liq) HHV (kJ/g)	O/C ratio	Product(Liq) HHV (kJ/g)	O/C mass ratio
n-Butanol	33.4	0.20	negligible	
Acetone	29.0	0.37	30 (org. phase)	0.32
Ethanol	29.7	0.34	8 (aq. phase)	1.23
ABE mixture	32.2	0.2	39(org. Phase)	0.03
			3 (aq. Phase)	--

Table 2.1(a) compares the higher heating value of the individual component and ABE as a mixture with the catalytic de-oxygenation liquid product from each of the components and the mixture. The aqueous dehydration product from n-butanol has less than 2000 ppm carbon, so the HHV was negligible. The organic product from acetone dehydration, the O/C ratio did not change much due to poor conversion. For liquid product from the ethanol dehydration, the O/C ratio increased as most of the organic carbon went in the gas phase in the form of ethylene. Interestingly, the ABE dehydration product possesses different characteristics; here the O/C mass ratio of organic liquid product is eight-fold lower when compared to that of the feed.

The liquid organic phase of the product from catalytic deoxygenation on γ-Al$_2$O$_3$ at 400˚C consists of a wide range of paraffins and olefins, oxygenated hydrocarbons and aromatic compounds. Form GC-MS analysis it was found that the organic liquid phase contains hydrocarbons in a range of carbon numbers C$_5$ to C$_{16}$. The GC-MS analysis of the organic phase of the liquid product from catalytic deoxygenation of ABE on γ-Al$_2$O$_3$ at 400˚C, showed a total of 135 components, out of which the major products are listed in Table 2.1(b) in the order of decreasing peak area in the chromatogram.

Table 2.1(b): Components in organic liquid product phase from catalytic dehydration of ABE mixture on γ-Al2O3 at 400˚C from GC-MS analysis, in an order of decreasing concentration.

Component	Formula	Chemical Structure
6-Undecanone	C$_{11}$H$_{22}$O	
2-Heptanone	C$_7$H$_{14}$O	
5-Undecene	C$_{11}$H$_{22}$	
Cyclohexene, 3-methyl-6-(1-methylethyl)-	C$_{10}$H$_{18}$	
Cyclodecene, 1-methyl-	C$_{11}$H$_{20}$	
4-Nonanone	C$_9$H$_{18}$O	
3-Heptene, 2-heptene	C$_7$H$_{14}$	

Cyclohexene, 4-propyl-	C_9H_{16}	
3-Hepten-2-one	$C_7H_{12}O$	
Naphthalene, decahydro-1,6-dimethyl-	$C_{12}H_{22}$	
Benzene, 1-methyl-3-propyl-	$C_{10}H_{14}$	
6-Tridecanone	$C_{13}H_{26}O$	
1,12-Tridecadiene	$C_{13}H_{24}$	

In addition, some smaller peaks representing higher hydrocarbon up-to C_{16} were also detected.

2.5.2 Effect of temperature
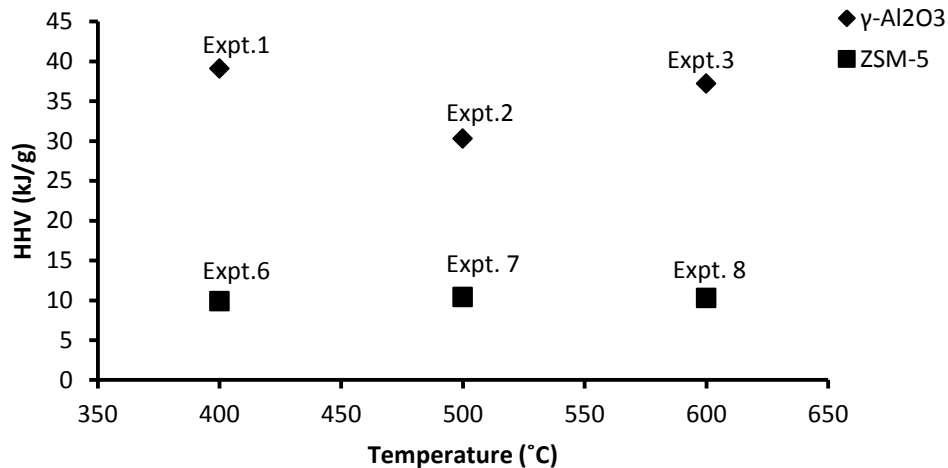
Figure 2.9 (a): HHV of ABE dehydration organic liquid product at varying

temperatures
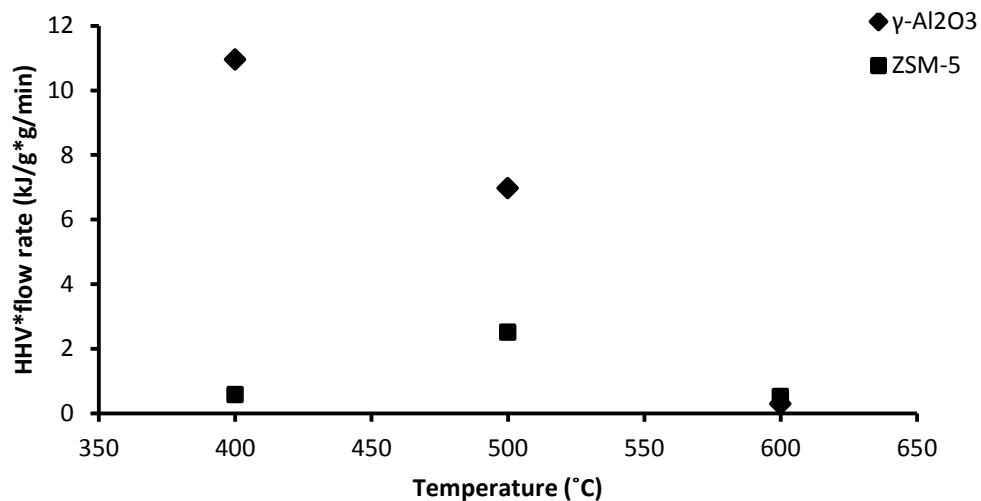
Figure 2.9 (b): Effect of temperature on production of organic liquid product and

its energy content at normalized feed flow rate of 0.8 g/min ABE mixture

The effect of temperature on the dehydration of ABE mixture was studied from 400 to 600°C for both γ-Al$_2$O$_3$ and ZSM-5 catalysts. The liquid product from the dehydration on ZSM-5 showed almost negligible change in HHV with temperature. Figure 2.9 shows

that using γ-Al$_2$O$_3$ catalyst, HHV of the liquid product from 500 °C was lower than that of 400°C. At the higher temperature more hydrocarbons were going to the gas phase so the decrease in liquid phase heating value was reasonable. But at 600 °C the HHV of organic liquid product increased again though the ratio of organic phase to aqueous phase was very small. This means at 600°C more oxygen is getting removed in forms of H$_2$O leaving a small amount of high energy content organic liquid product.

Figure 2.9 (b) shows the product of mass flow rate of organic liquid and the corresponding HHV value with varying temperature. At 600°C the HHV of the organic phase is very high but at this temperature the mass flow rate of the organic phase is very small (Figure 2.9 a). In Figure 2.9b the product of HHV and mass flow rate of the organic liquid produced are shown which depicts the actual energy flow in liquid product from dehydration of ABE mixture, given that the aqueous phase of the liquid product has negligible energy content. For γ-Al$_2$O$_3$ catalyzed dehydration at 400°C the energy flow rate is the highest as both the mass flow rate of organic liquid product and its HHV are high. In ZSM-5 catalyzed dehydration, the energy flow is much lower as the production rate of organic liquid phase or higher hydrocarbon was very low. The liquid phase has a low content of hydrocarbons which results in small HHV of the liquid product; and also the energy flow did not vary much with temperature for the ZSM-5 catalyzed dehydration.
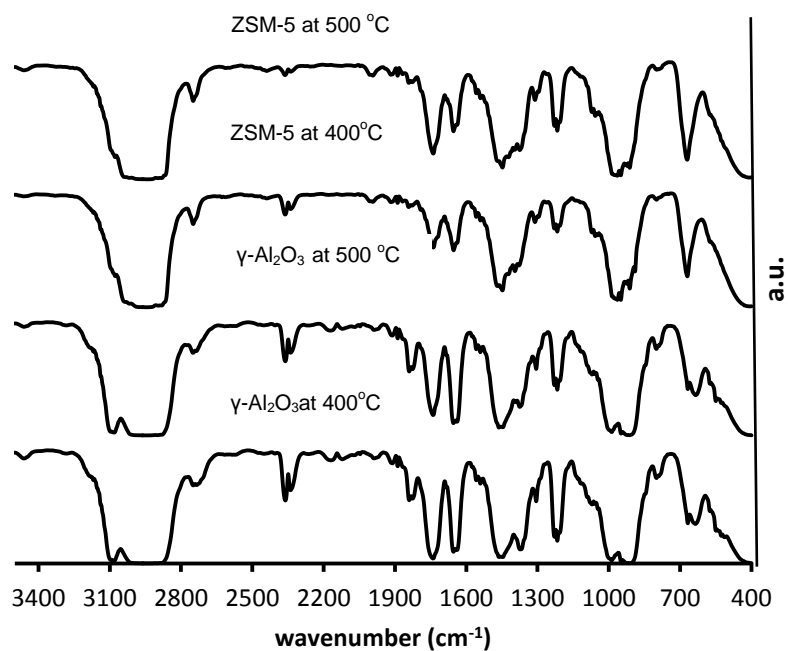
Figure 2.10: IR spectra of ABE dehydration gases produced at different reaction
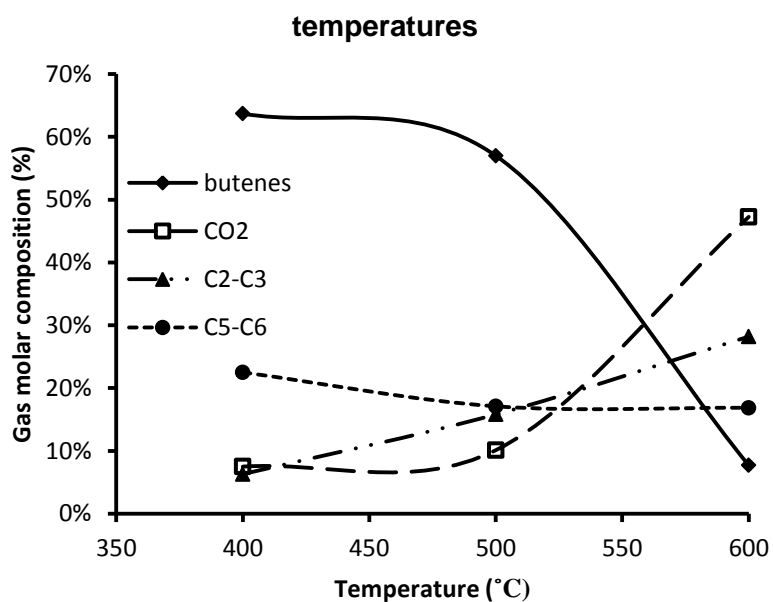
temperatures

Figure 2.11(a): Effect of temperature on gas product composition
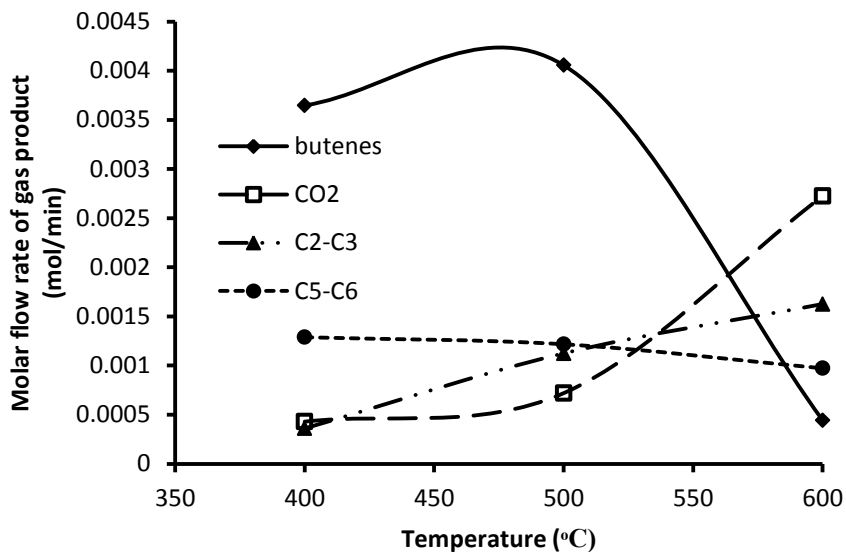
Figure 2.11(b): Effect of temperature on molar flow rate of gas products from

γ-Al2O3 at 0.8 g/min feed flow rate
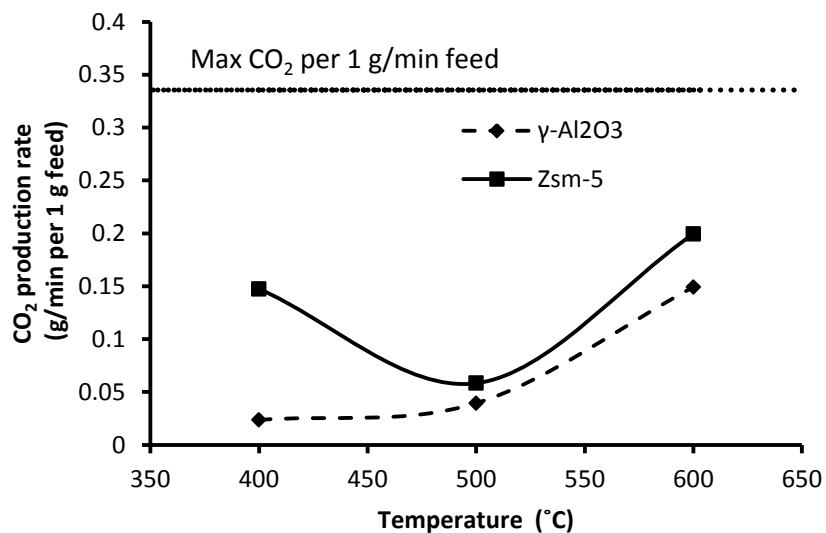
Figure 2.12: CO2 production rate in ABE dehydration on γ-Al2O3 and ZSM-5 at

varying temperatures

The effect of temperature gaseous product was noticeable only for the production rate which increases with the temperature. Figure 2.11(a) shows variation in the gas

compositions with temperature and catalysts. The composition did not vary significantly in the 400 to 500°C range, however, at 600°C CO_2 increased significantly for both γ-Al_2O_3 and ZSM-5 due to the increased conversion of acetone in the ABE mixture. With the increase in temperature, C_4 to C_5 composition decreases and CO_2 and C_2 to C_3 increase (Figure 2.11a). In Figures 2.11(b) and 12 the sudden rise of CO_2 production is shown for increasing temperature from 500 to 600°C in ABE dehydration on γ-Al_2O_3. CO_2 production rate in ZSM-5 catalyst is higher than that in γ-Al_2O_3 (Figure 2.8), as acetone conversion is higher in the ZSM-5 catalyzed process [18], [23], more oxygen is being removed as CO_2 than in the γ-Al_2O_3 catalyzed process at same operating temperatures. It can be summarized that with temperature CO_2 production rate increases, and ZSM-5 catalyzed ABE dehydration produces more CO_2 than of γ-Al_2O_3 catalyzed dehydration. Also with increase in temperature, the production of small hydrocarbon molecules and CO_2 dominates over the production of C_4 and higher hydrocarbons gases.

For zeolite catalyst at high temperatures, acetone conversion to aromatics was observed for both ABE and pure acetone feeds. This resembles the results from another study on n-butanol-acetone mixture where it showed that gaseous olefins and non-aromatic liquid hydrocarbons are the main products at low temperature like 375 °C, but as temperature is increased to 450 °C the yield in gaseous paraffins and aromatics increases [22]. From reaction mechanism and previous studies [14], [18], it was found that at lower temperatures than 400°C, dehydration of n-butanol and acetone to olefins are not the preferred reactions. In the experimental runs at low temperatures, both the yield of olefin and conversion was low. The conversion becomes high at 400°C which can be considered as an optimized temperature especially for γ-Al_2O_3 catalyzed dehydration.

2.5.3 Effect of feed flow rate
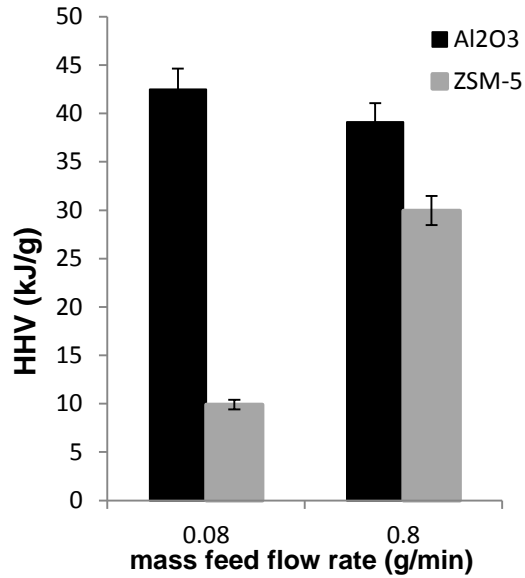
Figure 2.13: Effect of feed flow rate on energy content of organic liquid product

from ABE dehydration at 400 ˚C
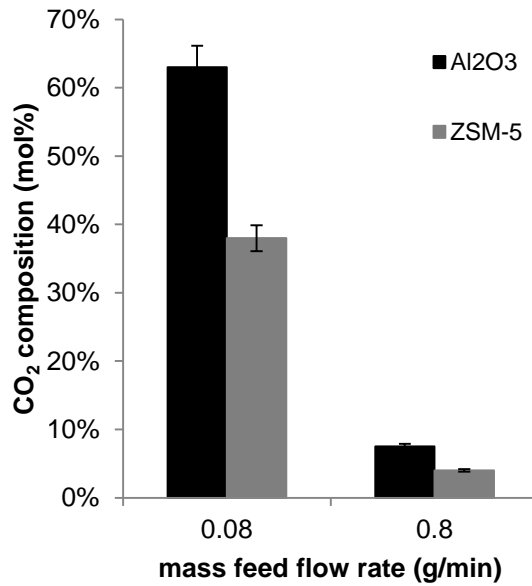
Figure 2.14: Change in gas composition of CO_2 produced from the ABE

dehydration at 400 ˚C

To examine the effect of reaction time, the feed flow rate was changed 10 fold. First the dehydration process was run with feed flow rate 0.8 g/min where the weight hourly space time was 0.22 h on γ-Al_2O_3 and 0.06 h on ZSM-5. And when the feed flow rate is lowered 10 folds the space times increases to 2.17 h and 0.6 h, respectively. With 0.8 g/min feed flow rate, CO_2 production was low in both cases which can be attributed to the low conversion of acetone in the ABE mixture. When the individual components were used as feed at the same flow rate of 1.0 ml/min (pump condition) and at operating temperature 400 °C, it could be seen that almost no conversion took place for acetone but n-butanol and ethanol conversions were above 90%. It is difficult to break the C=O bond in acetone than to break the C-OH bond in n-butanol or ethanol. With increasing space time, the conversion increases. This observation is also consistent with an increase in the HHV of the liquid products and increasing CO_2 composition in the gaseous product mixture with an increase in space time. In Figure 2.13, HHV of the organic liquid product from γ-Al_2O_3 catalyzed ABE dehydration is compared with the only 1-phase liquid product from ZSM-5 catalyzed dehydration at two different feed flow rates. HHV of organic phase is much higher compared to the 1-phase liquid product, and with increasing feed flow rate HHV decreased only by a small extent. CO_2 composition decreases with increasing flow rate or decreasing space time (Figure 2.14), which is consistent with the fact that increasing space time contributes to a higher conversion, a higher production of CO_2 and a lower yield of organic liquid.

Another important observation is that the liquid production rate decreases with increasing residence time. On γ-Al_2O_3 catalyst for decreasing feed flow rate from o.8 g/min to 0.08 g/min, the liquid production rate decreased from 55 to 10 wt.% of the feed. Hence, at the lower flow rate more gas is being produced as dehydration product which

47

indicates a better conversion and a better removal of oxygen from the alcohols and ketones than those at the high flow rate.

2.5.4 Effect of catalyst

As compared to that from ZSM-5, the liquid product from γ-Al$_2$O$_3$ catalytic dehydration of the ABE mixture is high in energy content and the gas product contains a good amount of unsaturated hydrocarbon (e.g., 1-butene). Thus γ-Al$_2$O$_3$ can be considered as a better catalyst than ZSM-5 for this dehydration process. The conversion of ABE on both γ-Al$_2$O$_3$ and ZSM-5 zeolite were comparable at high residence time (low feed flow rate but the catalytic activity of γ-Al$_2$O$_3$ was higher in producing heavy hydrocarbons as the liquid product. Though in other studies ZSM-5 demonstrated a high activity for acetone conversion [18] but it also showed low conversion when the selectivity is high towards isobutene products (~80%) [23], which might have been the case here as more gaseous hydrocarbon was produced than liquid in the ZSM-5 catalyzed dehydration of ABE. On the other hand it is well established that pure alumina do not catalyze the dehydrogenation of alcohols, while surface Lewis acid sites catalyze the dehydration of alcohols. Acid sites of γ-Al$_2$O$_3$ also contribute to the isomerization of dehydration products depending on the strength, amount distribution of these sites and reaction conditions. Recent experimental results suggested that isomerization on alumina was more dependent on the density of the acid sites and was structurally insensitive [29], [30]

.

(a) (b)

Figure 2.15: Liquid product of catalytic de-oxygenation of ABE: (a) two phase product from γ-Al2O3 catalyzed reaction (b) 1 phase liquid product from zsm-5 catalyzed reaction

ZSM-5 lattice   γ-Al$_2$O$_3$ lattice
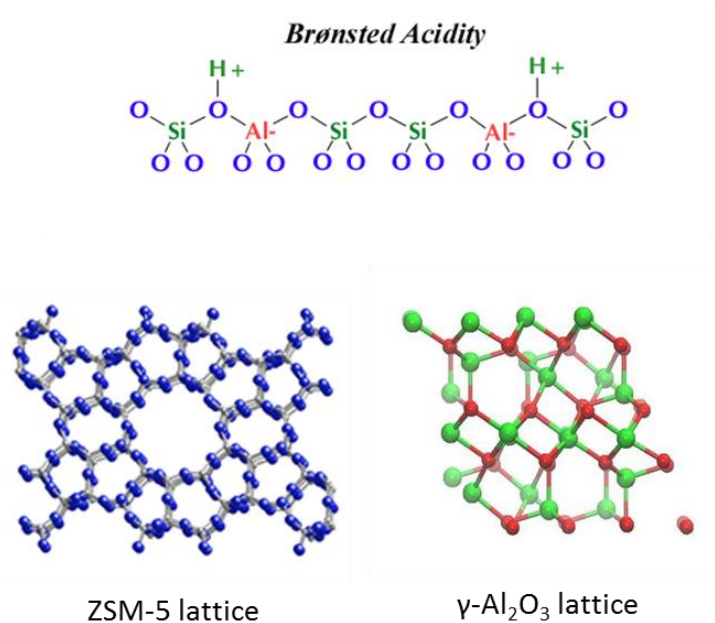
Figure 2.16: ZSM-5 and γ-Al2O3 lattice structures and Bronsted acidity in ZSM framework structure

The acidity of alumina and aluminosilicate catalysts depends on the coordination of alumina and its neighbors. In zeolites, it is accepted that the Bronsted acid site is the OH bridging from a framework silicon to a framework aluminium. Zeolites contain both

49

Bronsted and Lewis acid sites and in this way it is different from γ-Al$_2$O$_3$[33] and [34]. ZSM-5 type zeolite possess strong acidity and intracrystalline network which contributes in high activity and shape selectivity yielding light hydrocarbon from n-butanol acetone mixture [22]. Though ZSM-5 is well known for its activity in hydrocarbon cracking reactions, this type of catalyst also induces the aromatization and polymerization of olefins produced in the dehydration reaction [18],[27]. But the molecular sieve nature of the catalyst avoids condensation reactions among the olefins and carbonium ions and that was expected to be the reason for producing lower hydrocarbons in ZSM-5 catalyzed dehydration. The ratio of Si/Al in the ZSM-5 zeolite catalyst affects the acidity and acid strength distribution [35];Though study on the effect of different Si/Al ratio in ZSM-5 on the dehydration process was not performed in this work but from literature it was seen that in case of low SiO$_2$/Al$_2$O$_3$ ratio of ZSM-5 (i.e., high acid density), (%) conversion of acetone was high and didn't deteriorate much with time on stream. But for the higher Si/Al ratio the (%) conversion decreased with duration of reaction [18].

The principal differences between γ-Al$_2$O$_3$ and ZSM-5 catalysts are in the type and strength of acid sites which cause the difference in characteristics of dehydration products. Some coking took place on both the catalyst while performing the dehydration reactions, but the difference in measured weights of the catalyst before loading and after 20 hours of experimental run was almost negligible.

Table 2.2: Effect of catalyst, reaction time and temperature on dehydration products from ABE mixture

Expt. No.	Feed Mass flow rate (g/min)	Feed WHST* ($\frac{g}{g/h}$)	Catalyst	Temp (°C)	Liquid product					Gas product				
					Flow rate (measured) g/min		TOC Aq. ph. (ppm)	HHV (kJ/g)		Flow Rate (Calculated by subtraction) (g/m)	Composition (GC analysis) (mol%)			
					Org. liq.	Aq. liq.		Org. liq.	Aq. liq.		butene and isomers	CO_2	C_2-C_3	C_5-C_6
1	0.80	0.22	γ-Al_2O_3	400	0.280	0.165	185,784	39.1	3.0	0.36	63.7	7.5	6.3	22.5
2	0.80	0.22	γ-Al_2O_3	500	0.230	0.164	219,921	30.3		0.41	57.0	10.1	15.8	17.1
3	0.80	0.22	γ-Al_2O_3	600	0.008	0.072	34,752	37.2		0.72	7.70	47.3	28.2	16.9
4	0.08	2.17	γ-Al_2O_3	400	0.003	0.005	27,750	42.5		0.07	25.0	63.0	12.0	1.23
5	0.80	0.06	ZSM-5	400	0.022	0.27	265,789	26.4	7.5	0.51	69.0	4.0	0.8	26.2
6	0.08	0.60	ZSM-5	400		0.028	290,716		9.9	0.05	39.5	38.0	2.0	20.3
7	0.08	0.60	ZSM-5	500		0.033	335,325		10.4	0.05	60.0	11.6	3.0	25.7
8	0.08	0.60	ZSM-5	600		0.005	323,740		10.3	0.08	28.6	29.0	8.7	33.7

*Weight hourly space time, WHST = $\frac{Mass\ of\ catalyst\ loaded\ (g)}{Mass\ flow\ rate\ of\ ABE\ mixture\ (\frac{g}{h})}$

Table 2.3: Yield of 'hydrocarbon' in gas and in liquid organic product phases of γ-Al_2O_3 catalyzed dehydration of ABE Mixture

Expt. No.	Temp (°C)	Feed flow rate (g/min)	Feed HHV (kJ/g)	Energy flow in feed (kJ/min)	Liquid organic product flow rate (g/min)	HHV of organic liquid (kJ/g)	Energy flow out organic liquid (kJ/min)	Gas flow rate (cc/min)	Gas Density* (g/cc)	Gas mass flow rate (g/min)		Energy flow out as butene gas (kJ/min)
										butene	CO_2	
1	400	0.80	32.2	25.76	0.280	39.1	10.95	140	1-Butene:	0.242	0.020	11.70
2	500	0.80	32.2	25.76	0.230	30.3	6.06	174	2.72x 10^{-3}	0.270	0.033	13.05
3	600	0.80	32.2	25.76	0.008	37.2	0.30	141	CO_2:	0.003	0.125	0.14
4	400	0.08	32.2	2.57	0.003	42.5	0.13	6.81	1.87x 10^{-3}	0.005	0.008	0.24

*Gas density data are taken from literature 1.013 bar pressure and 15°C temperature

Residence time (WHST) of the reactant with the catalyst plays a major role in determining product characteristics (Table 2.2). In the case of γ-Al₂O₃, lowering the space velocity by 10 folds causes the HHV of the organic liquid product to increase but the production rate of organic liquid decreases compared to the aqueous liquid. That implies that a high amount of the light hydrocarbons were produced which went in the gas product. The concentration of 1-butene and isomers decreased as more acetone conversion took place to generate more CO_2 gas. On the other hand for ZSM-5 catalyst, mostly aqueous phase of liquid product was found. For a lower WHST a minimal amount (8 wt.%) of total liquid product was generated which went in the organic phase. The heating value of the liquid product was low for ZSM-5 catalyzed dehydration as most of the organic carbon went in the gas phase in the form of light hydrocarbons as 1-butene and its isomers.

In Table 2.2, experiment number 5 and 6 compare the products from dehydration using ZSM-5 at 400°C. It was found that on zeolite at low space time (0.06 h) a small amount of organic liquid product was produced but at ten-fold higher space time (0.6 h), only aqueous phase of liquid product was found. Also CO_2 production increased at the higher space time. This implies that, at the higher space time ZSM-5 is converting the ABE mixture mostly to light hydrocarbon and CO_2.

In Table 2.3, the distribution of hydrocarbon yield and energy flow of each stream i.e. feed, organic liquid product and butenes and its isomers in gas product stream are shown for different operating temperatures and feed flow rate in γ-Al₂O₃ catalyzed deoxygenation process. Comparing the energy distribution and hydrocarbon yield data it was found that at 400°C and 0.8 g/min feed flow rate high energy flow is coming out in terms of organic liquid hydrocarbon and butene and isomers in the gas phase product compared to at the other operating conditions. At the above mentioned temperature and

feed flow rate, yield of hydrocarbon in the organic liquid product phase is 35 wt.% and the yield of butenes and its isomers is 30.2 wt.%, and corresponding energy yields are 34% and 36%, respectively. The energy flow associated with lighter hydrocarbon (C_2 to C_3) product stream is not shown here.

As a goal toward producing gasoline, jet fuel or diesel, if a high energy content product is obtained from the first step of conversion (i.e., dehydration), it should be economically attractive. In the second step, the gaseous unsaturated hydrocarbons are oligomerized to liquid fuels.

2.6. Conclusion

Catalytic dehydration of the ABE mixture reveals an interesting synergy of the reacting components. The product from ABE mixture is not a simple sum of the products from the individual feed components, acetone, 1-butanol, and ethanol. The inter-reactivity of the components contributed to a liquid product with a high heating value.

The γ-Al_2O_3 catalyzed dehydration produces an organic liquid phase containing C_5 to C_{16} hydrocarbons along with an aqueous phase. But the ZSM-5 catalyzed dehydration produces only one liquid phase containing light hydrocarbons at low heating value. The gas phase product contains mostly butane and its isomers and CO_2, with varying composition depending on the reaction temperature and time. Out of the conditions studied here, γ-Al_2O_3 catalyzed dehydration at 400°C produced the highest amount of useful hydrocarbon products in terms of butene and high HHV organic liquid. At this operating condition more carbon is retained as hydrocarbon and oxygen is removed mostly as water. On the other hand, oxygen removal in ZSM-5 catalyzed dehydration

took place by the production of a higher amount of CO_2 which causes a loss of carbon generating low energy content products.

References

[1]   R. B. Gupta and A. Demirbas, *Gasoline, Diesel and Ethanol Biofuels from Grasses and Plants*. Cambridge University Press, 2010, pp. 140–157.

[2]   N. Qureshi, B. C. Saha, R. E. Hector, B. Dien, S. Hughes, S. Liu, L. Iten, M. J. Bowman, G. Sarath, and M. a. Cotta, "Production of butanol (a biofuel) from agricultural residues: Part II – Use of corn stover and switchgrass hydrolysates☆," *Biomass and Bioenergy*, vol. 34, no. 4, pp. 566–571, Apr. 2010.

[3]   N. Qureshi and T. Ezeji, "Butanol,'a superior biofuel'production from agricultural residues (renewable biomass): recent progress in technology," *Biofuels, Bioprod. Biorefining*, vol. 2, no. 4, pp. 319–330, 2008.

[4]   C. Weber, A. Farwick, F. Benisch, D. Brat, H. Dietz, T. Subtil, and E. Boles, "Trends and challenges in the microbial production of lignocellulosic bioalcohol fuels.," *Appl. Microbiol. Biotechnol.*, vol. 87, no. 4, pp. 1303–1315, Jul. 2010.

[5]   D. T. Jones and D. R. Woods, "Acetone-butanol fermentation revisited.," *Microbiol. Rev.*, vol. 50, no. 4, pp. 484–524, Dec. 1986.

[6]   P. H. Pfromm, V. Amanor-Boadu, R. Nelson, P. Vadlani, and R. Madl, "Bio-butanol vs. bio-ethanol: A technical and economic assessment for corn and switchgrass fermented by yeast or Clostridium acetobutylicum," *Biomass and Bioenergy*, vol. 34, no. 4, pp. 515–524, Apr. 2010.

[7]   K. Kraemer, A. Harwardt, and R. Bronneberg, "Separation of butanol from acetone-butanol-ethanol fermentation by a hybrid extraction-distillation process," in *20th European Simposium on Computer Aided Process Engineering*, 2010, no. iv.

[8]   T. C. Ezeji, N. Qureshi, and H. P. Blaschek, "Bioproduction of butanol from biomass: from genes to bioreactors.," *Curr. Opin. Biotechnol.*, vol. 18, no. 3, pp. 220–227, Jun. 2007.

[9]   I. Maddox and N. Qureshi, "Production of acetone-butanol-ethanol from concentrated substrate using< i> clostridium acetobutylicum</i> in an integrated fermentation-product removal process," *Process Biochem.*, vol. 30, no. 3, pp. 209–215, 1995.

[10]   T. C. Ezeji, N. Qureshi, and H. P. Blaschek, "Acetone butanol ethanol (ABE) production from concentrated substrate: reduction in substrate inhibition by fed-batch technique and product inhibition by gas stripping.," *Appl. Microbiol. Biotechnol.*, vol. 63, no. 6, pp. 653–658, Feb. 2004.

[11]   M. E. Wright, B. Harvey, and R. L. Quintana, "Creating new NAVY fuels from biobutanol," *ACS , Div Fuel Chem*, vol. 53, no. 1, pp. 252–253, 2008.

[12]   M. E. Wright, B. G. Harvey, and R. L. Quintana, "Highly Efficient Zirconium-Catalyzed Batch Conversion of 1-Butene : A New Route to Jet Fuels," *Energy & Fuels*, vol. 10, no. 12, pp. 3299–3302, 2008.

[13]   R. J. J. Nel and A. de Klerk, "Fischer−Tropsch Aqueous Phase Refining by Catalytic Alcohol Dehydration," *Ind. Eng. Chem. Res.*, vol. 46, no. 11, pp. 3558–3565, May 2007.

[14]   P. Berteau and M. Ruwet, "Reaction Pathways in 1-Butanol Dehydration on γ-Alumina," *Bull. Soc. Chim. Belg.*, vol. 94, no. 11, pp. 859–868, 1985.

[15]   H. ARAI, "Ethanol dehydration on alumina catalysts I. The thermal desorption of surface compounds," *J. Catal.*, vol. 9, no. 146–153, 1967.

[16]   M. Lu, G. Xiong, H. Zhao, and W. Cui, "Dehydration of 1 -butanol over y-AlTO catalytic membrane," *Science (80-.).*, vol. 25, pp. 339–344, 1995.

[17]   V. Macho, E. Jurecekova, and J. Hudec, "Dehydration of C4 alkanols conjugated with a positional and skeletal isomerisation of the formed C4 alkenes," *Appl. Catal. A*, vol. 214, pp. 251–257, 2001.

[18]   S. Setiadi, "Catalytic Conversion of Acetone to Monoaromatic Chemicals using HZSM-5," *Int. J. Eng. Technol.*, vol. 11, no. April, pp. 72–79, 2011.

[19]   H. Pines, "Alumina : Catalyst and Support. I. Alumina, its intrinsic acidity and catalytic activity," *J. Am. Chem. Soc.*, vol. 82, no. 10, pp. 2471–2483, 1960.

[20]   T. Zaki, "Catalytic dehydration of ethanol using transition metal oxide catalysts.," *J. Colloid Interface Sci.*, vol. 284, no. 2, pp. 606–13, Apr. 2005.

[21]   B. G. Harvey and H. a. Meylemans, "The role of butanol in the development of sustainable fuel technologies," *J. Chem. Technol. Biotechnol.*, vol. 86, no. 1, pp. 2–9, Jan. 2011.

[22]   E. Costa, J. Aguado, and G. Ovejero, "Conversion of n-butanol-acetone mixtures to C1-C10 hydrocarbons on HZSM-5 type zeolites," *Ind. Eng. Chem. Res.*, vol. 31, no. 4, pp. 1021–1025, 1992.

[23]   J. Hutchings, P. Johnston, and D. F. Lee, "Acetone conversion to isobutene in high selectivity using zeolite catalyst," *Catal. Letters*, vol. 21, pp. 49–53, 1993.

[24]   H. Arai, "Ethanol dehydration on alumina catalysts I. The thermal desorption of surface compounds," *J. Catal.*, vol. 9, no. 2, pp. 146–153, Oct. 1967.

[25]   J. D. Butler, "Kinetics of the catalytic dehydration of ethanol over alumina," *J. Chem. Soc. B Phys. Org.*, p. 905, 1968.

[26] B. G. Harvey and M. E. Wright, "The Oligomerization of 1-Butene ; A New Approach To Full Performance Jet Fuels."

[27] R. J. Quann, L. A. Green, S. A. Tabak, and F. J. Krambeck, "Chemistry of olefin oligomerization over ZSM-5 catalyst," *Ind. Eng. Chem. Res.*, vol. 27, no. 4, pp. 565–570, 1988.

[28] A. de Klerk, D. O. Leckel, and N. M. Prinsloo, "Butene Oligomerization by Phosphoric Acid Catalysis: Separating the Effects of Temperature and Catalyst Hydration on Product Selectivity," *Ind. Eng. Chem. Res.*, vol. 45, no. 18, pp. 6127–6136, Aug. 2006.

[29] H. Pines, "Alumina: Catalyst and Support. IX. 1 The Alumina Catalyzed Dehydration of Alcohols2, 3," *J. Am. Chem. Soc.*, vol. 173, no. 4, pp. 1956–1957, 1961.

[30] S. S. Ashour, "Factors affecting the activity and selectivity of alumina catalysts in the dehydration of 1-butanol," *Adsorpt. Sci. Technol.*, vol. 22, no. 6, pp. 475–483, 2004.

[31] H. Solomon and H. Bliss, "Catalysis of alcohol and ether dehydration on gamma-alumina," *Ind. Eng. Chem. Res.*, vol. 6, no. 3, pp. 325–333, 1967.

[32] S. Kumar, "Hydrothermal treatment for biofuels: Lignocellulosic biomass to bioethanol, biocrude, and biochar," Auburn University, 2010.

[33] D. Coster, a. L. Blumenfeld, and J. J. Fripiat, "Lewis Acid Sites and Surface Aluminum in Aluminas and Zeolites: A High-Resolution NMR Study," *J. Phys. Chem.*, vol. 98, no. 24, pp. 6201–6211, Jun. 1994.

[34] M. Digne, "Use of DFT to achieve a rational understanding of acid?basic properties of ?-alumina surfaces," *J. Catal.*, vol. 226, no. 1, pp. 54–68, Aug. 2004.

[35] L. Shirazi, E. Jamshidi, and M. R. Ghasemi, "The effect of Si/Al ratio of ZSM-5 zeolite on its morphology, acidity and crystal size," *Cryst. Res. Technol.*, vol. 43, no. 12, pp. 1300–1306, Dec. 2008.

Chapter 3

Separation of ABE (acetone, n-butanol, ethanol) mixture from dilute model aqueous solution

3.1 Introduction

Separation of ABE from the very dilute aqueous solution of water coming out as the fermentation product from the bioreactor has always been a big challenge since the establishment of ABE fermentation process. The highest concentration of ABE produced by genetically modified clostridium strain is found to be 8.2 g/l acetone, 17.6 g/l n-butanol and 2.2 g/l ethanol [1]. Many research works are going on for increasing the yield of ABE and also for selective production of n-butanol by improvement in production techniques and genetic modification of the strains [2],[3],[4],[5]. Separation of n-butanol from the fermentation broth is also very important not only because of the low yield but also due to the toxic effect it has on the fermentation process and on the microbial catalysts. That is why selective separation of n-butanol has been a matter of research for quite some time since the ABE fermentation process began. In this work, one of the main goals was to treat the ABE as a mixture from dilute simulated aqueous solution having similar concentration of the fermentation broth and deoxygenate all the three components i.e. acetone, n-butanol and ethanol, so that the energy and other resources required to separate n-butanol to use it as the only fuel component can be saved in this way. All the hydrocarbons being produced in the fermentation process can

be utilized in forms of fuel only. Though the catalytic ABE de-oxygenation process shown in the previous used model ABE mixture with the similar wt.% ratio as it is produced in the fermentation process, but according to the proposed process scheme the ABE solution coming out in the fermentation broth will be fed to the de-oxygenation unit after separation, So separation of the ABE is a very vital part of this project. Many research groups and also government organizations like USDA and DoE have worked and still working on this separation process of ABE from the dilute aqueous solution. The principal separation techniques or unit operations which are being studies are as follows:

1. Distillation
2. Adsorption and desorption
3. Membrane separation
4. Pervaporation
5. Perstraction
6. Liquid- liquid extraction
7. Supercritical fluid extraction

A summary of the merits and demerits and yield of these separation processes is being discussed here.

3.1.1 Distillation

Separation of ABE components from water by the establishment of an external distillation column is common as a chemical separation process. But due to its high energy requirement it has not been established as an attractive industrial process for its lower economic feasibility. In one study it was found that for steam stripping distillation process 24314 kilojoules of energy is required per kilogram wt. of n-butanol recovered which is the highest among all other possible separation processes [6]. To make the distillation process a feasible one it has to be coupled up with another separation

mechanism. Hybrid separation processes of distillation and solvent extraction together mesitylene leads to less energy consumptions in the hybrid process. This hybrid distillation process coupled with solvent extraction decreases the energy consumption from around 20 MJ for pure distillation process to 5.7 MJ for the hybrid process per kg of butanol recovery. Other mixture of solvents like oleyl and decane mixture have also been tried for this purpose to improve the efficiency of separation by pure distillation [8].
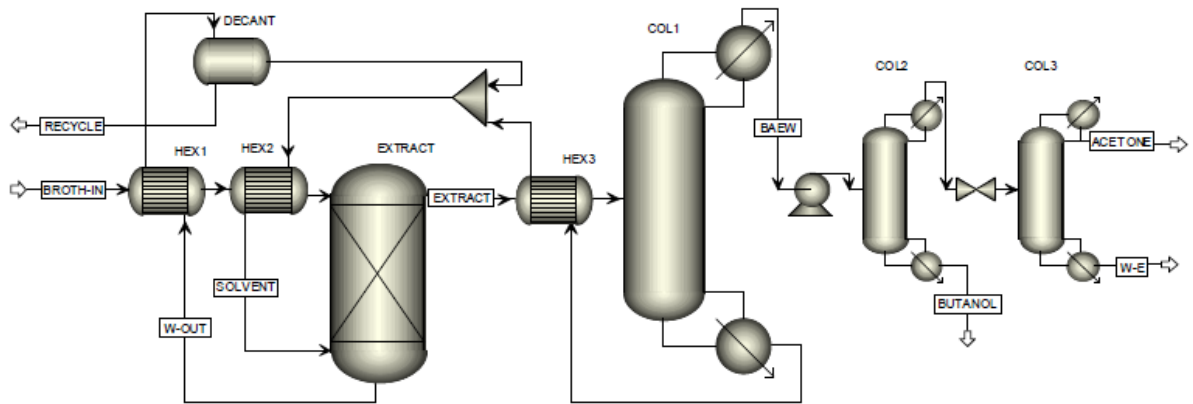
Figure 3.1: Process flow-sheet for hybrid extraction-distillation process [7]

3.1.2 Adsorption and desorption

Adsorption

Adsorption is usually a convenient separation process for many chemicals as adsorbent materials are usually cheap, selective to specific components and regeneration and reuse if possible. But the regeneration process by desorption and chemical recovery usually takes place at high temperature which is again an energy intensive process involving higher cost. For ABE extraction silicates, zeolites, activated carbon polymeric resins can be used as adsorbent materials. Both packed bed and fluidized bed adsorptions are possible. Packed bed adsorption process often faces with the problems like high pressure drop, fouling, channeling etc. Again fluidized bed adsorption process

has increased surface area available for the same particle size but continuous energy source is needed to keep the bed fluidized. Again chance of entrainment of particles is also possible in continuous flow adsorbers. Zeolites consisting of mainly silicates have been proven good for adsorption of ABE. Comparing three different types of zeolites, Zeolite Y type with SiO_2/Al_2O_3 ratio 80 found to have the highest adsorption capacity whereas Zeolite ZSM-5 with SiO_2/Al_2O_3 ratio 280 showed the highest affinity for n-butanol at aqueous n-butanol concentration below 2 gL^{-1}[9]. In the ABE separation process the initial concentration of n-butanol is almost 20 gL^{-1} which is much higher than the 2 gl^{-1} working concentration mentioned in that research work [9]. It has also been showed that ZSM-5 has the highest affinity towards n-butanol among the other components of the ABE mixture and it also has very high affinity towards the butyric acid of the fermentation broth which is not preferred to be removed. Because of the hydrophobicity of zeolites, adsorption of water is very low at all the temperatures. For desorption purpose and ABE recovery CO_2 can be used as a displacement agent. For desorption of zeolites energy required is in the range of 1000 to 1200 kJ per kg of n-butanol recovered. The desorption rate varies for different zeolites with different SiO_2/Al_2O_3 ratio and usually with higher temperature higher desorption rate is achieved. The heat of desorption of n-butanol is higher than heat of evaporation of pure n-butanol for zeolites, which makes it an energy intensive process [10]. From another study it was found that using ZSM-5 zeolites as adsorbent, fractions of water and ethanol can be

separated at 50°C and n-butanol fraction is separated at around 150°C. N-butanol concentration could be increased from 1.28 wt.% to 84.3 wt.% [11].
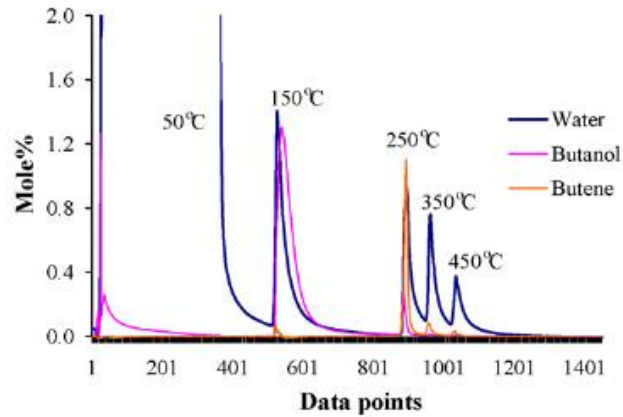
Figure 3.2: Desorbed components from ZSM-5, zeolite based with ABE solution (16-24 mesh alumina based extrudates)

Another attractive adsorbent material according to adsorption capacity is the activated charcoal. Comparative study between activated charcoal and silicalites or zeolites showed that silicalite has a n-butanol adsorption capacity 97 mg g^{-1} whereas activated carbon can have n-butanol adsorption capacity as high as 252 mg g^{-1}. But the main adversity of using activated carbon is that the desorption is incomplete and leads to maximum 60% to 85% adsorbed alcohol can be recovered whereas complete recovery can be achieved using the silicalites [6]. Comparative energy balance of the separation processes also shows that separation of n-butanol by the adsorption-desorption process requires the lowest energy compared to the other processes which is around 1948 kcal per kg n-butanol recovered [6].

3.1.3 Membrane separation

Membrane separation process has been studied for the separation of ABE in different ways. Membrane separation is a common process in chemical engineering separation processes and to improve the process efficiency, it has been tried combine other unit operations with the regular membrane for effective separation. Among the membrane separation processes pervaporation, perstraction, reverse osmosis and microfiltration processes can be mentioned as probable separation techniques for ABE separation. From these, pervaporation and perstraction processes have drawn more interest of the researchers because of their potentials in ABE separation. Composite membranes are also used for separation purpose. In a study a silicone-silicalite-1 composite membrane was used to recover ABE from model solutions. The synthesized composite membrane mentioned above has a n-butanol selectivity of 100-108 and a flux of 89 g/m^2 at feed n-butanol concentrations at feed n-butanol concentrations but elevated temperature is needed for desorption of n-butanol from the silicalite which will create a process economics problem [12].

3.1.4 Pervaporation

In the pervaporation process separation takes place based on the concentration gradient of the solute over the membrane. Due to the partial pressure difference on both sides of the membrane the solute diffuses through it and the pressure difference is created usually by creating vacuum in one side of the membrane or putting a sweep gas but the vacuum induces better mass flux through the membrane. FOR separation of ABE from aqueous solution, the alcohol flux along the membrane will decrease as concentration of the feed solution decreases [8]. Characteristics of membrane, its thick ness, feed concentration, operating temperature play important role in the separation process [13]. Performance of silicone or silicate-1/PDMS hybrid membranes has been

studied for pervaporation separation of ABE. Competing adsorption of the ABE components takes place on the membranes. N-butanol could be preferentially adsorbed on silicate-1 but acetone hinders n-butanol adsorption whereas ethanol promotes n-butanol transport through the membrane. Also the increasing vacuum pressure seems to have adverse effect on the permeate fluxes [14]. Another study on integrated fermentation process with silicone membrane pervaporation the product concentration of n-butanol could be increased form 24.2 g/L to 51.5 g/L. The total productivity of fermentation product also found to be increased as n-butanol toxicity could be reduced by maintaining lower concentration due to integrated separation and also as pervaporation has no adverse effect on the microbial strain [15]. Pervaporation can also be applied along with ionic liquid separation method which could also be called Supported Ionic Liquid Membrane (SILM) technology where nylon and polypropylene have been tested as support and tris trifluorophosphate as ionic liquid and silicone layer membrane. It was found in the study that application of ionic liquid in pervaporation increased the permeability of the membrane by three times and also with increasing Ionic liquid content , mass flux seemed to increase through the membrane with n-butanol concentration change form 5 wt.% to 55 wt.% [16].

In pervaporation separation, high selectivities and high flux values could be achieved at 80°C and high sweep gas flow rate which will cost higher cost for energy consumption. Again from the comparative energy study of the separation processes it is said that pervaporation process is also an energy intensive process requiring 13839 kJ energy per kg of n-butanol recovered[6]. Pervaporation is selective and simple to operate but the achievable flux through the membrane is generally and other problems like clogging and fouling of the membrane can decrease the efficiency of the separation significantly [17]

3.1.5 Perstraction

Perstraction is a membrane assisted fluid extraction separation process. In a study in Auburn University by Dr. Y.Y. Lee silicone tubing was used as the separation membrane and the membrane was immersed in several extractants like oleyl alcohol, polypropylene glycol, dodecanol, methyl oleate etc. one at a time. The silicone rubber tubing has a high permeability for n-butanol and acetone, autoclavability, biological inertness and compatibility with many organic solvents. Also by perstraction extractant loss can be reduced compared to the liquid-liquid extraction process. The toxic effect of extractant on the fermentation can also be reduced. The total solvent yield increased by 23% in the fed batch process compared to the regular batch process of fermentation [18].
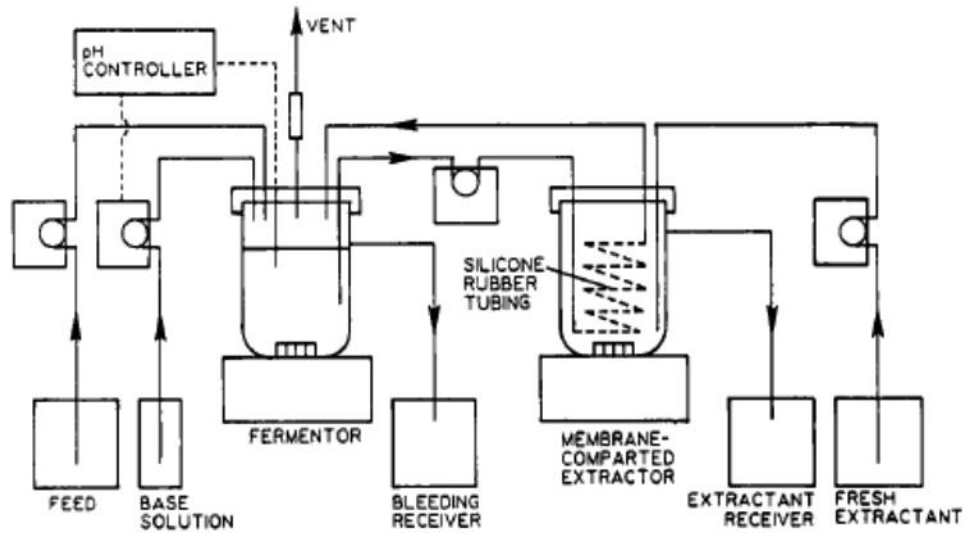
Figure 3.3: Schematic diagram of the experimental set up of fed batch fermentation coupled with membrane assisted extraction [18]

Another study showed the perstraction separation process using hollow fiber modules in the extraction column and oleyl alcohol as the extractant. The aqueous phase and organic phase are considered to be well mixed in the individual loops of the membrane module. The mass transfer coefficient for that specific membrane system was found to be k_m =5.7x 10^{-7} with a membrane area of 840 m^2. This high membrane area requirement causes problem while designing a separation unit in an industrial scale. On the other hand designing a liquid-liquid extraction unit can be tedious but may have a more reasonable size for industrial establishment [8].

In another study of ABE fermentation from whey permeate medium supplemented by lactose and coupled with perstarction separation process using oleyl alcohol and as extractant and silicate membrane of 0.1130 m^2 were suggested. In this process it was shown that removal of ABE by perstraction had a higher rate than of ABE production and the maximum concentration of ABE in the extract phase was 9.75 gL^{-1} compared to the productivity from lactose fermentation 0.21 $gL^{-1}h^{-1}$. It was also found that recovery of ABE from the extractant was more economical than recovery from the fermentation broth [19]. But in this perstraction separation process, the acid concentration in the fermentation broth was found to be significantly low compared to other separation processes which have a positive effect in reducing the product inhibition.

3.1.6 Liquid-liquid extraction

Production of ABE with integrated product removal process by liquid-liquid extraction using different solvents like oleyl alcohol, benzoyl benzoate, dibutyl terephthalate etc. has been studied in several research works. Among other extractants, oleyl alcohols have been taken as the standard one in different studies. Though it was found that productivity decreases a bit due to the integrated product removal by LLE, but considering all other aspects like energy usage, it can be considered as one of the best

appropriate separation methods for ABE. It has almost similar product recovery as pervaporation and superior to distillation considering the technical difficulties the stripping process involves [20].
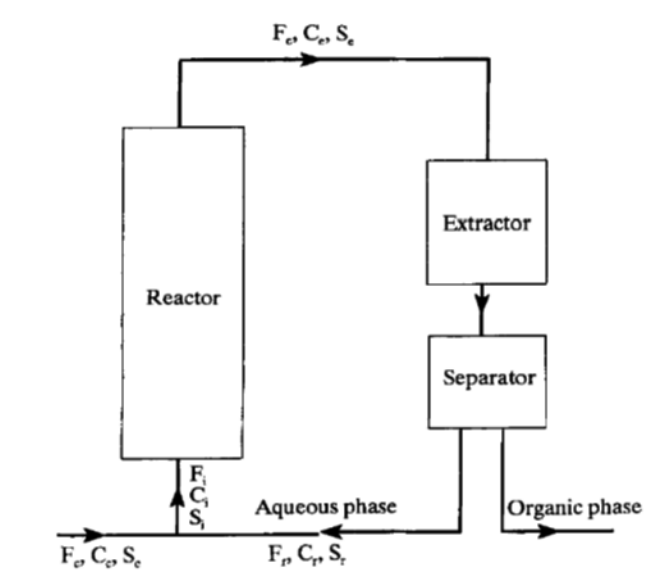
Figure 3.4: Schematic diagram of an experimental setup for extraction system

By continuous removal of toxic n-butanol for the fermentation process by a countercurrent flow of oleyl alcohol in an extraction column enables the process to ferment a concentrated feed solution of 300 g/L glucose producing 1.0 g/L h n-butanol which 70% higher than normal batch fermentation process [21]. In another study soybean derived biodiesel has been used as the extractant of n-butanol from n-butanol, 1,3 propanediol and ethanol mixture. The partition coefficient for n-butanol in biodiesel was determined to be 0.91. Though the partition coefficient is lower compared to oleyl alcohol as extractant for n-butanol, extraction from a system where biodiesel derived glycerol is fermented to produce n-butanol, biodiesel can be used as it has no toxic effect on the system and the microbial culture [22].

Another comparative study of three different extractants for n-butanol which are oleyl alcohol, 2-ethyl-1-hexanol crude palm oil ester showed that changing the volume ratio of fermentation broth to extractant by increasing the extractant amount, increases the n-butanol productivity. 2-ethyl-1-hexanol was found to show the highest partition coefficient among the other two at a temperature range of 10°C to 70°C. The partition coefficient was in the range of 7 to 10 which is pretty high [23]. 100% recovery of the solute is very difficult by LLE, so several additional approaches have been taken. Membrane assisted liquid-liquid extractions, which are also called perstraction and supercritical fluid extraction processes, are couple of advanced separation processes to increase the product recovery. The energy requirement in the regular liquid-liquid extraction process is around 8900 kJ per kg n-butanol recovered which is quite low compared to the stripping and pervaporation processes [6]. The main problem for the extraction separation processes is that the high capacity extractants or solvents have low selectivity to the solute whereas the low capacity solvents are selective enough. But in most of the cases, these low selectivity solvents are least toxic for ABE separation [24]. So selection of appropriate solvents having moderate partition coefficient, high selectivity and low toxic effect to the microbial strain is very important for an efficient LLE process.

3.1.7 Supercritical fluid extraction

This separation process has the same methodology as liquid-liquid extraction. The only exception it has is that it utilizes the supercritical properties of the fluid. Supercritical CO_2 at 100 bar and 40°C was used as a solvent in a study and over 99.7% of initial n-butanol amount was removed from the feed stream of 5 wt.% 1-n-butanol in a mechanically agitated extraction column. The optimized solvent to feed ratio was 2.7 [25]. Compared to regular liquid- liquid extraction process, the above mentioned work showed better efficiency and productivity,
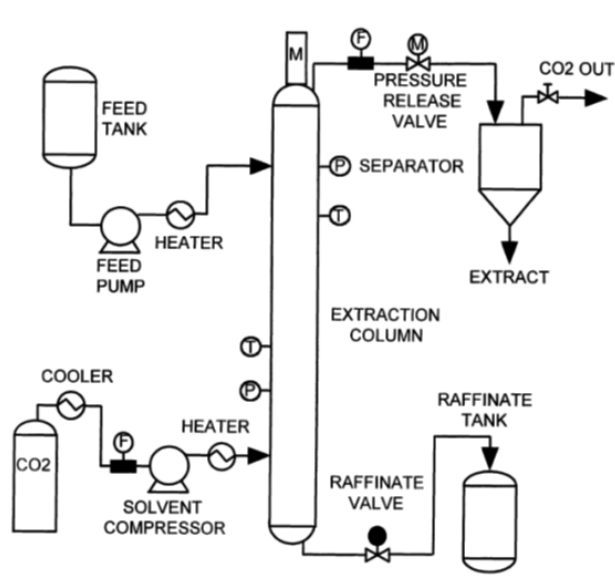
Figure 3.5: Schematic diagram of experimental setup for supercritical fluid extraction

This is a very high pressure system and the separator column had the maximum pressure up to 400 bars which may increase the cost of the process quite a bit.

In another study supercritical butene has been used for extraction of 5wt% secondary n-butanol solution critical temperature and pressure of butene is 146.4°C and 39.7 atm respectively. The experiments were done at both supercritical and subcritical conditions by varying temperature and pressure of the extraction process. It was found that in supercritical conditions buetne solubility in water is higher but if residence time is increased enough to reach the thermodynamic equilibrium, similar extraction level was found with both supercritical and subcritical butene [26]. So due to the cost of the supercritical condition and not much additional extraction efficiency offered by the process, it has not been considered as a very popular method for ABE separation. Comparison of all the separation processes mentioned here showed that every process

has its own advantage and disadvantages. But considering three main criteria which are, the separation capacity or efficiency, industrial design feasibility and economics due to energy requirement, it can be said that liquid- liquid extraction can be an attractive option for the separation of ABE. Again another approach can be coupling two processes and for that adsorption coupled with liquid-liquid extraction can be a probable method in respect of all the three criteria mentioned above.

3.2 Proposed process of ABE separation by liquid-liquid extraction using butene as extractant

In the previous chapter where the ABE deoxygenation step was discussed thoroughly, It was shown that a good amount butene and its isomers are getting produced in the gas phase of the deoxygenation product which is in the range of 60 to 70 vol% of the gaseous phase product and yield of around 27wt% based on the mass flow rate of ABE feed. A part of this butene produced can be used as the extractant in a liquid- liquid extractor which can be placed right after the bioreactor in the process flow (Figure 3.6).
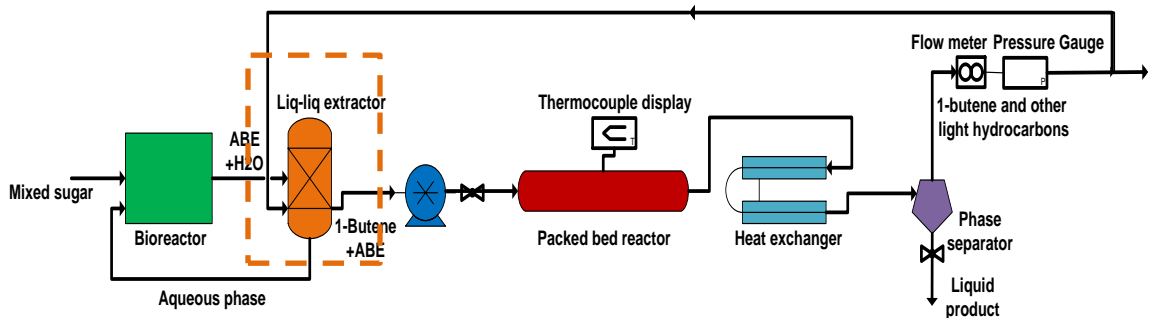
Figure 3.6: Schematic diagram of the process flow of ABE production extraction and deoxygenation

3.3 Two-step separation approach

One of the main goals of the project is to develop an efficient process where very minimal hydrocarbon loss is achieved as from current fermentation technology ABE yield is still very low. So to improve the efficiency and feasibility of the process, it has to be ensured that minimal loss of ABE takes place during the de-oxygenation and further processing steps. The higher the separation of ABE from the fermentation broth can be achieved the lower the energy requirement and higher the yield of higher hydrocarbon will be achieved based on the studies and previous research works mentioned before, it can be seen that two step approach for separation of ABE will be more efficient if the total energy requirement for two steps does not go very high compared to the energy required from one step to get the same yield. Comparing all the current technologies for separation a new combination of separation steps is being proposed in this work and the unit operations are selected based on several major criteria which is as follows:

- Yield of ABE form separation

- Selectivity of the ABE in the specific separation media used

- Total energy consumption in the process of separation and recovery of ABE

- Operational simplicity on basis of industrial scale design

- Economical feasibility

Based on the above mentioned criteria liquid- liquid extraction followed by adsorption is proposed as the best option. Specially these two processes are the least energy consuming processes among the others which are 8182 kJ/ kg and 8900 kJ/kg butanol recovered for adsorption and LLE separation processes respectively [27] . Also on the basis of selectivity and separation yield both of these processes has moderate to good efficiency. From liquid- liquid extraction experiments and also from previous studies it

could be seen that from liquid- liquid extraction process 100% separation of ABE has not been possible, whereas adsorption and desorption has shown 100% separation of the process but it has some other drawbacks like regeneration of the adsorption bed and recovery by desorption which have been discussed before. So to offset the drawbacks of each process and to find out a low energy but high yield separation process for ABE, this two-step approach is expected to contribute largely. Again as extractant, the butene gas generated from the ABE deoxygenating step will be used, which makes this integrated process more energy efficient and cost effective. As adsorption material in the adsorber column, activated carbon will be used, which is also not expensive and has proven results showing good adsorption of ABE [6]. Also for desorption process for the recovery of the adsorbed ABE a fraction of ABE de-oxygenation product gas will be used so that the heat energy required for desorption process can be reduced.

In the second part of this work, to measure the adsorption and extraction efficiency for separation of ABE mixture from aqueous phase a simplified set up is made for a batch separation process. Percent adsorption and percent extraction are measured separately for each of the component of ABE mixture using activated charcoal for adsorption surface and then pure 1-butene gas pressurized to be in the liquid form as the extractant to recover the adsorbed ABE components from activated charcoal in a single step. As liquid-butene extraction is the less efficient part of the whole separation process, to increase extraction efficiency, increased extraction temperature and increased extract concentration are also studied.

3.4 Objectives

Integrating the ABE catalytic dehydration process and separation process from fermentation broth by using the dehydration by-product 1-butene in a liquid-liquid or liquid- solid extraction

(I)   Estimating the liquid-liquid extraction efficiency and distribution coefficient between liquid-1 butene phase and ABE aqueous solution phase

(II)   Comparing efficiency of extraction and percent recovery of each individual component acetone, n-butanol, ethanol and butyric acid.

(III) Determining the effect of temperature and initial concentration of solute on the liquid-solid extraction process with activated charcoal and liquid 1 butene.

(IV)   Comparing the distribution coefficients between the liquid- liquid and liquid-solid extraction with 1-butene as the extractant.

(V)   Comparing percent recovery in extraction with 1-butene of each individual component and components in ABE mixture.

3.5 Experimental section

3.5.1 Materials

ACS grade n-butanol (99.4%), acetone (99.9%), ethanol (99.98%) were used in this study. ABE mixture is prepared as a mixture of n-butanol (62.9 wt.%), acetone (29.3 wt.%) and ethanol (7.8 wt.%). 99.5% 1-butene gas cylinder (Airgas, Opelika, AL), untreated, granular activated charcoal of 408 mesh size (Sigma-Aldrich, St. Louis, MO).

3.5.2 Apparatus and procedure

For experimental purpose the extraction process was done with individual components i.e. n-butanol solution, acetone solution and ethanol solution and also with the ABE mixture model solution. The concentration of each of the solutions has been taken from that of the standard fermentation broth dilute solution having the concentration of 17.6 g/L n-butanol, 8.2 g/L acetone and 2.2 g/L ethanol in water [1]

To determine the efficiency and capacity of buetne as an extractant for ABE separation, the partition coeffcient of each of the components of ABE has been experimentally

determined between the two phases: the organic phase (butene phase) and the aqueous phase. Pure butene gas was used for experimental purpose directly from the speciality gas cylinder. A high pressure stainless steel vessel of 46.26 ml volume with a glass window was used as the extraction unit. The extraction was done in a batch process and the feed solution was preloaded to the vessel. 1-butene gas was fed directly from the cylinder through an input connection valve in the middle of the vessel. The inlet temperature was maintained at 8 to 10 °C by immersing the inlet valve in ice water. All the outlet valves were closed butene was being fed for 45 mins. The liquid butene level could be seen increasing through the glass window if the vessel and within 35 mins it reached the top of the level. But butene was fed extra 10 minutes after that to ensure the pressure inside the vessel to be high enough to keep the butene in liquid phase. Inlet pressure of butene from the cylinder was 2.77 bars that is 40.7 psia and the same pressure was maintained during the extraction in the batch process. After filling up liquid butene for 45 mins, it is left for 20 to 24 hours for reaching the equilibrium. In another process, recirculation pump was added to the system so that it takes the liquid solution from the bottom and again puts in from the top of the vessel so that it travles through the organic phase and better contact was achieved by this means. So thermodynamic equilibrium is also achieved quickly.

(a)   (b)
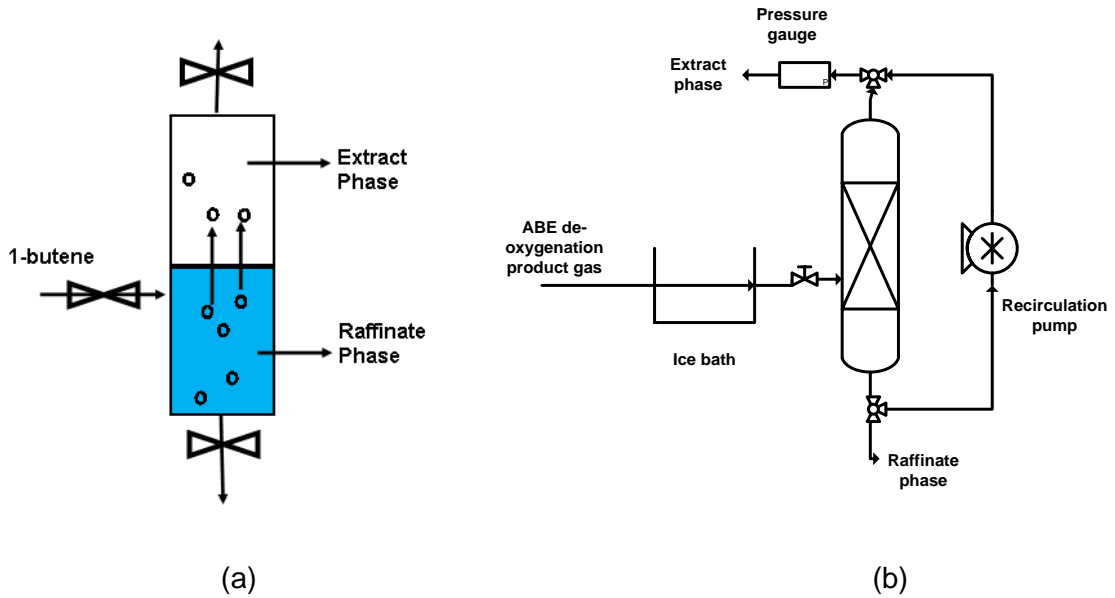
Figure 3.7: Schematic diagram of the experimental setup of liquid -liquid extraction using 1 butene as extractant a) batch extraction process b) setup with recirculation pump
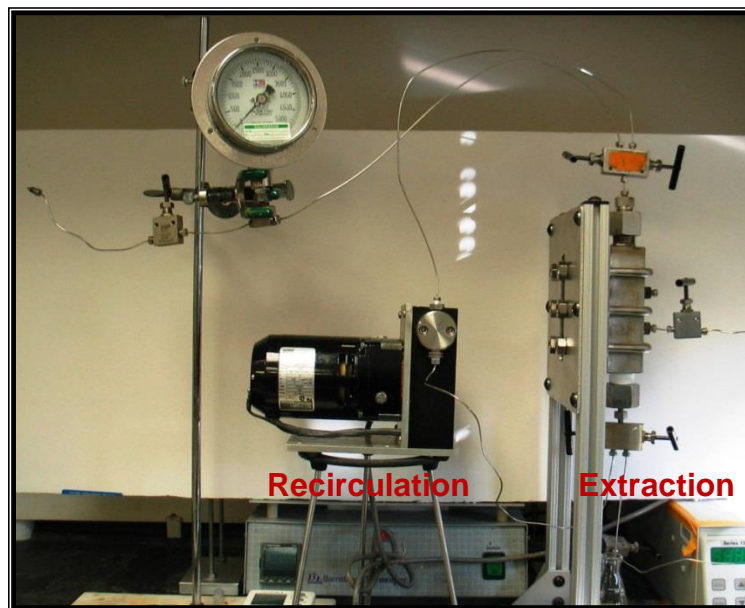
Figure 3.8: Experimental set up for liquid -liquid extraction of ABE using 1-butene (with recirculation system)

Figure 3.9: Extraction vessel and input-output lines for feed and products

For the experiments with two steps separation that is adsorption on activated charcoal followed by liquid-solid extraction with liquid butene, a different experimental setup was used. A HIP steel tube of 10 ml volume and 8 mm inner diameter was used as the extraction vessel closed at both sides with HIP adaptors. At each end of the tube a gate valve was connected. At one end gaseous 1-butene cylinder was connected with 1/16" steel tubing. A pressure gauge from Omega Engineering having a range up to 60 psig was connected to the valve of the other end of the extraction tube. A 2.0 g batch of activated charcoal was loaded in the extraction cylindrical tube with 0.2 g or 0.6 g of acetone, n-butanol, ethanol or butyric acid one component at a time. For temperature control of the extraction process the whole setup was submerged in a steel water bath

and an Isotemp Immersion Circulator (model 730) from Fisher Scientific was connected to the water bath with a mercury thermometer dipped in the water (Figure 3.10 b). The isotemp immersion circulator has an electric heating coil and the heater temperature can be set with a regulator. When the set temperature is reached, it is automatically switched off and again starts up when water tends to cool down. In Figure 3.10 (a) it is shown that 1-butene was fed directly from the cylinder at 25 psig pressure and 0° to 5°C loading temperature maintained by continuous putting ice in the water in the bath where the extraction tube was immersed. When the pressure gauge connected to the extraction vessel reaches 25 psig and stays constant then the 1-butene feed was stopped and the and the system was kept at constant temperature of either 25°C or 60°C for 24 hours extraction time. After 24 hours the extractant liquid has been collected by opening the bottom valve of the cylindrical tube vessel and bubble in 10 ml of distilled water in a vial immersed in ice water bath shown in Figure 3.10 (c).

(a)

(b)

(c)

Figure 3.10: Experimental set-up for liquid solid extraction of ABE components from activated charcoal using 1-butene (a) liquid 1-butene in equilibrium with solid phase of activated charcoal (b) Isotemp Immersion Circulator in the water bath (c) collection of extractant product

3.5.3 Analysis Methods

3.5.3.1 Total organic carbon (TOC) analyzer

The organic carbon content of the liquid product was measured using a TOC analyzer ('TOC-Vcsn',Shimadzu).

3.5.3.2 High Pressure Liquid Chromatography (HPLC) analysis

An HPLC instrument, Waters 600 with a C18 column was used to find the mass fraction of the solute at the extract phase.

3.6 Results and Discussion

3.6.1 Direct liquid-liquid extraction

Individual components of ABE i.e. acetone, n-butanol, ethanol were extracted separately from the dilute model solutions and extracted as a mixture as well. The concentration of the feed solutions was maintained as the same as the fermentation broth concentration of those components individually which are 8.2 g/L acetone, 17.6 g/L n-butanol, 2.2 g/L ethanol [1]. Though the concentration of solutes were different the amount of feed solution and liquid butene extractant are taken almost same for each of the experimental run. The extraction measurement is done in terms of total organic carbon (TOC) content of the feed solution and the raffinate phase.

- 1-Butene loading temperature : 8 to 10 °C
- Operating temperature: 22 °C
- Operating pressure: 40.7 psia or 2.77 bars

Table 3.1: Percent recovery and distribution coefficient from liquid-liquid

extraction between liquid 1-butene phase and aqeous phase

Components	Feed solution	Raffinate phase		Extract phase	Percent Extracted	Distribution coefficient
	ppm	wt. (g)	ppm	wt. (g)	(%)	mol/mol
n-butanol	9400	18.92	6250	17.2	33.7	1.71
acetone	5489	21.98	3895	15.33	24.5	1.45
ethanol	1673	20.4	1608	16.13	3.9	0.41
ABE	14870	20.8	9960	16.01	33	--

A sample calculation for measurement of the distribution coefficient is shown

here:

Water + n-butanol :18.92 g

N-butanol in the solution: 0.331 g

Total volume of the extraction vessel: 46.206 ml

Volume of feed solution loaded: 18.92 ml

So, butene loaded in the extraction vessel: (46.206 ml-18.92) ml

Density of liquid butene: 0.63 g/ml

Weight of butene loaded: 0.63 g/ml * 27.3 ml = 17.2 g

Feed solution TOC : 9400 mg/l = 9.4 g/l 'C'

So calculated amount of n-butanol in feed:

$$\frac{9.4\ g\ 'C' * 1\ l * 18.92\ ml * 74\ g\ n-butanol}{1\ l * 1000\ ml * 48\ g\ 'C'} = 0.274\ g\ n-butanol$$

Raffinate phase TOC measurement: 6250 mg/l = 6.25 g /l 'C'

$$\frac{6.25\ g\ 'C' * 1\ l * 18.92\ ml * 74\ g\ n-butanol}{1\ l * 1000\ ml * 48\ g\ 'C'} = 0.182\ g\ n-butanol$$

So, amount of n-butanol in Extract phase (by subtraction): (0.274-0.182) g= 0.092 g

Mol fraction of n-butanol in butene (extract) phase, y_{butene}:

$$\frac{\frac{0.092}{74}}{\frac{0.092}{74} + \frac{17.2}{56}} = 0.00403$$

Mol fraction of n-butanol in aqueous (raffinate) phase, y_{H2O}:

$$\frac{\frac{0.182}{74}}{\frac{0.182}{74} + \frac{18.738}{18}} = 0.00236$$

Distribution coefficient = y_{buetne} /y_{H2O} = 0.00403/ 0.00236 = 1.71

Distribution coefficients for acetone ethanol and also were calculated in a similar way.

From the distribution coefficients it was found that ethanol has very low distribution coefficient which reflects its affinity towards water much higher than that of organic components like 1-butene. This can be explained from the dipolar moments of the components. Ethanol has a dipole moment very close to that of water which is 1.69 and 1.85 respectively. Again ethanol has a very small hydrocarbon chain (2 carbons) which cannot repel water molecule as strongly as n-butanol and acetone do because of higher carbon numbers in the molecule. Again n-butanol has higher distribution coefficient than both acetone and ethanol (from Table 3.1) because of the presence of longer

hydrocarbon chain which makes n-butanol more non polar than acetone and ethanol and thus more soluble in organic solvent like liquid butene than polar solvent like water.

Though from the experimental results it could be seen, the distribution coefficient was higher than '1' that means molar concentration of the solute was higher in the extract phase than the raffinate phase, still for further extraction or for improving the value of distribution coefficient, operating parameters of the extraction process can be changed. At this temperature and pressure 1-buetne concentration in pure H_2O is 0.39 g/l which can be subtracted from the TOC measurement of the raffinate phase to get the concentration of organic 'C' from the sample only. 0.39 g/l can be considered as the solubility of buetne measured in pure water at 22°C and 40.7 psia/ But with changing pressure and temperature the solubility of butene will change as and it may influence the extraction results.

To improve separation efficiency, a two-step approach was taken in this next phase of experiments where in the first step adsorption of the ABE components and also butyric acid were tested on granulated activated charcoal having high surface area in the range of 600 to 800 m²/g at dry basis. Then at the second step the extraction efficiency was measured by using liquid 1-butene to extract the adsorbed ABE components from the activated charcoal surface.

First, the adsorption and extraction were done from the aqueous solutions of ABE and butyric acid with their known concentrations in ABE fermentation broth which are 8.2 g/L acetone, 17.6 g/L n-butanol, 2.2 g/L ethanol[1] and also 20 g/l butyric acid which is also a by product of ABE fermentation having a different route of microbial metabolism[28],[29]. Butyric acid can also be produced directly from biomass with a high yield up to 60 wt%.

In Table 3.2 the adsorption efficiency of activated charcoal in separation of ABE mixture, n-butanol, butyric acid and methanol from their aqeous solutions of above mentioned concentrations are shown.

Table 3.2: Separation efficiency calculated from total organic carbon content for adsorption on activated charcoal

Fermentation products	Activated Charcoal (g)	Feed solution TOC (mg/l)	Raffinate phase TOC (mg/l)	Adsorption Efficiency (%)
ABE (aq)	7.04	15090	3029	79.9
n-butanol (aq)	7.02	10190	511	95.0
butyric acid	5.0	1567	476	69.6
methanol	5.0	9349	2700	71.1

From Table 3.2 it is observed that adsorption efficiency is high for the aqueous solution of ABE mixture but when only aqueous solution of pure n-butanol is used as the feed solution the adsorption efficiency is found as high as 95%. From these data, it can be inferred that among acetone, n-butanol and ethanol, most of the n-butanol is adsorbed on activated charcoal and due to slightly lower adsorption of ethanol and acetone the adoption efficiency of ABE mixture as a whole is lower than n-butanol aqueous solution. For fermentation products other than ABE components like butyric acid and methanol, the adsorption efficiency from their aqueous solutions maintaining the fermentation broth concentrations were found to be lower than ABE adsorption.

The results shown above are for extraction using liquid butene directly from aqueous solutions of acetone, n- butanol and ethanol separately and from the mixture and again adsorption of these components on activated charcoal from the aqueous solution done separately one process at a time. As the direct liquid-liquid extraction efficiency were observed to be low in Table 3.1 from the two step separation approach, a liquid-solid extraction has been undertaken for improving the overall acetone, n- butanol, ethanol recovery from the feed solution.

3.6.2 Adsorption followed by liquid-solid extraction

For simplicity of measuring the extraction efficiency and for comparison of the extraction capacity for each individual component of ABE and butyric acid, only pure components of acetone, n-butanol, ethanol and butyric acid were adsorbed on the same amount of activated charcoal. Two different loadings of ABE and butyric acid were taken for each of the components keeping all other parameters constant to observe the effect of concentration of solute on the extraction efficiency. In Figure 3.11, except for acetone all other components showed distinctive differences in recovery from activated charcoal by liquid butene extraction. At higher loading of the components that is 30wt% concentration of solute higher percent recovery were achieved than 10wt% solute concentration in activated charcoal. Only acetone showed similar percent recovery for both concentration which could be due to its low boiling point it tends to be on the surface of activated charcoal not penetrating much in the pores and thus easier to retrieve even at low concentrations.
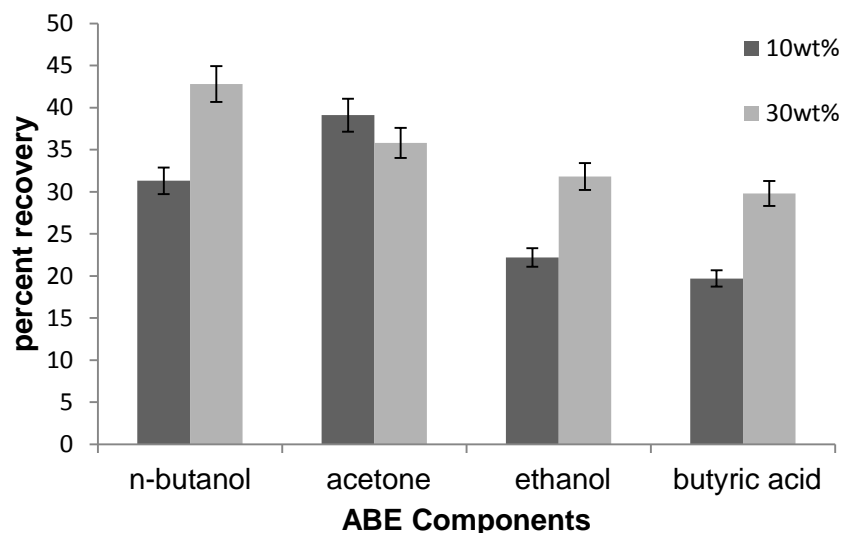
Figure 3.11: Effect of solute concentration adsorbed in activated charcoal on extraction efficiency

To improve the extraction furthermore that is to recover more of the adsorbed components, a double stage extraction experiment was held for n-butanol and butyric acid separately. After single stage extraction the activated charcoal was not unloaded from the vessel, fresh liquid butene was fed in the batch extraction vessel in the same amount at 25 psig pressure. Extraction was done again for 24 hours at 25°C and the extract phase was collected and total organic carbon content was measured. In Table 3.3 from the results of two-stage extraction, it can be inferred that doubling the amount of extractant i.e. liquid butene, higher extraction can be achieved in a single stage. In the batch process without any circulation of liquid butene, the contact of liquid butene and activated charcoal might have played a role but it has been assumed that at 24 hours of time equilibrium of distribution in these two phases must have been achieved and only the solubility of the components in butene was playing the role in extraction efficiency. Approximately 5.1 g of liquid butene is loaded at each stage of separation for each 2.0 g of activated charcoal.

Table 3.3: Two stage Liquid-solid extraction data with repeated butene loading

Solute component	No. of extraction stage	Time= 0 hr Wt. of solute (g)	Time = 24 hr Wt. of solute (g)		Percent extracted
		A.C Phase	A.C. Phase	butene phase	
n-butanol	1	0.6	0.36	0.24	40.0
	2	0.36	0.24	0.12	31.9
Butyric acid	1	0.61	0.43	0.18	29.8
	2	0.43	0.32	0.11	24.5

Effect of extraction temperature was observed on the percent extraction or percent recovery for each 2.0 g of activated charcoal with 30 wt.% solute adsorbed in it. Experiments were performed for acetone, n-butanol, ethanol and butyric acid separately at 25°C and 60°C constant extraction temperature. In Figure 3.12 it is shown that at

higher temperature the percent recovery slightly increased other than butyric acid, but this increase is only significant for ethanol extraction. Ethanol being a highly polar molecule has less solubility in non-polar liquid butene, but at higher temperature the solubility increased and thus percent extraction also increased. For butyric acid at higher temperature, chemisorption might have taken place on activated charcoal surface and thus some new chemical bonds were formed due to the corrosive properties of butyric acid which might have increased with temperature. This chemisorption contributed in lower extraction as it has become more difficult to break the bonds formed at the surface using the extractant only.
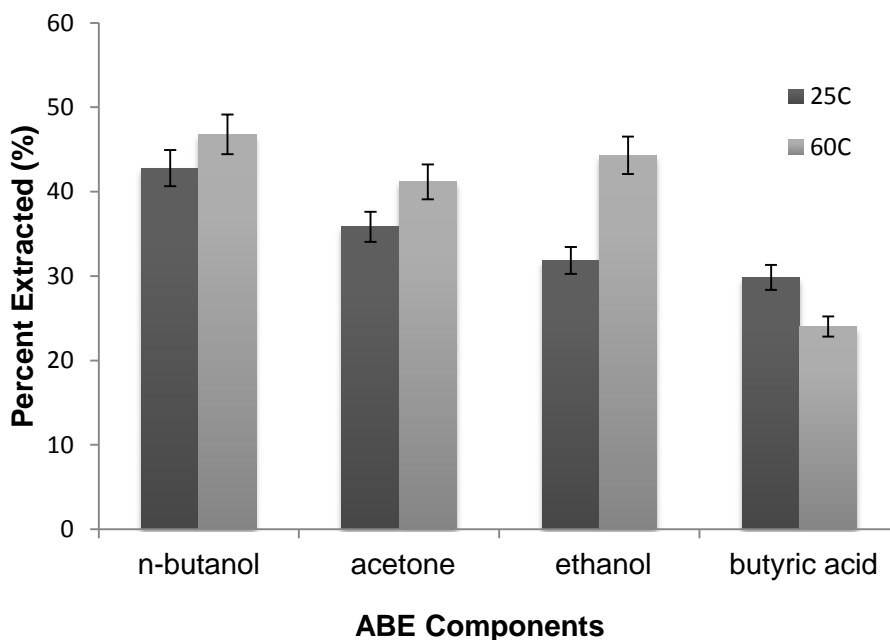
Figure 3.12: Effect of temperature on percent extraction
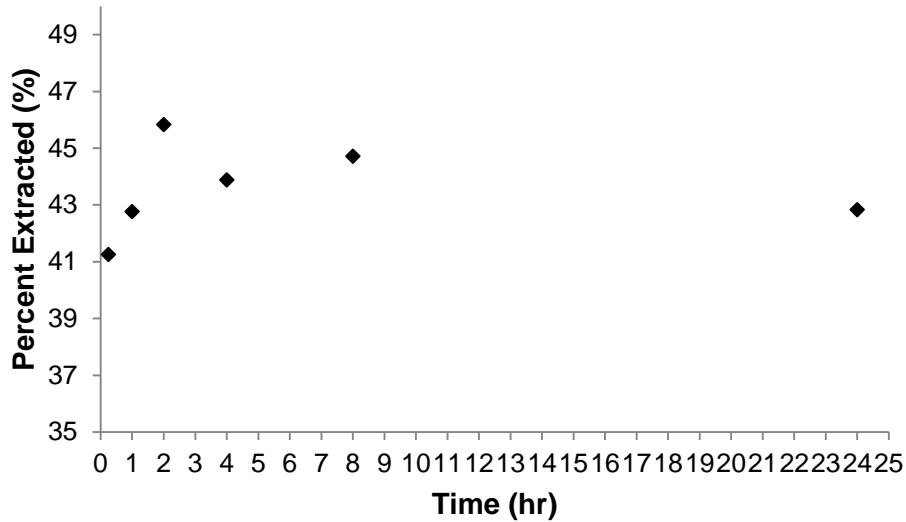
Figure 3.13: Effect of extraction time on percent extraction of butanol

Though most of the extraction experimental runs were performed for 24 hours, to determine the optimum extraction time a few experiments were done with duration starting from 15 minutes to 24 hours and the concentration n-butanol is measured both in the extract phase and solid activated charcoal phase. In Figure 3.13, it is observed that percent recovery of n-butanol increased with time at the beginning. By the time of 8 hours of extraction, it reached the optimum level that is equilibrium is reached. At the end of 24 hours the percent recovery went down slightly.

The above percent recovery data shown in Figures 3.11-13 and Table 3.3 are showing comparison of extraction capacity and recovery of each component of ABE fermentation products and also of butyric acid varying with different operating parameters. To show the exact separation efficiency at a certain operating condition distribution coefficient based on mass fractions and mol fractions were calculated of the components in each phase after extraction was completed.

Table 3.4: Distribution coefficient in liquid 1-butene and activated charcoal phases

Components	Concentration in A.C. phase at t=0 hr (wt.%)	Mass distribution Co-efficient		Mol distribution coefficient	
		25°C	60°C	25°C	60°C
n-Butanol	10	0.15	--	0.8	--
	30	0.33	0.38	1.37	1.6
Acetone	10	0.26	--	1.18	--
	30	0.25	0.31	1.55	1.62
Ethanol	10	0.12	--	0.54	--
	30	0.21	0.35	1.13	1.2
Butyric Acid	30	0.2	0.15	0.79	0.6

$$mass\ distribution\ coefficient = \frac{mass\ fraction\ in\ liq\ 1-butene\ phase\ (x_{butene})}{mass\ fraction\ in\ activated\ charcoal\ phase\ (x_{A.C})} \quad .... (3.1)$$

$$mol\ distribution\ coefficient = \frac{mol\ fraction\ in\ liq\ 1-butene\ phase\ (y_{butene})}{mol\ fraction\ in\ activated\ charcoal\ phase\ (y_{A.C.})} \quad .... (3.2)$$

In Table 3.4 mass distribution coefficient values are much less than 1, which implies that lower amount of solute traveled to per gram of extract phase than retained in per gram of solid activated charcoal phase. That also referred, higher mass ratio of liquid butene to solid activated charcoal needed to be taken for getting high extraction or recovery. Comparing the mole based distribution coefficients in Table 3.4 with that of Table 3.1 showing the distribution coefficients for direct extraction of ABE components from dilute aqueous solution using same extractant i.e. liquid butene, it was observed that liquid solid extraction from activated charcoal is not more efficient than the liquid- liquid extraction for n-butanol. But for ethanol and acetone the distribution coefficients were much higher for liquid –solid extraction. As in the liquid-liquid extraction, the raffinate phase is water and ethanol and acetone are hydrophilic components compared to the other solutes, it was found to be easier to extract these two components from the activated charcoal than directly from aqueous solution.

In all extraction measurement and calculation showed above, it was not possible to show the analysis data for ABE extraction as a mixture maintaining the concentration as in fermentation broth as with the total organic carbon measurement of a sample of extract phase, it could not be differentiated that which component contributed how much organic carbon count from the mixture. For ABE mixture extraction from activated charcoal with liquid butene, the extract phase has been analyzed with high performance liquid Chromatography (HPLC) and the percent recovery was calculated and presented in Table 3.5.

Table 3.5: HPLC analysis results for extraction of ABE mixture at 60°C

Components Of ABE	Solute in A.C phase (at t=0 hr) (mg)	Solute in liq. Butene phase (at t= 8 hr) (mg)	Percent extracted
n-butanol	389	256	65.8
acetone	183	70	38.2
ethanol	60	23	38.3

It was observed that when a mixture of ABE was extracted, a preferential extraction had been taking place and being the least polar component among the three, n-butanol was been preferentially going to the liquid butene phase and higher percent recovery was achieved. While performing single component extraction, n-butanol and acetone recovery were much similar specially at 60°C temperature but for the extraction of the mixture the components had to compete with one another and the least polar one was preferentially extracted.

3.7 Conclusion

In this work, liquid- liquid extraction (LLE) of dilute model ABE aqueous solution having the standard concentration of ABE as in the fermentation broth was performed using liquid 1-butene as extractant to integrate the processes of catalytic dehydration and ABE separation from fermentation broth as 1-butene is a by-product of the ABE catalytic upgrading process. A two-step separation process of adsorption of activated charcoal surface and then liquid-solid extraction again using liquefied 1-butene was also carried out to compare the efficiency of extraction with the direct one step approach. The highest percent recovery and distribution coefficient have been achieved for n-butanol compared to the other components in ABE when single component extraction was performed. The distribution coefficient found in this process based on mol fraction in butene phase divided by mol fraction in aqueous phase was 1.71 which was higher than that found in liquid-solid extraction process. Higher percent recovery and higher distribution coefficient was achieved for ethanol and acetone in adsorption and liquid-solid extraction combined process. Increasing extraction temperature contributed in higher percent of recovery of the ABE components and higher distraction coefficients as well. Increase in solute concentration on activated charcoal surface also showed positive impact on extraction efficiency. Butyric acid showed poor extraction efficiency even at high temperature due to its corrosive properties and possible occurrence of chemisorption on the activated charcoal which makes it increasingly difficult to extract. Comparing the polarity indices of ABE components it has been inferred that the higher extraction of n-butanol in liquid butene was observed as it possesses the lowest polarity index and thus more non-polar than the other two components. Also that is the reason

for n-butanol was observed to be preferentially extracted above acetone and ethanol when extraction of ABE as a mixture was performed.

In conclusion this work showed a feasible integration of the separation process of ABE fermentation broth and ABE catalytic dehydration and direct liquid- liquid extraction using the by-product 1-butene in a pressurized condition can be potential separation approach optimizing the cost and efficiency.

References

[1]   C. Weber, A. Farwick, F. Benisch, D. Brat, H. Dietz, T. Subtil, and E. Boles, "Trends and challenges in the microbial production of lignocellulosic bioalcohol fuels.," *Appl. Microbiol. Biotechnol.*, vol. 87, no. 4, pp. 1303–1315, Jul. 2010.

[2]   T. C. Ezeji, N. Qureshi, and H. P. Blaschek, "Bioproduction of butanol from biomass: from genes to bioreactors.," *Curr. Opin. Biotechnol.*, vol. 18, no. 3, pp. 220–227, Jun. 2007.

[3]   I. Maddox and N. Qureshi, "Production of acetone-butanol-ethanol from concentrated substrate using< i> clostridium acetobutylicum</i> in an integrated fermentation-product removal process," *Process Biochem.*, vol. 30, no. 3, pp. 209–215, 1995.

[4]   Q. Li, H. Cai, B. Hao, C. Zhang, Z. Yu, S. Zhou, and L. Chenjuan, "Enhancing clostridial acetone-butanol-ethanol (ABE) production and improving fuel properties of ABE-enriched biodiesel by extractive fermentation with biodiesel.," *Appl. Biochem. Biotechnol.*, vol. 162, no. 8, pp. 2381–6, Dec. 2010.

[5]   O. Mutschlechner, H. Swoboda, and J. R. Gapes, "Continuous two-stage ABE-fermentation using Clostridium beijerinckii NRRL B592 operating with a growth rate in the first stage vessel close to its maximal value.," *J. Mol. Microbiol. Biotechnol.*, vol. 2, no. 1, pp. 101–105, Jan. 2000.

[6]   N. Qureshi and S. Hughes, "Energy-efficient recovery of butanol from model solutions and fermentation broth by adsorption," *Bioprocess Biosyst Eng*, vol. 27, pp. 215–222, 2005.

[7]   K. Kraemer, A. Harwardt, and R. Bronneberg, "Separation of butanol from acetone-butanol-ethanol fermentation by a hybrid extraction-distillation process,"

in *20th European Simposium on Computer Aided Process Engineering*, 2010, no. iv.

[8]   W. Groot and R. Van der Lans, "Technologies for butanol recovery integrated with fermentations," *Process Biochem.*, 1992.

[9]   A. Oudshoorn, L. A. M. Van Der Wielen, and A. J. J. Straathof, "Adsorption equilibria of bio-based butanol solutions using zeolite," vol. 48, pp. 99–103, 2009.

[10]   a. Oudshoorn, L. a. M. van der Wielen, and a. J. J. Straathof, "Desorption of butanol from zeolite material," *Biochem. Eng. J.*, vol. 67, pp. 167–172, Aug. 2012.

[11]   V. Saravanan, D. a. Waijers, M. Ziari, and M. a. Noordermeer, "Recovery of 1-butanol from aqueous solutions using zeolite ZSM-5 with a high Si/Al ratio; suitability of a column process for industrial applications," *Biochem. Eng. J.*, vol. 49, no. 1, pp. 33–39, Mar. 2010.

[12]   N. Qureshi, M. M. Meagher, and R. W. Hutkins, "Recovery of butanol from model solutions and fermentation broth using a silicalite / silicone membrane 1," vol. 158, pp. 115–125, 1999.

[13]   F. Liu, L. Liu, and X. Feng, "Separation of acetone–butanol–ethanol (ABE) from dilute aqueous solutions by pervaporation," *Sep. Purif. Technol.*, vol. 42, no. 3, pp. 273–282, Apr. 2005.

[14]   H. Zhou, Y. Su, X. Chen, and Y. Wan, "Separation of acetone, butanol and ethanol (ABE) from dilute aqueous solutions by silicalite-1/PDMS hybrid pervaporation membranes," *Sep. Purif. Technol.*, vol. 79, no. 3, pp. 375–384, Jun. 2011.

[15]   N. Qureshi and H. P. Blaschek, "Production of acetone butanol ethanol (ABE) by a hyper-producing mutant strain of Clostridium beijerinckii BA101 and recovery by pervaporation.," *Biotechnol. Prog.*, vol. 15, no. 4, pp. 594–602, 1999.

[16]   S. Heitmann, J. Krings, P. Kreis, a. Lennert, W. R. Pitner, a. Górak, and M. M. Schulte, "Recovery of n-butanol using ionic liquid-based pervaporation membranes," *Sep. Purif. Technol.*, vol. 97, pp. 108–114, Sep. 2012.

[17]   G. Jurgens, S. Survase, O. Berezina, E. Sklavounos, J. Linnekoski, A. Kurkijärvi, M. Väkevä, A. van Heiningen, and T. Granström, "Butanol production from lignocellulosics.," *Biotechnol. Lett.*, vol. 34, no. 8, pp. 1415–34, Aug. 2012.

[18]   Y. J. Jeon and Y. Y. Lee, "Membrane-assisted extractive butanol fermentation.," *Ann. N. Y. Acad. Sci.*, vol. 506, pp. 536–542, 1987.

[19]   N. Qureshi and I. S. Maddox, "Reduction in Butanol Inhibition by Perstraction," *Food Bioprod. Process.*, vol. 83, no. 1, pp. 43–52, Mar. 2005.

[20] I. A. N. S. Maddox, "Continuous Production of Acetone-Butanol-Ethanol Using Immobilized Cells of," vol. 80, no. 2, pp. 185–189, 1995.

[21] S. R. Roffler, H. W. Blanch, and C. R. Wilke, "In situ extractive fermentation of acetone and butanol.," *Biotechnol. Bioeng.*, vol. 31, no. 2, pp. 135–43, Feb. 1988.

[22] L. Adhami, B. Griggs, P. Himebrook, and K. Taconi, "Liquid–Liquid Extraction of Butanol from Dilute Aqueous Solutions Using Soybean-Derived Biodiesel," *J. Am. Oil Chem. Soc.*, vol. 86, no. 11, pp. 1123–1128, Aug. 2009.

[23] S. Chuichulcherm and J. Chutmanop, "Butanol separation from ABE model fermentation broth by liquid-liquid extraction," 2000.

[24] G. Jurgens, S. Survase, O. Berezina, E. Sklavounos, J. Linnekoski, A. Kurkijärvi, M. Väkevä, A. van Heiningen, and T. Granström, "Butanol production from lignocellulosics.," *Biotechnol. Lett.*, vol. 34, no. 8, pp. 1415–34, Aug. 2012.

[25] A. Laitinen and J. Kaunisto, "Supercritical fluid extraction of 1-butanol from aqueous solutions," *J. Supercrit. Fluids*, vol. 15, no. 3, pp. 245–252, Jul. 1999.

[26] D. L. Petre, "Investigations on secondary butanol extraction by supercritical butene.," *Rev. Chim. Bucharest Rom.*, vol. 58, no. 8, pp. 833–837, 2007.

[27] N. Qureshi, S. Hughes, I. S. Maddox, and M. a Cotta, "Energy-efficient recovery of butanol from model solutions and fermentation broth by adsorption.," *Bioprocess Biosyst. Eng.*, vol. 27, no. 4, pp. 215–22, Jul. 2005.

[28] D. E. Ramey, "Production of butyric acid and butanol from biomass," *Final Report DOE*, 2004. [Online]. Available: http://www.afdc.energy.gov/pdfs/843183.pdf. [Accessed: 20-Apr-2014].

[29] J. Zigová, E. Šturdík, D. Vandák, and Š. Schlosser, "Butyric acid production by Clostridium butyricum with integrated extraction and pertraction," *Process Biochem.*, vol. 34, no. 8, pp. 835–843, Oct. 1999.

Chapter 4

Catalytic Deoxygenation of Butyric Acid to Energy-Dense Hydrocarbons and Aromatics

4.1. Introduction

Bioethanol has been considered as the well-recognized biofuel around the world derived from biomass like corn stovers, wood chips, grasses, etc. It is being used as fuel blend mostly with petroleum products like gasoline in automobile engines, but due to its corrosiveness, high volatility and aqueous solubility and low heating value compared to gasoline and equivalents, solely bioethanol is not close enough to replace the petroleum products as transportation fuel[1]. The Renewable Fuel Standard enacted by the US Energy Independence and Security Act of 2007 gives a strong incentive to increase the production of renewable liquid fuel with a production goal of 36 billion gallons of liquid biofuel use by year 2022. Moving away from corn-starch ethanol and focusing more on lignocellulosic biofuel production is another motto of the policy makers to avoid the food versus fuel issue. To meet these requirements biofuels beyond bioethanol are coming into production, among them biobutanol is the most promising one[2][3][4]. Compared to bioethanol, biobutanol has 33% higher energy content per mass and also the physical and chemical properties are more comparable to those of gasoline[5][6]. Biochemical production of biobutanol from biomass has also been studied more in last two decades.

Despite of having fuel-compatible physicochemical properties, the low yield in the production process is the major challenge in producing biobutanol. The toxic effect of product 1-butanol on the microbial strain, limits the product concentration to less than 20 g/l [1][7][3].

Though extensive research work is going on to improve the yield of biobutanol by creating genetically modified microbial strain which can withstand the 1-butanol environment[3][8][9] and by continuous energy efficient separation of 1-butanol from the fermentation broth, the increment in yield is still not economical. On the other hand biochemical production of butyric acid can be considered as a potential precursor for producing biofuels. Butyric acid is also produced as by product in the two-step ABE fermentation process using Clostridium acetobutylicum[10][11].Depending on effective gene expressions of enzymes the end product may vary in a fermentation process that is shown in Figure 4.1.
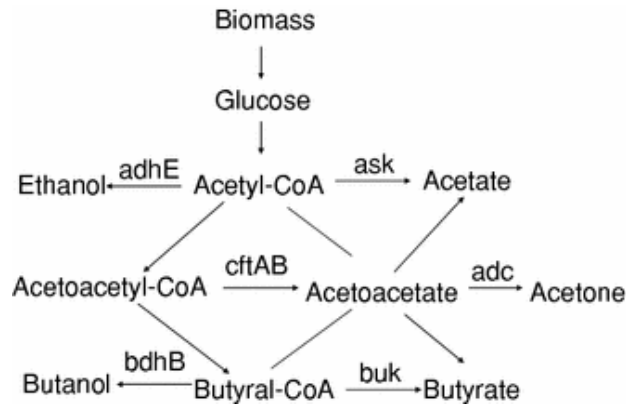
Figure 4.1: Metabolic pathway of ABE fermentation depending on effect of different genes on end product [12]

For producing butyric acid as the main fermentation product, several other microbial strain of Clostridium genus showed high productivity, such as Clostridium butyricum[13], Clostridium beijerinckii[14][15] and Clostridium tyrobutyricum; out of these Clostridium tyrobutyricum gave the highest product concentration in a fed-batch (with immobilized cell) fermentation. The fermentation reaction type and mode also has significant effect on the productivity. A summary of different studies on biochemical production of butyric acid with several microbial strains and process types are shown in Table 4.1.

Table 4.1: Biochemical production of butyric acid having a high product concentration, using different substrates and Clostridial strains[16]

Strain	Substrate	Final butyric acid concentration (g/L)	Fermentation mode
C. *butyricum ZJUCB*	Glucose	12.2 16.7	Batch Fed batch
C. butyricum S21	Lactose	18.6	Batch
C. *thermobutyricum*ATCC48975	Glucose	19.4	Continuous
C. *tyrobutyricum* CIP 1-776	Glucose	62.8	Fed-batch
C. *tyrobutyricum* ATCC 25755	Glucose	53.0 44.0	Fed-batch (immobilized cell) Batch
C. *tyrobutyricumc* ZJU 8235	Jerusalem Artichoke hydrolysate	60.4	Fed-batch (immobilized cell)

This high throughput of butyric acid from biomass fermentation compared to that of biobutanol can make it a very attractive option for producing liquid transportation fuel from renewable sources. As a raw material for producing liquid biofuel, butyric acid possesses a lower HHV (higher heating value, 24 kJ/g) compared to biobutanol (33 kJ/g) due to the higher O/C mass ratio in its molecular structure. But this acid can be converted to a good hydrocarbon fuel by catalytic deoxygenation which will produce

longer chain hydrocarbon with low O/C ratio thus a higher HHV product. Studies on catalytic deoxygenation of biobutanol showed very positive results in terms of producing a higher energy content organic liquid which can be used as a drop in fuel or fuel blend[5][17][18][19].   Similarly butyric acid produced in biomass fermentation process can be catalytically deoxygenated to produce liquid hydrocarbon fuel; however, the deoxygenation of organic acids is more difficult than that of alcohols and ketones due to the high bond dissociation energy required as there are two strong carbon-oxygen bonds in the carboxylic acid group [20][21].

In this study catalytic deoxygenation of butyric acid was examined for determining the appropriate catalyst and operating conditions. The oxygen removal is expected to take place in the form of water and/or carbon dioxide, with a preference to water so that carbon is retained in the product for a high yield of the hydrocarbon liquids. Three common commercial acid catalysts, well-known for catalyzing dehydration reactions, γ-Al_2O_3, ZrO_2 and ZSM-5, were selected for this study. These catalysts have been selected for their slightly different acid sites and properties so that the effect of the acidity can be examined. The γ-Al_2O_3 only has Lewis acid sites, but ZrO_2 has amphoteric property as it has both Lewis acid and Lewis basic sites. ZSM-5 possess' both Bronsted and Lewis acid sites thus it has very strong acidity[22].

Recent studies have shown that the major product from deoxygenation of mono carboxylic acids over metal oxide catalysts are usually ketones[23][24][25]. For carboxylic acid ketonization a good number of studies are done with CeO_2 and ZrO_2 catalysts [26][27] and in the comparative studies ZrO_2 showed a higher conversion efficiency than CeO_2[28], but combination of these catalysts can modify the acid-base properties and the catalyst surface structure and properties are changed[29]. A review on catalytic ketonization of carboxylic acids proposed mechanisms via intermediate products such as ketenes, beta-keto-acids, carboxylates and acyl carbonium ions[22].

DFT calculation of the heat of adsorption and energy barrier of α-hydrogen abstraction on a zirconia surface imply that the lattice oxygen of the (111) plane of ZrO_2 crystal structure can abstract the α-hydrogen from the carboxylic acid molecules [30]. Formation of esters from deoxygenation of carboxylic acid on metal oxide catalysts at < 300°C is observed in a previous study[31]. The activation energy required for ketonization is much higher (132 kJ/mol) than that for esterification (40 kJ/mol), hence the latter is favored at low temperatures. Above 400°C, higher ketone production from carboxylic acids on metal oxide catalysts are expected via beta-keto-acids or ketenes intermediates.

In this work a single step conversion of butyric acid to aromatic hydrocarbons is examined on a series catalyst bed of (a) ZrO_2 followed by ZSM-5, and (b) γ-Al_2O_3 followed by ZSM-5. The main goal in the series catalyst bed is to first deoxygenate the butyric acid molecules, and then to aromatize the deoxygenation product in a single step reactor using the aromatization properties of ZSM-5 zeolites [32][33].

4.2 Objectives

The objective of this work is catalytic deoxygenation of butyric acid to produce energy dense higher hydrocarbon.

(I)   Comparison of performance of three different inorganic acid catalysts γ-Al_2O_3, ZSM-5 and ZrO_2 in single catalyst beds in deoxygenation of butyric acid.

(II)   Effect of operating parameters   temperature and feed flow rate on deoxygenation process for each of the catalyst beds

(III)   Comparison of the products from a series catalyst bed of ZrO_2 followed by ZSM-5 with the products of single catalysts and predicting the reaction mechanism taking place

4.3. Experimental Section

4.3.1 Materials

Butyric acid (i.e., butanoic acid) of purity >99% from Sigma-Aldrich was used as the feed material in this study. Catalysts γ-Al_2O_3 as cylindrical pellets (0.32 cm dia, 220 m^2/g surface area and 0.62 mL/g pore volume), ZSM-5 as powder (23:1 SiO_2:Al_2O_3 molar ratio, m^2/g surface area and 0.118 mL/g pore volume) are used as received from Alfa Aesar (Ward Hill, MA). 3 mm pellets of monoclinic ZrO_2 (0.32 cm dia, 5.6 m^2/g surface area and 0.26 ml/g pore volume) were used as catalysts received from Saint-Gobain NorPro (Stow, OH). Silica sand (0.853 to 2.00 mm dia) is used as the filler material. Anhydrous calcium sulfate was used as desiccant for gases.

4.3.2 Apparatus and procedure:

A schematic of the apparatus is shown in Figure 4.2. The feed, liquid butyric acid was pumped to the reactor using a high pressure positive displacement pump in which flow rate was controlled and pressure was adjusted automatically to overcome the pressure drop across the catalysts bed. A stainless steel tubular reactor (High Pressure Equipment Company, Erie, PA) with 0.8 cm internal diameter (i.d.) and 20.4 mL internal volume has been placed inside an electric furnace. The feed was pumped through coiled tubing inside the furnace to be preheated before entering the reactor. Fluid temperature in the reactor has been monitored by a thermocouple (Omega). The reactor was packed with either 10.5 g of γ-Al_2O_3 cylindrical pellets, or 12.76 g of ZrO_2 cylindrical pellets. When a catalyst bed of γ-Al_2O_3 or ZrO_2 and then ZSM-5 were used in a series, 4-5 g of γ-Al_2O_3 or ZrO_2 was loaded in the reactor and after that 1.5 g of ZSM-5 mixed with 3.5 g of silica sand was loaded so that half of the reactor was full with the cylindrical pellets and the rest of it was filled with zeolite powder mixed with silica sand. The product outlet

line from the reactor was a 1/16" 316 stainless steel tubing which was first air cooled and then water cooled using a double tube heat exchanger of which the outer tube was made of copper. After passing through the heat exchanger, the product, a gas/liquid mixture, was fed to a 'phase separator' consisting of a 30 ml Jerguson gage with sight glass. The product mixture entered at the middle of the separator and the separated gas exited from the top. A volumetric gas flow meter (Cole Parmer, Vernon Hills, IL) of maximum capacity 500 mL/min calibrated with respect to air was connected to the top outlet of the phase separator. At the outlet of the flow meter, a pressure gauge of maximum capacity of 60 psig was placed to measure the pressure. The gas product then passed through a tubular steel vessel packed with anhydrous calcium sulfate to remove the moisture before entering gas chromatograph.
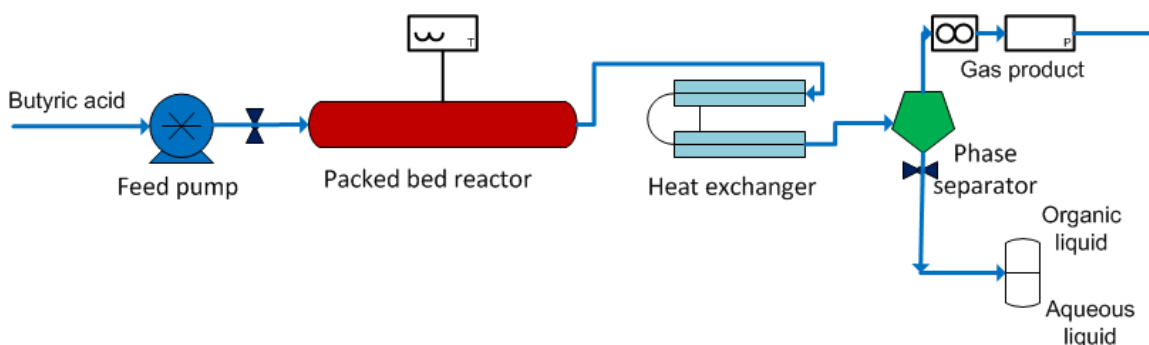
Figure 4.2: Apparatus for the catalytic deoxygenation of butyric acid

A control valve, at the bottom outlet of the phase separator, was opened intermittently to collect the liquid product gathered in a given duration. After collection of the liquid product, due to density difference the organic phase and the aqueous phase get separated distinctively and they are separately decanted. Each phase of the liquid product was weighed separately and the mass flow rate of each phase of liquid product stream was calculated. After every two experimental runs, nitrogen gas is passed through the reactor at 400°C to remove any chemical residue or coke deposit.

Two operating parameters, reaction temperature and feed flow rate, were varied to examine the deoxygenation kinetics for two different catalysts and also series catalyst beds with ZSM-5. Pressure drop across the catalyst bed was measured from the difference of the pressure reading of the feed pump and the gas product outlet pressure, which varied with changing feed flow rate and with changing temperature. The pressure drop across the bed varied from 3 to 5 bars depending on the feed flow rate.

4.3.3 Product Characterization

4.3.3.1 GC Chromatography: A SRI 8610C gas chromatograph (GC) with a thermal conductivity detector (TCD) was used to determine the composition of the gas product. A capillary Supel-Q PLOT column (Supelco, Sigma-Aldrich, St. Louis, MO) with divinylbenzene polymer as the stationary phase and 27 m in length and 0.32 mm i.d. was used for the gas chromatographic analysis. This column was selected as the stationary media of fused silica can separate CO_2 and C_1-C_5 hydrocarbons. The column oven was maintained at 70˚C. Helium has been used as the carrier gas. Sample injection to the GC was done online by means of a six-port injection valve attached through a 10 µL sample loop.

4.3.3.2 Fourier Transform Infrared (FTIR) Spectroscopy: The IR analysis of the gas mixture was done using a Nicolet IR100 FTIR instrument and Spectra Tech Econo gas cell of 50 mm path length and NaCl windows. Product gas was collected by connecting the top outlet tubing from the phase separator to a 1-liter flex film gas sampling bag (SKC, Inc., PA). A gas tight syringe of 5 ml capacity (SGE, Austin, TX) was used to transfer gas from the sample bag to the gas cell. The cell was flushed with gas several times to ensure that no air or previous gases were left inside. The background taken for subtraction was the IR spectrum of the empty cell containing pure nitrogen. The IR

analysis was done especially to detect the type of bonds in the gaseous products which couldn't be detected in the GC analysis.

4.3.3.3 Calorific value analysis: The calorific value of the liquid feed and dehydration products were analyzed by an IKA C 200 calorimeter. As the feed and product are both very combustible and volatile, they were first soaked in cotton and then combusted in a bomb calorimeter on a stainless steel crucible pressurized with oxygen at 34 bars. The HHV of the cotton was subtracted from the total reading to obtain the HHV of the sample only.

4.3.3.4 Gas Chromatography-Mass Spectrometry (GC-MS) analysis: The organic liquid product phase was analyzed using a GC-MS. The GC-MS was equipped with a DB-1701 column (30m, 0.25mm, 0.25um) from Agilent Technologies to separate the hydrocarbon and oxygenated hydrocarbon components. The GC is also from Agilent (Model 7890) contains a flame ionization detector and can detect and detect hydrocarbons from C_2 to C_{20}. The injection volume taken of each product sample is 1 µL.

4.4. Reactions Involved

The principal reaction involved in the catalytic deoxygenation of butyric acid produces 4-heptanone, water and carbon dioxide. From 2 butyric acid molecules 3 out of 4 total oxygen atoms get removed resulting in a 7-carbon ketone product with higher energy content.
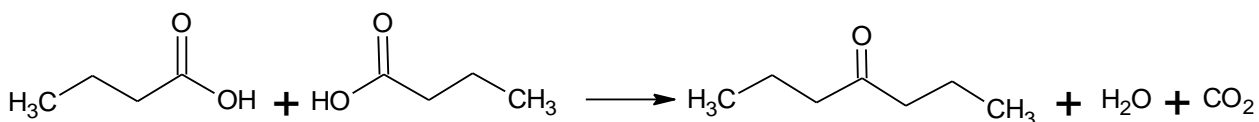
The oxygen atoms are removed in terms of water in the liquid product phase and carbon dioxide in the gaseous product phase.

$$CO_2$$
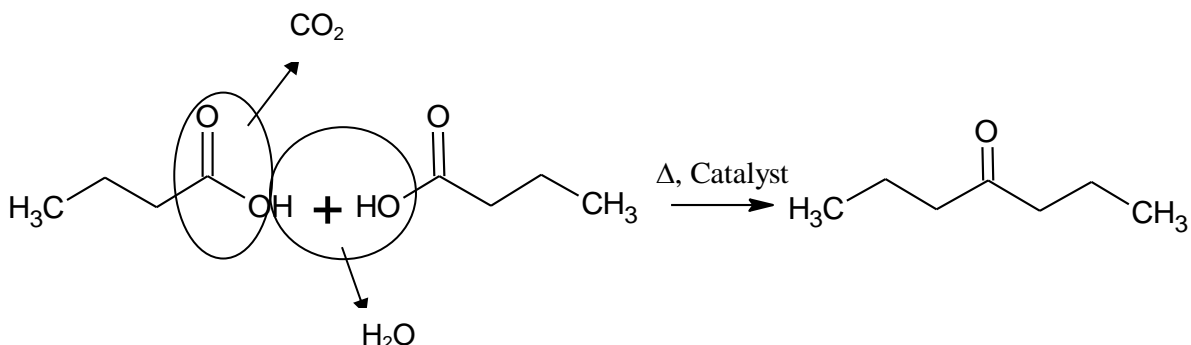
Higher hydrocarbons, other than 4-heptanone were also detected in the organic product phase. In addition, the aromatic compounds are produced at > 400°C.

The probable reaction mechanism for formation of the major product 4-heptanone from butyric acid is via the formation of β-ketoacid, where an α-hydrogen in a butyric acid molecule is abstracted on the active catalyst site and then get coupled with another adsorbed butyric acid molecule on the catalyst surface to produce the β-ketoacid which is actually formed by coupling an enolate and carboxylate or a carbonyl or acyl fragment [22]. Formation of β-ketoacid intermediate is the kinetically favored mechanism over the other routes [34]. This β-ketoacid structure goes under a redistribution of electrons to produce an enol which undergoes instant tautomerization to form the corresponding ketone as ketone is a more chemically stable structure than an enol. As β-ketoacid structures are very much likely to go under decarboxylation, CO_2 is formed in this reaction mechanism after the dehydration step [35]. A proposed mechanism for butyric acid deoxygenation on the metal oxide catalysts in this study is as follows:
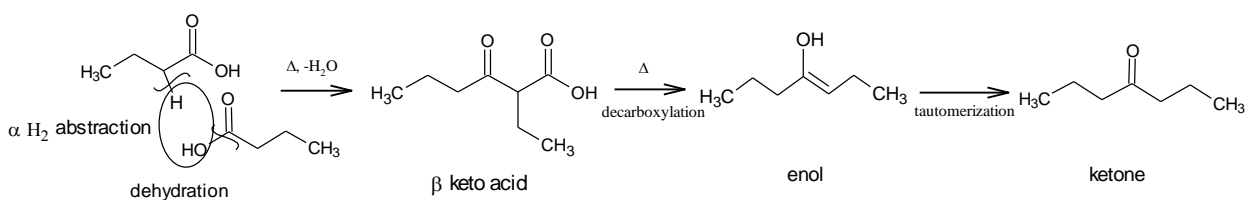
Other than 4-heptanone other log chain hydrocarbon, oxygenated hydrocarbon, cyclic and aromatic products are also produced in this process at higher operating temperature or for zeolite catalyst activity.

4-heptanone → (400 °C, ZSM⁻5) → toluene + P-xylene + ethyl benzen + 1-methyl naphthalene
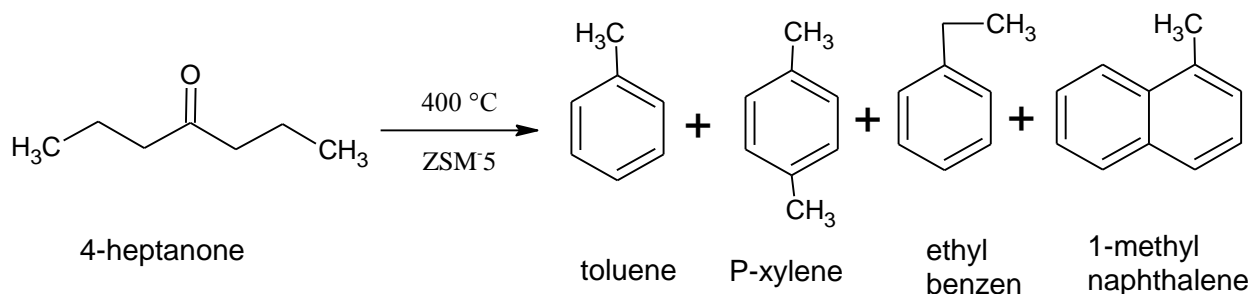
When ZSM-5, zeolites are used in a series catalyst bed after a deoxygenation catalyst, further conversion of product 4-heptanone and other ketones take place. On ZSM-5 catalyst bed, deoxygenation of ketone and consecutive redistribution of bonds create cyclic hydrocarbons and mostly aromatics due to the frame work structure of the pores in ZSM-5.

4.5. Results and Discussion

The deoxygenation products of pure butyric acid consist of a gaseous product and a liquid product collected at room temperature. The liquid phase is again separated into an organic phase and a small fraction of aqueous phase. The organic phase contains mostly 4-heptanone and other liquid aliphatic and aromatic hydrocarbons when ZrO_2 is used and catalyst. The composition of the organic liquid product varies with operating conditions especially with temperature.

Table 4.2: Summary of butyric acid deoxygenation experimental result (inlet and outlet flow) on different catalysts, operating temperatures and feed flow rates

Expt. No.	Feed Mass flow rate (g/min)	Feed WHST* ($\frac{g}{g/h}$)	Catalyst (catalyst[1] is followed by catalyst[2] in a series bed)	Temp (°C)	Liquid product				Gas product
					Flow rate (measured) g/min		Organic phase		Flow Rate (Calculated by subtraction) (g/m)
					Org. liq.	Aq. liq.	HHV kJ/g	Yield (wt.%)	
1	0.96	0.18	γ-Al_2O_3	400	0.770	0	23.50	80.2	0.190
2	0.96	0.18	γ-Al_2O_3	500	0.860	0	23.20	89.6	0.100
3	0.96	0.18	γ-Al_2O_3	600	0.150	0.120	31.74	15.6	0.690
4	0.96	0.08	γ-Al_2O_3[1], ZSM-5[2]	500	0.270	0	25.05	28.1	0.680
5	0.096	1.06	γ-Al_2O_3	400	0.083	0	23.09	86.5	0.013
6	0.096	1.06	γ-Al_2O_3	600	0.021	0.008	27.03	21.9	0.067
7	0.096	0.81	γ-Al_2O_3[1], ZSM-5[2]	400	0.057	0	23.20	59.4	0.039
8	0.96	0.22	ZrO_2	400	0.792	0	25.86	82.5	0.168
9	0.96	0.22	ZrO_2	600	0.739	0	20.37	77.0	0.221
10	0.096	2.22	ZrO_2	400	0.067	0.006	36.20	69.8	0.023
12	0.096	2.22	ZrO_2	500	0.042	0.005	34.40	43.7	0.049
13	0.096	2.22	ZrO_2	600	0.019	0.003	33.80	19.8	0.074
14	0.096	0.88	ZrO_2[1], ZSM-5[2]	400	0.047	0.008	27.10	49.0	0.041

*Weight hourly space time, WHST $= \dfrac{Mass\ of\ catalyst\ loaded\ (g)}{Mass\ flow\ rate\ of\ ABE\ mixture\ (\frac{g}{h})}$

The major component of the gaseous phase of the product is CO_2. It also contains smaller amount of C_2 to C_3 hydrocarbon gases which can be confirmed by GC and FTIR

analysis of the gaseous product. The composition of the gas mixture also depends on the catalyst and the operating temperature.

Performance of four different acid catalysts i.e. γ-Al$_2$O$_3$, γ-Al$_2$O$_3$ and ZSM-5 in series, ZrO$_2$, ZrO$_2$ and ZSM-5 in series bed are tested for the deoxygenation of pure butyric acid. The product phases, quality, conversion and yield vary with the catalysts, operating temperature and feed flow rate as shown in Table 4.2.

4.5.1 Comparison of liquid organic phase of the deoxygenation product on different catalysts

In the case of γ-Al$_2$O$_3$, very low conversion is found at 400°C. From GC-MS analysis of the organic liquid product it is seen that less than 10% is converted to 4-heptanone and above 90% of the liquid product composition is unconverted butyric acid. Combining γ-Al$_2$O$_3$ and ZSM-5 in a series catalyst bed did not improve the conversion to liquid product much. On the other hand ZrO$_2$ catalyzed deoxygenation liquid product consists of two separate phases: a larger amount of organic phase and a small aqueous phase in a mass ratio of 11 is to 1. At 400°C operating temperature the conversion of butyric acid to 4-heptanone is higher than 90%. Using a series combination of ZrO$_2$ and ZSM-5 catalysts, yield of organic phase decreased but the conversion of butyric acid increased as negligible amount of unconverted butyric acid could be found in the organic liquid product phase. Also in the series bed of ZrO$_2$ and ZSM-5, ZrO$_2$ first butyric acid to 4-heptanone as in the case of pure ZrO$_2$ catalysis, then the heptanone and other similar hydrocarbon molecules go through aromatization on the ZSM-5 bed resulting in almost equal composition of aromatics being produced as 4-heptanone.
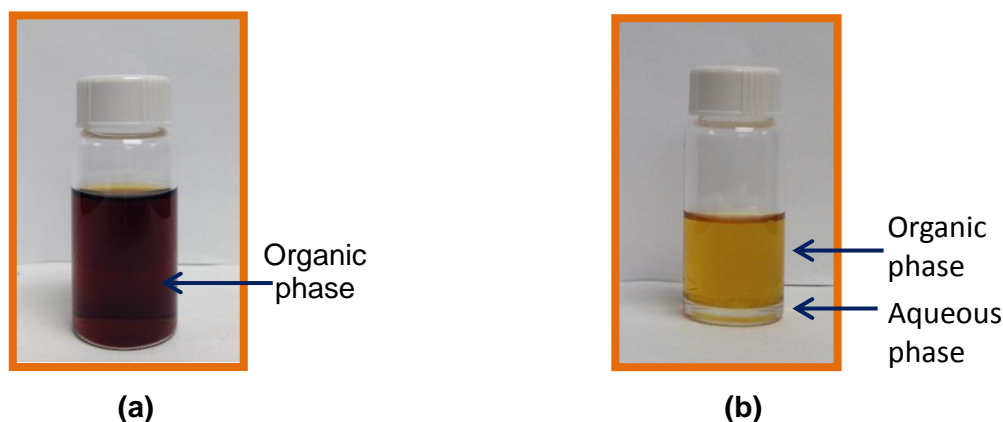
Figure 4.3: Liquid products from deoxygenation of butyric acid at 400°C on (a) γ-Al$_2$O$_3$ and (b) ZrO$_2$ catalyst bed

Table 4.3: Yield and composition of organic liquid product from pure butyric acid deoxygenation over different catalysts at 400°C and 1.0 ml/min (0.096 g/min) feed flow rate

Catalyst	Organic product yield (wt%)	Composition of the liquid organic phase		
		4-Heptanone (GCMS area%)	Aromatics (GCMS area%)	Butyric acid (GCMS area%)
γ-Al$_2$O$_3$	85.9	7.7	--	83.8
γ-Al$_2$O$_3$ followed by ZSM-5	59.4	15.3	--	84.0
ZrO$_2$	69.8	90.2	--	7.6
ZrO$_2$ followed by ZSM-5	48.9	33.1	29.5	9.3

Comparison of the HHV of the organic liquid product also show that ZrO$_2$ catalyzed liquid product has the highest energy content (Figure 4.4). ZrO$_2$ catalyzed deoxygenation gives an organic product with 36 kJ/g HHV at 400°C and 0.45 h WHST. Compared to the HHV of pure butyric acid measured as 23 kJ/g ZrO$_2$ catalysed process increased the energy content by 56.5% in a single step. In constrast, at the same operating conditions the three other catalysts produce liquid of only one phase containing a low HHV. The HHV values of the liquid products can be explained from the GC-MS analysis showed in Table

4.3 as well. Only γ-Al$_2$O$_3$ and γ-Al$_2$O$_3$ and ZSM-5 catalyzed liquid product consists of almost 84% of unconverted butyric acid, thus they possess the HHV almost similar to that of pure butyric acid. ZrO$_2$ and ZSM-5 in a series produces a better energy product of 27.1kJ/g but much lower than ZrO$_2$. From Table 4.3, it can be seen that the yield decreases when ZSM-5 is added in a series with γ-Al$_2$O$_3$ or with ZrO$_2$ as more carbon from the feed is goes to the gas phase product. That is why when ZrO$_2$ and ZSM-5 are used together it produces a liquid product with lower HHV than that in only ZrO$_2$. But again ZSM-5 contributes in producing larger fraction of aromatics in the liquid organic phase of the product.
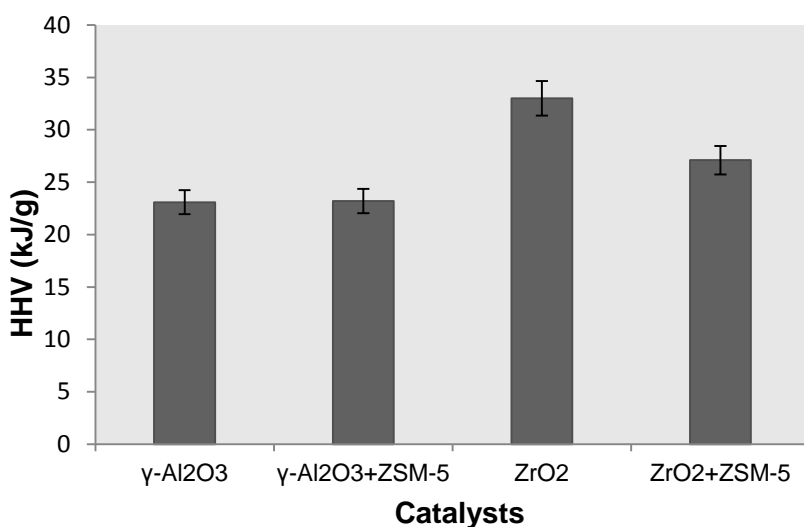
Figure 4.4: Comparison of heating value of deoxygenation liquid product using different catalysts
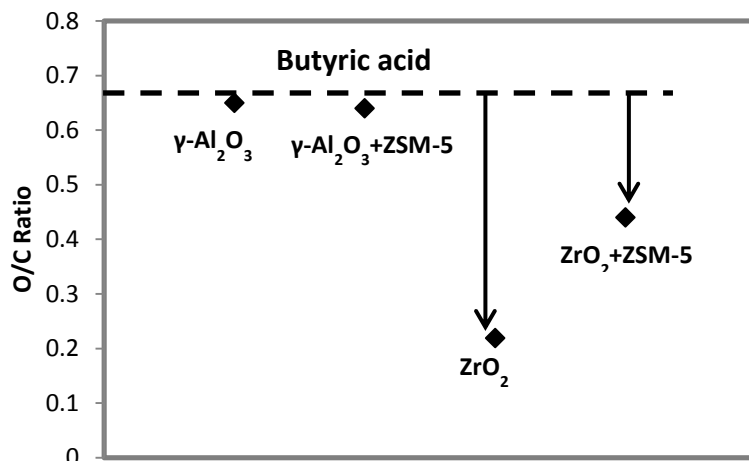
Figure 4.5: Change in oxygen to carbon mass ratio from feed that is butyric acid to the deoxygenation liquid product in case if different catalysts

In Figure 4.5, the oxygen to carbon mass ratio in the organic liquid product phase using different catalysts for the deoxygenation reaction are compared from the base line of pure butyric acid. The oxygen to carbon mass ratios shown in Figure 4.5 is calculated from the analyzed HHV of the products. The empirical correlation[36] that is used for calculating the O/C mass ratio from the HHV is as follows:

$$y = 14.371x^2 - 35.542x + 40.106 \tag{4.1}$$

Where y is the HHV of the sample in kJ/g and x is O/C mass ratio.

The main objective of this study is to deoxygenate butyric acid and produce hydrocarbons with a low O/C ratio so that it can be used as a fuel. Higher O/C ratio leads to low HHV and does not possess properties to qualify as a good fuel. Using four different catalysts and catalyst mixtures it is seen that ZrO_2 catalyzed deoxygenation liquid product possess the lowest O/C mass ratio compared to the products using other catalysts. So among the three acid catalyst and their mixtures shown in Figure 4.5, ZrO_2 removed the most of the oxygen from pure butyric acid and produced the desired liquid

organic product with an O/C mass ratio of 0.22. In cases of γ-Al_2O_3, and γ-Al_2O_3 and ZSM-5 catalyzed reactions, the conversion of butyric acid is very low and that is why in Figure 4.5 it is seen that the change in O/C mass ratio from feed to product are negligible.

4.5.2 Comparison of gas phase of the deoxygenation product from different catalysts

Gaseous product from the deoxygenation of butyric acid using different acid catalysts also shows difference in composition by FT-IR and GC analyses. In Figure 4.6, the IR spectra of the gaseous products of the deoxygenation processes on each of the four different catalyst and catalyst combinations are compared. The deoxygenation reaction temperature is kept constant at 400°C and the feed mass flow rate is 0.096 g/min.
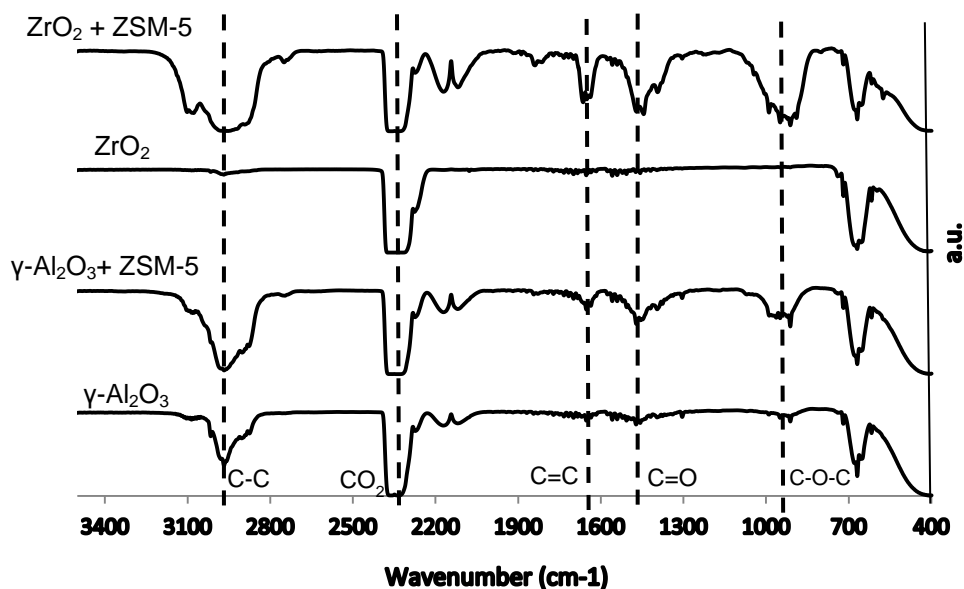
Figure 4.6: IR spectra of the gas product from deoxygenation of butyric acid on different catalysts at reaction temperature of 400°C

From Figure 4.6, it can be seen that the common component in all the gaseous product mixture is CO_2. Except for ZrO_2 catalyzed product gas all the other 3 cases produced some amount of hydrocarbon gases are formed as carbon-carbon single bond peak can be seen at wavenumber 2950 cm^{-1}. Upon using ZSM-5 in series with γ-Al_2O_3 or ZrO_2, more hydrocarbon gases and oxygenated-hydrocarbon gases are produced. This finding can be explained by previous studies which show that ZSM-5 can act as a cracking catalyst and breaks the hydrocarbon chains into smaller molecules due to the presence of strong Bronsted acid sites [5][37][38][39]. As from liquid organic product analysis we could see that in ZrO_2 catalyzed deoxygenation the conversion of butyric acid is the highest compared to the other catalysts, mostly producing heavy hydrocarbons. This finding is supported by the spectrum of the gas phase product from ZrO_2 catalyzed deoxygenation as no peaks for hydrocarbons or oxygenated hydrocarbons can be seen. For γ-Al_2O_3 catalyzed process, the conversion is very low but some hydrocarbon gases are generated. The gas chromatography analyses of the product gas show the change in composition in terms of change in CO_2 production and hydrocarbon gases for different catalysts (Table 4.4).

Table 4.4: Area composition of the product gas mixtures from GC analysis on different catalysts at 400°C operating temperature and 1.0 ml/min (0.096 g/min) feed flow rate.

Catalyst	Gas mass flow rate* (g/min)	Components (area%)	
		CO$_2$	C$_2$-C$_3$
γ-Al$_2$O$_3$	0.014	53.8	46.2
ZrO$_2$	0.023	88.7	11.3
ZrO$_2$+ZSM-5	0.041	38.6	61.4

*By subtraction of feed and liquid product mass flow rate

For ZrO_2 catalyzed deoxygenation, the gas phase of the product consisted of mostly CO_2 and negligible amount of C_2- C_3 hydrocarbons. But When ZSM-5 zeolite was used in the series after ZrO_2, a higher amount of lighter hydrocarbon gases were produced, which implies that some of the heavier hydrocarbon molecules generated on the ZrO_2 catalyst bed were being converted to smaller hydrocarbons due to the cracking activity of the ZSM-5 catalyst.

4.5.3 Effect of temperature

The effect of temperature on the deoxygenation of butyric acid on different catalysts studied from 300 to 600°C. The previous studies have shown that below 300°C carboxylic acid groups prefer to undergo esterification reaction on metal oxide catalysts rather than deoxygenation as the activation energy needed for esterification is much lower than ketonization[31]. From the discussion on section 4.1 and 4.2 it is seen that ZrO_2 had the highest conversion of butyric acid (table 4.2) the organic liquid product from this process had the lowest butyric acid content. Hence, ZrO_2 catalyzed process was further studied to find out the optimum operating range for a high conversion, yield and HHV. Catalytic activity on γ-Al_2O_3 was examined for two temperatures.
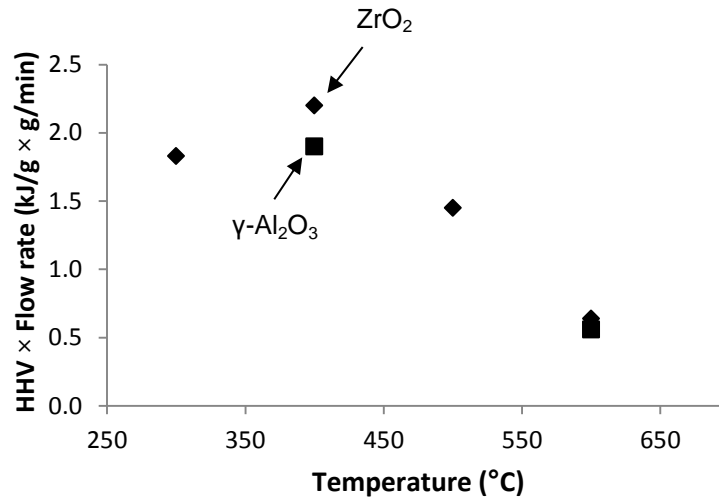
Figure 4.7: Energy flow rate in organic liquid product from deoxygenation of butyric acid at different reaction temperature

In Figure 4.7, the rate of energy flow out as organic liquid product is shown at four different temperatures for ZrO_2, and at two different temperatures for γ-Al_2O_3. The rate of energy flow (kJ/min) is calculated by multiplying the organic liquid product mass flow rate (g/min) with HHV of the respective product stream.

At 400°C, the rate of energy flow is the highest in the ZrO_2 catalyzed deoxygenation process. The rate of energy flow decreases at lower operating temperature due to the low HHV value of the product attributed to the low conversion of butyric acid. With increasing temperature to 500 and 600°C, the HHV value do not vary much but the yield of organic liquid product decreases which results in a lower rate of energy flow. For γ-Al_2O_3 catalyzed deoxygenation process similar trend can be found but the energy flow rate is much lower than that of ZrO_2 catalyzed process at 400°C, but almost similar at 600°C. In the case of γ-Al_2O_3, the HHV value is much lower than that in ZrO_2 but the

mass flow rate of organic liquid product is higher which makes the energy flow rate somewhat comparable.

Based on the GC-MS composition analysis of the organic liquid products (Table 4.5a), γ-Al₂O₃ has almost no activity in conversion of butyric acid at 400°C but at 600°C approximately 20% of the organic liquid product phase is consisted of n-heptanone and aromatics.

Table 4.5 (a): Major components of organic liquid product from γ-Al₂O₃ catalyzed deoxygenation

T (°C)	Yield (%)	Components	GC-MS Area %
400	85.9	4-heptanone	7.8
		butyric acid	90.2
		4-heptanone	11.6
		butyric acid	26.3
600	21.9	toluene	3.9
		0-xylene	2.8
		Benzene	1.5
		2-pentanone	1.0

Table 4.5 (b): Major components of organic liquid product from ZrO₂ catalyzed deoxygenation

T (°C)	Yield (%)	Components	GC-MS Area %
300	78.7	4-heptanone	21.6
		butyric acid	78.4
400	69.8	4-heptanone	92.4
		butyric acid	7.6
		4-heptanone	41.5
		3,4-heptadiene	5.7
500	44.1	3-heptene	4.4
		4-methyl3-heptene	3.2
		3-hexanone	3.0
		4-octanonone	2.2
		4-heptanone	30.1
		dimethyl-pentadiene	4.0
600	19.8	toluene	3.8
		paraxylene	3.3
		3-methyl phenol	2.4
		3-hexanone	2.0

For ZrO$_2$ (Table 4.5 b), a dramatically change in conversion of butyric acid can be seen from 300 to 400°C. At the higher temperatures of 500 and 600°C the conversion is even higher as almost negligible amount of butyric acid is detected in the organic phase. But at these high temperatures, high-carbon alkenes, cyclic hydrocarbons and aromatics in a small amount are getting produced along with 4-heptanone. As operating temperature increases, conversion of butyric acid increases but the yield of organic liquid decreases. Also with increasing temperature, 4-heptanone composition in the product decreases and other unsaturated hydrocarbons, cyclic compounds and aromatic composition increase. But the amount of aromatics produced at the high temperature on pure ZrO$_2$ catalyst bed is not comparable with that of the series bed of ZrO$_2$ and ZSM-5. In the series catalyst bed of ZrO$_2$ and ZSM-5 equal amount of n-heptanone and aromatic compounds are produced; the conversion of butyric acid is high as only 9% unconverted butyric acid can be seen in GC-MS analysis of the organic liquid product. But the HHV of the product is lower than that from ZrO$_2$ as ZSM-5 along with aromatization also catalyzes the cracking process of higher hydrocarbon molecules producing lighter hydrocarbons in the gaseous phase which was confirmed from the IR spectrum of the gaseous product phase from ZrO$_2$ and ZSM-5 catalyzed deoxygenation in Figure 4.6.
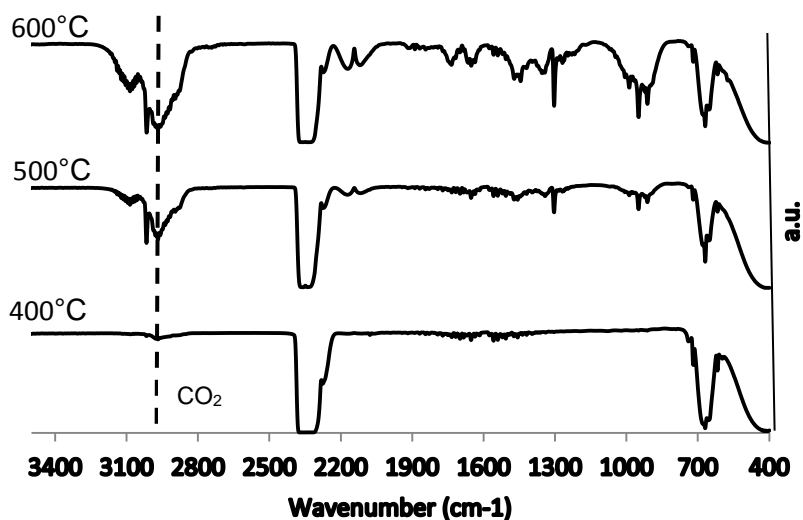
Figure 4.8: Comparison of IR spectra of ZrO2 catalyzed deoxygenation gaseous product mixture at different reaction temperature.

Effect of temperature on the gaseous product composition can be deduced from the IR spectra (Figure 4.8) of the product gas mixtures. At 400°C the gaseous product was mainly comprised of CO_2 which is represented by the peak at wavenumber 2350 cm^{-1}. At 500°C, along with the CO_2 peak, hydrocarbon and oxygenated hydrocarbon bonds could be seen. At 600°C, the hydrocarbon peaks were observed to be prominent and the area under the peaks increased indicating the presence of more hydrocarbons in the gaseous products. The higher the composition of hydrocarbons in the gaseous phase, the lower it was in the liquid phase. As a result the yield and as well as the higher heating value of the organic liquid phase decreased which can be supported by the liquid product heating value (HHV) analysis and mass flow rate. So from both the gaseous and organic liquid product phases analyses, it can be inferred that in ZrO_2 catalyzed deoxygenation of butyric acid the optimum temperature was 400°C in respect of desired organic liquid product yield and energy content.

4.5.4 Effect of Feed flow rate

The effect of feed flow rate in other words the effect of contact or residence time of the reactants on the catalyst bed are studied for pure γ-Al_2O_3 and pure ZrO_2 catalyst beds. First experiments were done with a higher feed flow rate of 0.96 g/min of butyric acid (1 ml/min volumetric rate, 0.18 and 0.22 h WHST for γ-Al_2O_3 and ZrO_2 catalyst beds, respectively) but almost no conversion could be seen for both cases of γ-Al_2O_3 and ZrO_2. But when the feed flow rate was lowered to one tenth (i.e., 0.096 g/min or 0.1 ml/min volumetric rate, 1.06 and 2.22 h on WHST γ-Al_2O_3 and ZrO_2 catalyst beds, respectively), in case of γ-Al_2O_3 catalyst the conversion did not change much which can be assumed from the organic product HHV value and the GC-MS analysis. On the other hand the lowered feed flow rate that is higher contact time has great effect in conversion of butyric acid on ZrO_2 catalyst bed. The heating value of the organic liquid phase of the deoxygenation product was found to increase much higher compared to that of high feed flow rate.
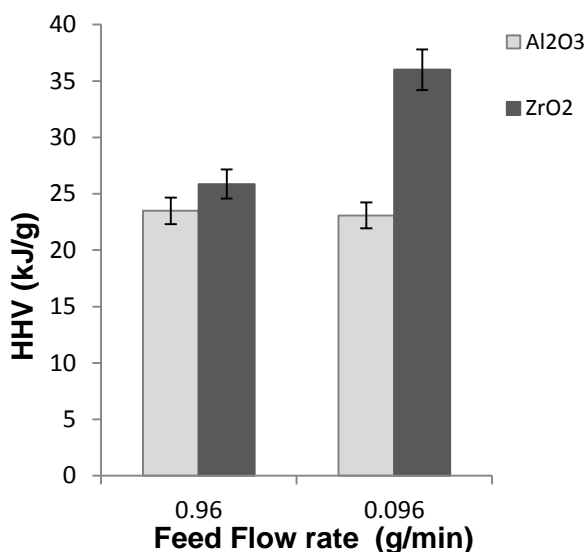
Figure 4.9: Comparison of liquid product heating value at different feed flow rates for γ-Al_2O_3 and ZrO_2 catalyzed deoxygenation

From Figure 4.9 it can be seen that even at higher feed flow rate (0.96 g/min) ZrO_2 catalyzed deoxygenation liquid product contains higher HHV than that of γ-Al_2O_3.
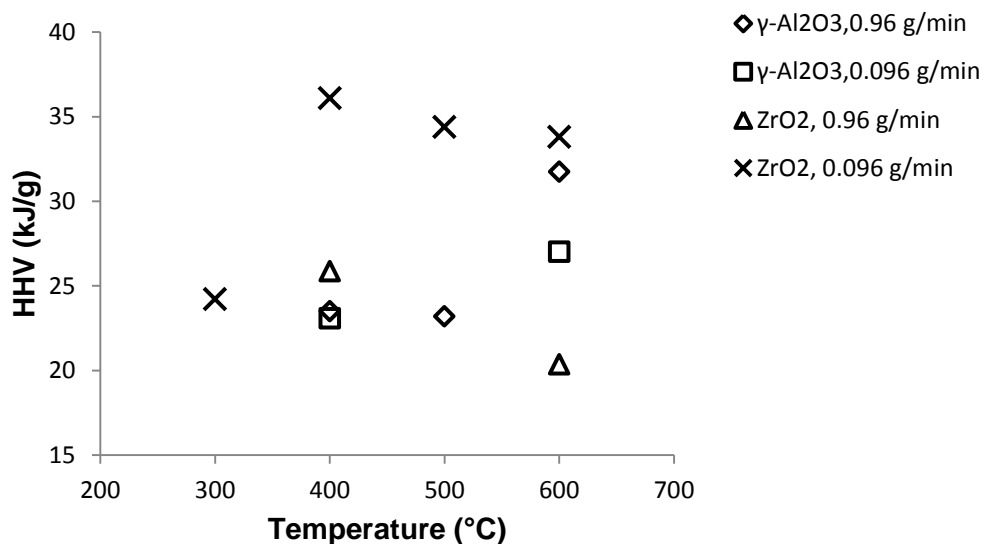
Figure 4.10: Effect of operating parameters on the energy content of both ZrO2 and γ-Al2O3 catalyzed deoxygenation organic liquid product

In Figure 4.10, effect of operating temperature and mass feed flow rate are shown on the product energy content in terms of HHV for ZrO_2 and γ-Al_2O_3 catalysts. At all operating temperatures and at the lower feed flow rate (0.096 g/min) the HHV of ZrO_2 catalyzed deoxygenation product was higher than that of γ-Al_2O_3 catalyzed product both at high and low feed flow rates. From all the experimental results presented in this study, it can be said that the catalyst activity of γ-Al_2O_3 for the deoxygenation of butyric acid or carboxylic acid groups was not high enough to lower the activation energy to the desired level for deoxygenation reactions to take place.

4.5.5 Effect of catalysts

Despite of all being acid catalysts, γ-Al_2O_3, ZrO_2 and ZSM-5 acted very differently in deoxygenation of butyric acid. γ-Al_2O_3 and ZrO_2 both have Lewis acid sites but ZSM-5 possess' both Bronsted and Lewis acid sites. Without using any metal precursor, γ-Al_2O_3 itself as a catalyst was not active enough to break the strong '–COOH' bond and remove the oxygen. The 'C=O' bond in the carboxylic acid group possess average bond energy approximately 833.17 kJ/mol which is higher than 'C=O' bond in ketones and aldehydes [20]. 'C-O' single bond possess an average bond energy of 351.7 kJ/mol. Compared to the 'C-C' single bond in hydrocarbons average bond energy of 335 kJ/mol, the 'C=O' bond is much higher and thus more difficult to break. Based on the experimental result in this study, γ-Al_2O_3 itself as a catalyst could not decrease the activation energy sufficiently to have the desired deoxygenation even at high WHST of 1.06 h and at 400°C operating temperature.

On the other hand, deoxygenation on ZrO_2 showed that at high WHST of 2.22 h (0.096 g/min) that is at higher residence time, above 90% conversion of butyric acid was achieved (Tables 4.2-4.3) at 400°C operating temperature. Though γ-Al_2O_3 and ZrO_2 both possess lewis acid sites and both of these metal oxides are known to convert carboxylic acid group to acetone, in this study it was found that ZrO_2 performs as an active catalyst for not only deoxygenation but condensation of butyric acid, producing mostly n-heptanone, water and carbon dioxide at 400°C. On the other hand for γ-Al_2O_3 no aqueous phase was produced and less than 30% butyric acid converted (Table 4.2).

ZSM-5

γ-Al$_2$O$_3$ ZrO$_2$
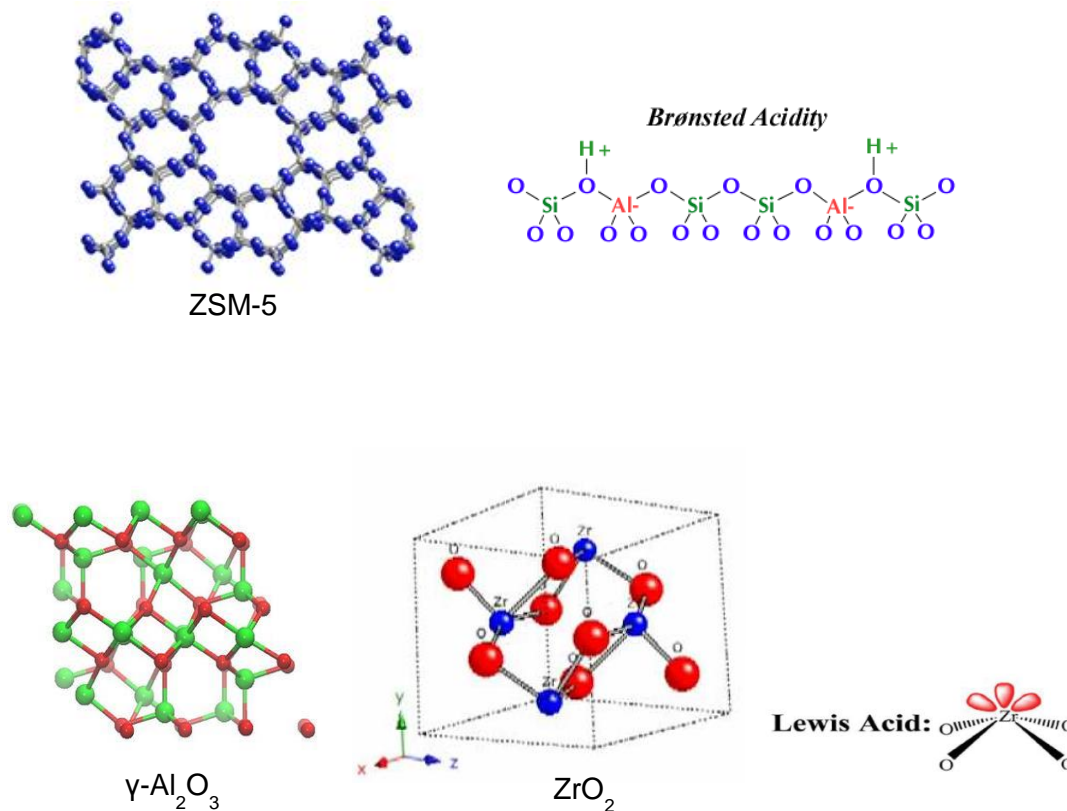
Figure 4.11: Lattice structures of the catalysts and types of acidity

The difference in surface properties and characteristics in γ-Al$_2$O$_3$ and ZrO$_2$ might play the main role in the activity specific to butyric acid deoxygenation. Though the ZrO$_2$ used in this study has a lower surface area and pore volume compared to that of γ-Al$_2$O$_3$, and both the catalysts were used in similar amounts (approximately 10.5 g), experimental results showed that ZrO$_2$ has better catalytic activity in this deoxygenation reaction. A possible reason behind this phenomenon can be attributed to the difference in bond lengths between the metal and oxygen atoms in each of the unit cell of γ-Al$_2$O$_3$ and ZrO$_2$. The bond length between Zr and O atoms is 2.45 Å whereas the bond length between Al and O atoms is 1.89 Å. The greater bond lengths in ZrO$_2$ unit cell possibly provide more space to butyric acid to interact with the metal atom on the surface as butyric acid is

bulkier than acetic acid (Figure 4.12). In previous studies γ-Al₂O₃ is used as catalyst for conversion of acetic acid[40][24]. But in this study for butyric acid γ-Al₂O₃ showed negligible conversion.
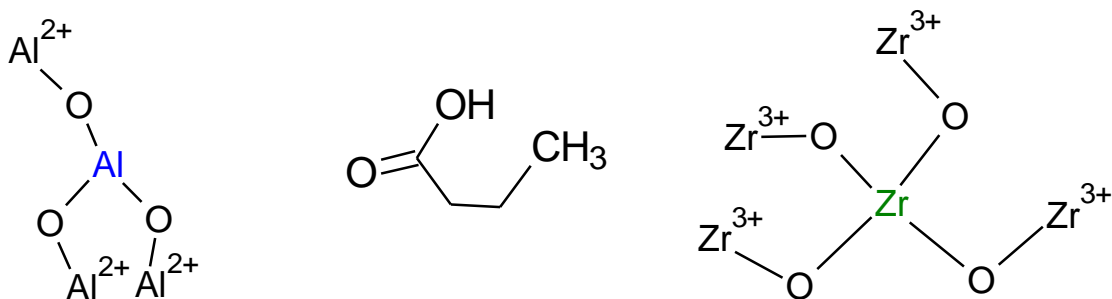
Figure 4.12: Molecular structures of γ-Al₂O₃, ZrO₂ and butyric acid

Also the amphoteric properties of ZrO_2 catalyst might have provided some additional benefits in catalyst activity for deoxygenation of butyric acid. ZrO_2 has both acid and basic sites; the exposed metal cations on the catalyst surface acts as the lewis acid cites and oxide anions act as lewis basic sites. For conversion of carboxylic acids it utilizes the dehydration sites i.e. the acid sites and the dehydrogenation sites as well i.e. the basic sites of the catalyst surface and thus ZrO_2 acts as a better catalyst for butyric acid[22]. The higher oxygen concentration in the ZrO_2 molecular structure contributes in higher aprotonic charge (3+) on Zn cation which makes it a stronger acid site for the deoxygenation catalysis compared to γ-Al₂O₃ which contains smaller positive charged metal ions.

Introducing ZSM-5 in a series packed bad produced aromatic products from 4-heptanone which was formed after deoxygenation on ZrO_2 catalyst. Though the cracking catalytic activity of ZSM-5 also gave higher yield of light hydrocarbon and carbon dioxide and decreased the yield of organic liquid hydrocarbon, it selectively

aromatized the deoxygenation product to produce ethyl benzene, toluene, para-xylene, naphthalene and other aromatics.

4.5.6 Deactivation of ZrO₂ catalyst
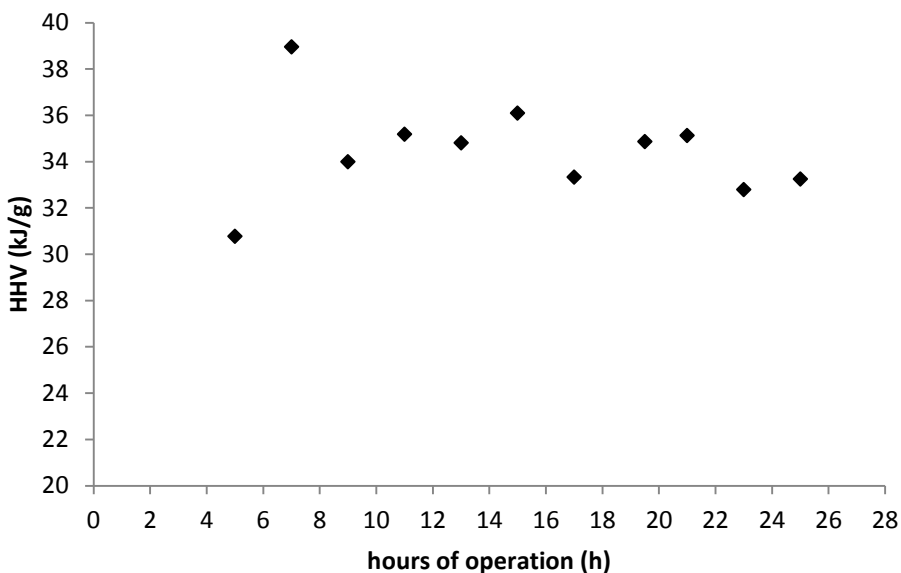
Figure 4.13: Catalyst performance in terms of HHV of the organic liquid product in 27 hours of continuous operation

As ZrO$_2$ showed good performance in conversion of butyric acid, the stability of the performace of this catalyst was tested in a continuous run of 27 hours for the reaction. Organic liquid product sample has been collected every two hours and the HHV was checked to find when the product quality started to deteriorate (Figure 4.13). Till 1st 6 hours of operation on the fresh catalyst the product HHV increased, but starting from 8 hours it started being stable and varied little. The HHV of the product after every two hours till 27 hours of continuous operation showed that the catalyst activity did not change that much as the product quality remained almost same. Also from the BET surface area and pore volume analysis of the fresh ZrO$_2$ catalyst and after continuous

use of 27 hours without flowing any nitrogen gas in between, it was seen that the surface area and pore volume have not decreased much (Table 4.6).

Table 4.6: Surface area and pore volume of ZrO$_2$ catalyst before and after 27-hr continuous use

Time (h)	Surface area (m^2/g)	Pore volume (cc/g)
0	55.6	0.259
27	48.9	0.249

Based on the results in Figure 4.13 and Table 4.6 it can be deduced that ZrO$_2$ is a stable catalyst in terms of performance in deoxygenation of butyric acid and also coke deposition was found to be minimum up to 27 hours of continuous operation.

From table 4.2 and from the effect of catalyst, feed flow rate and operating temperature on the deoxygenation of butyric acid, it was observed that ZrO$_2$ successfully catalyzed the deoxygenation process at the WHST of 2.22 h (0.096 g/min) and 400°C and produced an organic liquid product with a HHV of 36 kJ/g. For converting butyric acid directly to aromatics, the butyric acid feed was passed on a catalyst bed of ZrO$_2$ followed by ZSM-5 in a series in a single step reaction.

4.6 Conclusion

Comparing the rate of conversion of butyric acid and product quality in terms of HHV, ZrO$_2$ was found to be a better catalyst than γ-Al$_2$O$_3$. In γ-Al$_2$O$_3$ catalyzed process no dehydration took place so the oxygen removal was also minimal but in ZrO$_2$ catalyzed process, a separate aqueous product phase was formed showing the removal of oxygen in the form of water. By varying the temperature and feed flow rate, it was found that at

400°C and a low mass feed flow rate of 0.096 g/min (0.45 h weight hourly space velocity) the organic liquid product from the deoxygenation of butyric acid possessed a higher heating value of 36 kJ/g. Here, the organic liquid phase contained above 90% of 4-heptanone, but more cyclic and aromatic compounds were found to be produced at the higher temperatures. With increasing temperature, the organic liquid product yield decreased and gaseous product yield increased due to cracking at higher temperatures. On the series catalyst bed of ZrO_2 and ZSM-5, butyric acid first got converted to ketone and then to aromatic compounds such as ethyl benzene, toluene, para-xylene, naphthalene and other aromatics. Almost equal compositions of 4-heptanone and aromatics were found at 400°C. This series catalyst bed can be used for a single step conversion of butyric acid to aromatic hydrocarbons.

References

[1]   P. H. Pfromm, V. Amanor-Boadu, R. Nelson, P. Vadlani, and R. Madl, "Bio-butanol vs. bio-ethanol: A technical and economic assessment for corn and switchgrass fermented by yeast or Clostridium acetobutylicum," *Biomass and Bioenergy*, vol. 34, no. 4, pp. 515–524, Apr. 2010.

[2]   M. Köpke and P. Dürre, "Biochemical production of biobutanol.," in *Handbook of biofuels production processes and technologies*, R. Luque, J. Campelo, and J. H. Clark, Eds. Woodhead Publishing Ltd, 2011, pp. 221–257.

[3]   T. C. Ezeji, N. Qureshi, and H. P. Blaschek, "Bioproduction of butanol from biomass: from genes to bioreactors.," *Curr. Opin. Biotechnol.*, vol. 18, no. 3, pp. 220–227, Jun. 2007.

[4]   P. Dürre, "Fermentative butanol production: bulk chemical and biofuel.," *Ann. N. Y. Acad. Sci.*, vol. 1125, pp. 353–362, Mar. 2008.

[5]   S. Nahreen and R. B. Gupta, "Conversion of the Acetone–Butanol–Ethanol (ABE) Mixture to Hydrocarbons by Catalytic Dehydration," *Energy & Fuels*, vol. 27, no. 4, pp. 2116–2125, Apr. 2013.

[6]   R. B. Gupta and A. Demirbas, *Gasoline, Diesel and Ethanol Biofuels from Grasses and Plants*. Cambridge University Press, 2010, pp. 140–157.

[7]   T. C. Ezeji, N. Qureshi, and H. P. Blaschek, "Acetone butanol ethanol (ABE) production from concentrated substrate: reduction in substrate inhibition by fed-batch technique and product inhibition by gas stripping.," *Appl. Microbiol. Biotechnol.,* vol. 63, no. 6, pp. 653–658, Feb. 2004.

[8]   C. Weber, A. Farwick, F. Benisch, D. Brat, H. Dietz, T. Subtil, and E. Boles, "Trends and challenges in the microbial production of lignocellulosic bioalcohol fuels.," *Appl. Microbiol. Biotechnol.*, vol. 87, no. 4, pp. 1303–1315, Jul. 2010.

[9]   D. T. Jones and D. R. Woods, "Acetone-butanol fermentation revisited.," *Microbiol. Rev.*, vol. 50, no. 4, pp. 484–524, Dec. 1986.

[10]   W.-C. Huang, D. E. Ramey, and S.-T. Yang, "Continuous Production of Butanol by Clostridium acetobutylicum Immobilized in a Fibrous Bed Bioreactor," *Appl. Biochem. Biotechnol.*, vol. 115, no. 1–3, pp. 0887–0898, 2004.

[11]   D. Ramey, "Continuous two stage, dual path anaerobic fermentation of butanol and other organic solvents using two different strains of bacteria," *US Pat. 5,753,474*, vol. 258, no. 1980, pp. 253–258, 1998.

[12]   X. Gao, H. Zhao, G. Zhang, K. He, and Y. Jin, "Genome shuffling of Clostridium acetobutylicum CICC 8012 for improved production of acetone-butanol-ethanol (ABE)," *Curr. Microbiol.*, vol. 65, pp. 128–132, 2012.

[13]   J. Zigová, E. ŠturdÄ±Ì• k, D. Vandák, and Š. Schlosser, "Butyric acid production by Clostridium butyricum with integrated extraction and pertraction," *Process Biochem.*, vol. 34, pp. 835–843, 1999.

[14]   O. Mutschlechner, H. Swoboda, and J. R. Gapes, "Continuous two-stage ABE-fermentation using Clostridium beijerinckii NRRL B592 operating with a growth rate in the first stage vessel close to its maximal value.," *J. Mol. Microbiol. Biotechnol.*, vol. 2, no. 1, pp. 101–105, Jan. 2000.

[15]   N. Qureshi and H. P. Blaschek, "Production of acetone butanol ethanol (ABE) by a hyper-producing mutant strain of Clostridium beijerinckii BA101 and recovery by pervaporation.," *Biotechnol. Prog.*, vol. 15, no. 4, pp. 594–602, 1999.

[16]   M. Dwidar, J.-Y. Park, R. J. Mitchell, and B.-I. Sang, "The future of butyric acid in industry.," *ScientificWorldJournal.*, vol. 2012, pp. 1–9, Jan. 2012.

[17]   M. E. Wright, B. Harvey, and R. L. Quintana, "Creating new NAVY fuels from biobutanol," *ACS , Div Fuel Chem*, vol. 53, no. 1, pp. 252–253, 2008.

[18]   P. Anbarasan, Z. C. Baer, S. Sreekumar, E. Gross, J. B. Binder, H. W. Blanch, D. S. Clark, and F. D. Toste, "Integration of chemical catalysis with extractive fermentation to produce fuels.," *Nature*, vol. 491, no. 7423, pp. 235–239, Nov. 2012.

[19]   B. G. Harvey and H. a. Meylemans, "The role of butanol in the development of sustainable fuel technologies," *J. Chem. Technol. Biotechnol.*, vol. 86, no. 1, pp. 2–9, Jan. 2011.

[20]   S. J. Blanksby and G. B. Ellison, "Bond dissociation energies of organic molecules.," *Acc. Chem. Res.*, vol. 36, no. 4, pp. 255–263, Apr. 2003.

[21]   R. M. West, E. L. Kunkes, D. a. Simonetti, and J. a. Dumesic, "Catalytic conversion of biomass-derived carbohydrates to fuels and chemicals by formation and upgrading of mono-functional hydrocarbon intermediates," *Catal. Today*, vol. 147, no. 2, pp. 115–125, Sep. 2009.

[22]   T. N. Pham, T. Sooknoi, S. P. Crossley, and D. E. Resasco, "Ketonization of Carboxylic Acids: Mechanisms, Catalysts, and Implications for Biomass Conversion," *ACS Catal.*, vol. 3, no. 11, pp. 2456–2473, Nov. 2013.

[23]   A. J. M. Glinski, J. Kijenski, "Ketones from monocarboxylic acids : Catalytic ketonization over oxide systems," *Appl. Catal. A Gen.*, vol. 128, pp. 209–217, 1995.

[24]   V. P. R. Pestman, R.M. Koster, A. van Duijine, J.A.Z. Pieterse, "Reactions of Carboxylic Acids on Oxides 2. Bimolecular Reaction of Aliphatic Acids to Ketones," *J. Catal.*, vol. 168, no. 2, pp. 265–272, Jun. 1997.

[25]   R. Pestman, A. van Duijne, J. a. Z. Pieterse, and V. Ponec, "The formation of ketones and aldehydes from carboxylic acids, structure-activity relationship for two competitive reactions," *J. Mol. Catal. A Chem.*, vol. 103, no. 3, pp. 175–180, Nov. 1995.

[26]   O. Nagashima, S. Sato, R. Takahashi, and T. Sodesawa, "Ketonization of carboxylic acids over CeO2-based composite oxides," *J. Mol. Catal. A Chem.*, vol. 227, no. 1–2, pp. 231–239, Mar. 2005.

[27]   K. Parida and H. Mishra, "Catalytic ketonisation of acetic acid over modified zirconia: 1. Effect of alkali-metal cations as promoter," *J. Mol. Catal. A Chem.*, vol. 139, pp. 73–80, 1999.

[28]   Y. a. Zaytseva, V. N. Panchenko, M. N. Simonov, a. a. Shutilov, G. a. Zenkovets, M. Renz, I. L. Simakova, and V. N. Parmon, "Effect of Gas Atmosphere on Catalytic Behaviour of Zirconia, Ceria and Ceria–Zirconia Catalysts in Valeric Acid Ketonization," *Top. Catal.*, vol. 56, no. 9–10, pp. 846–855, Apr. 2013.

[29]   A. A. Shutilov, M. N. Simonov, Y. A. Zaytseva, G. A. Zenkovets, and I. L. Simakova, "Phase composition and catalytic properties of ZrO2 and CeO2-ZrO2 in the ketonization of pentanoic acid to 5-nonanone," *Kinet. Catal.*, vol. 54, no. 2, pp. 184–192, Apr. 2013.

[30]   A. Ignatchenko, "Density Functional Theory Study of Carboxylic Acids Adsorption and Enolization on Monoclinic Zirconia Surfaces," *J. Phys. Chem. C*, vol. 115, no. 32, pp. 16012–16018, Aug. 2011.

[31] C. A. Gaertner, J. C. Serrano-Ruiz, D. J. Braden, and J. A. Dumesic, "Catalytic coupling of carboxylic acids by ketonization as a processing step in biomass conversion," *J. Catal.*, vol. 266, no. 1, pp. 71–78, Aug. 2009.

[32] P. Oliveira, P. Borges, R. R. Pinto, M. A. N. D. A. Lemos, F. Lemos, J. C. Védrine, and F. R. Ribeiro, "Light olefin transformation over ZSM-5 zeolites with different acid strengths – A kinetic model," *Appl. Catal. A Gen.*, vol. 384, no. 1–2, pp. 177–185, Aug. 2010.

[33] R. J. Quann, L. A. Green, S. A. Tabak, and F. J. Krambeck, "Chemistry of olefin oligomerization over ZSM-5 catalyst," *Ind. Eng. Chem. Res.*, vol. 27, no. 4, pp. 565–570, 1988.

[34] A. Pulido, B. Oliver-Tomas, and M. Renz, "Ketonic decarboxylation reaction mechanism: a combined experimental and DFT study," *ChemSusChem*, vol. 6, pp. 141–151, 2013.

[35] F. Bettelheim, W. Brown, M. Campbell, S. Farrell, and O. Torres, *Introduction to organic and biochemistry*, 9th ed. 2012, pp. 187–228.

[36] S. Kumar, "Hydrothermal treatment for biofuels: Lignocellulosic biomass to bioethanol, biocrude, and biochar," Auburn University, 2010.

[37] A. Corma and A. V. Orchillés, "Current views on the mechanism of catalytic cracking," *Microporous Mesoporous Mater.*, vol. 35–36, pp. 21–30, Apr. 2000.

[38] "Catalytic activity of Bronsted acid sites in zeolites: Intrinsic activity, rate-limiting step, and influence of the local structure of the acid sites," *J. Catal.*, vol. 244, no. 2, pp. 163–168, Dec. 2006.

[39] J. A. van Bokhoven, B. A. Williams, W. Ji, D. C. Koningsberger, H. H. Kung, and J. T. Miller, "Observation of a compensation relation for monomolecular alkane cracking by zeolites: the dominant role of reactant sorption," *J. Catal.*, vol. 224, no. 1, pp. 50–59, May 2004.

[40] V. P. R. Pestman, R.M. Koster, J.A.Z. Pieterse, "Reactions of Carboxylic Acids on Oxides 1. Selective Hydrogenation of Acetic Acid to Acetaldehyde," *J. Catal.*, vol. 168, no. 2, pp. 255–264, Jun. 1997.

Chapter 5

Catalytic upgrading of methane to higher hydrocarbon in by a non-oxidative chemical conversion

5.1 Introduction

Methane, the first member of the organic hydrocarbons, possess' very significant chemical properties because of its very stable tetrahedral structure. Methane itself is valuable as a combustible gaseous fuel for vastly used for electric power generation, Industrial heating and raw material especially for hydrogen production and for domestic cooking and HVAC systems. In 2013, the United States consumed approximately 26.13 trillion cubic feet (Tcf) of natural gas.

Table 5.1: U.S. natural gas consumption by major end uses, 2013 [1]

End uses	mount (Tcf)	Share of Total
Electric power generation	8.15	31%
Industrial	7.41	28%
Residential	4.91	19%
Commercial	3.28	13%
Lease and plant fuel consumption	1.48	6%
Pipeline and distribution	0.86	3%
Vehicle fuel	0.03	0.03%

A very minute amount of the total share natural gas is being used as vehicle fuel due to and the inconvenience of using gaseous fuel for regular automobile design. Also storage and transportation of gaseous fuel, to make it available all over the country is still not a feasible process in USA.

There are various sources from which gaseous methane is produced. The main source of methane is natural gas consisting of above 70% of methane found in on shore and off shore gas wells. With the discovery of huge amount of shale gas in the last two decades increased the production of dry natural gas in USA which effected in reduction of price of natural gas from $10 per mBTU to half of it i.e. $5 per mBTU in the duration of 2 years, 2008 to 2010 (Figure 5.1) and remained consistently low till 2014 [1].

energy spot prices
2012 dollars per million Btu

Source: EIA, Annual Energy Outlook 2014 Early Release
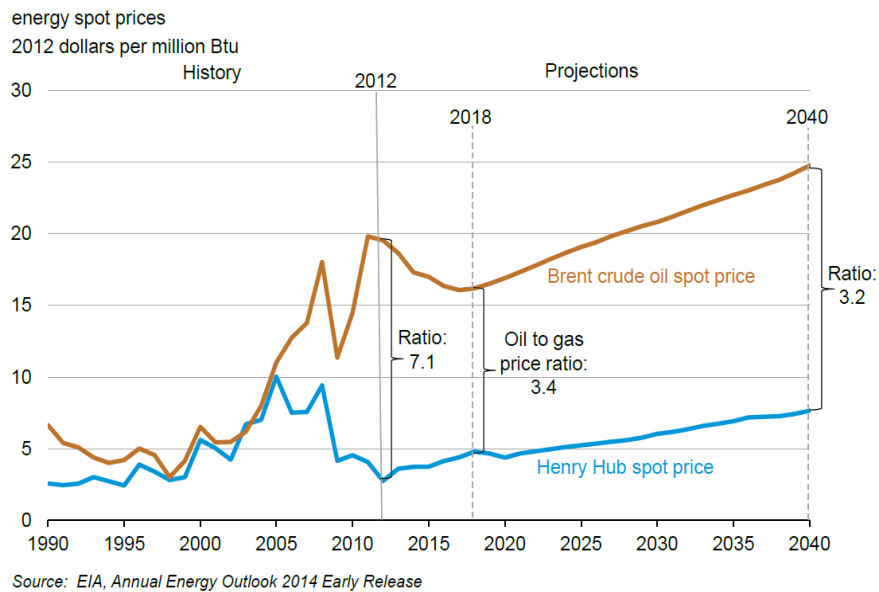
Figure 5.1: Projection of price per million BTU of Henry Hub natural gas compared to Bent crude oil

Other than mineral resources, methane is also found from renewable resources like biomass, domesticated animal and dairy waste and compost, landfill, industrial and municipal waste etc. But capturing all these naturally generated methane and proper

storage is difficult. For methane production from biomass in an industrially controlled system, there are two principal processes: i) thermal gasification ii) biological methanogenesis. Thermal gasification process is very energy intensive on the other hand biological conversion process needs lower energy but anaerobic microbial digestion and conversion to methane depends on the quality of the feed material and its biodegradability[1]

Also methane emission to the atmosphere is very harmful for the ozone layer as it is a 21 times higher potential greenhouse gas (GHG) compared to CO_2. Approximately 560 million metric tons CO_2 equivalent methane gas was emitted in the year 2012 according to US Environmental Protection Agency (EPA) report [2]. Government has taken strategies to reduce the emission by making new policies for lowering the allowable limit for industries as well as encouraging them by providing subsidies for reducing carbon footprints [3]. These government subsidies can help the renewable biomethane sources to become more compatible in term of cost effectiveness to be used as energy source or as raw materials for chemical processes in comparison with the petroleum and mineral sources.

Methane, being the main component of shale gas and renewable natural gas, has abundant resources at present. So it can be considered using methane as source of energy other than for power generation and industrial utility usage. From Table 5.1, it can be seen that less than 1% natural gas resource is being used as vehicle fuel. The main reason behind this low representation in transportation sector is mostly due to the inconvenience caused by the low density, undeveloped storage and transportation facilities and suitability of using it for the huge number of automobile engines already on the road and in market. Converting methane to transportation fuel or value added

chemicals have drawn interests both to the academic and industrial research community since production of methane is increasing in USA.

Conversion of methane to higher hydrocarbon gases and liquids has been investigated extensively in the last two decades. Different chemical reactions and processes with different additives and raw materials and catalysts have been studied for activation of methane and conversion to value added chemicals. Among all the processes of methane conversion, the most conspicuous ones are as follows[4]:

    a) Steam and CO_2 reforming or partial oxidation of methane to form syngas (CO +H_2) followed by Fischer-Tropsch chemistry

    b) Direct oxidation of methane to methanol and formaldehyde

    c) Oxidative coupling of methane to ethylene

    d) Non-oxidative direct conversion to aromatics and hydrogen

Steam reforming of methane is the most well established process among all of the processes mentioned above. Steam reforming is highly endothermic process and also requires high pressure of steam[4]. The catalysts used for the steam reforming reaction also face the coking problem and thus has a high deactivation rate due to the lack of heat circulation in the catalyst bed[4]. Other than Fischer-Tropsch synthesis process a considerable application of steam reforming of methane is performed for ammonia synthesis via production of syngas in chemical and fertilizer industries[5].

Direct conversion of methane to C_1 oxygenates takes place under specific reaction temperature range of 350 to 500°C with a definite oxygen flow as the limiting agent to control the oxidation of methane to produce methanol or formaldehyde [6]. Different solid catalysts especially metal salts such as Pt or Pd salts in sulfuric acid solvent found to

increase the yield of methanol by producing an intermediate product of methyl bisulphate a very high yield of 72%. After hydrolyzing the methanol product of difficult to separate from the sulfuric acid solvent and also due to the corrosive property of the strong acid is detrimental for the reactor and thus difficult for industrial applications [7][6].

Oxidative coupling of methane has drawn interest with the increasing demand of ethylene product in the polymerization industry. In this process, separation of oxygen form air is required which increases cost as well as the usual yield of ethylene is 25% to 30% as a significant amount of methane is oxidized to produce CO_2[8]. The pioneer of this work Keller and Bhasin [9] showed the results of OCM process with different metal oxide catalysts. In latter works SrO/La_2O_3 and Mn/Na_2WO_4 showed better results with 20% CH_4 conversion and 80% selectivity of C_2 hydrocarbon products [10]. But in this process it is seen that high selectivity of C_2 hydrocarbons are achieved only at low methane conversion [6]. Also the high reaction temperature range of the oxidative coupling process leads to deterioration of catalyst activity made the industrial application of this process more difficult.

Facing the limitations and challenges of oxidative conversion routes for methane to higher hydrocarbon or oxygenate chemicals; the non-oxidative single step catalytic conversion of methane to hydrocarbon or aromatic products has drawn more attention of researchers for upgrading methane. In a gas to liquid (GTL) process plant, 60% of the capital cost is associated with the synthesis gas production unit which is one of the largest motivation to come up with a cost effective process of methane conversion to higher hydrocarbon avoiding the intermediate step via synthesis gas production [5]. Finding out the right catalyst for high conversion of methane and higher yield of aromatics or hydrocarbon products with considerable selectivity is a very challenging area of research in Chemical Engineering.

The different routes of direct and indirect methane conversion and upgrading to useful chemical products and hydrocarbon can be shown in a simplified way with following diagram:
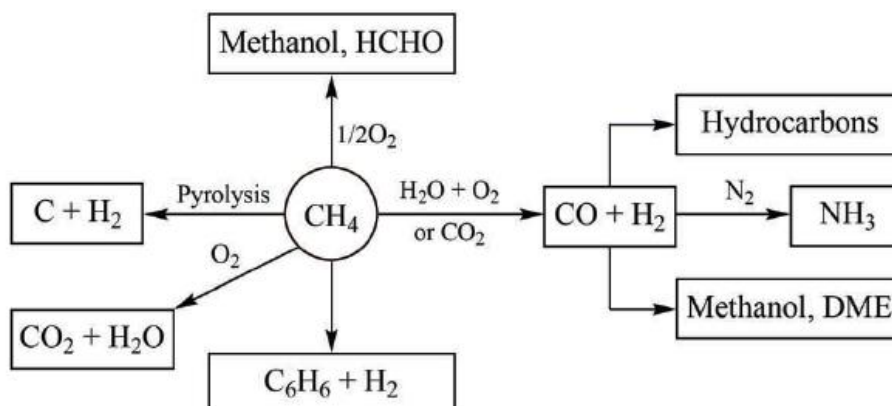
Figure 5.2: Different routes of methane conversion[11]

This experimental study focuses on the direct conversion of methane to higher hydrocarbon gases or liquids by application of catalysis and heat energy in an oxygen-free operating condition. In this condition, from Figure 5.3 it can be predicted that probable products will be either the pyrolysis products, that is carbon black and hydrogen or the dehydroaromatization products that is higher hydrocarbon gases and aromatics along with hydrogen. The non-oxidative conversion is the most attractive process of upgrading methane for industrial scale production of value added higher hydrocarbons as it is a single step conversion process and mostly controlled by catalysis. It has a potential to be a very cost efficient process because of the simplicity of the process operation parameters and technology. Again to find out the right catalyst for activation of methane and to undergo coupling or ring formation is very challenging as the stable and symmetrical structure of methane results in a high activation energy of 425 kJ/mol and has no functional group to contribute in polarity or magnetic moment

which can make a chemical substituent vulnerable to be attacked by other molecules or ions [5]. Researchers tried to study the activity of different metal catalysts specially transition metal catalysts for methane activation reaction. Different metal catalysts and support combinations found to catalyze the methane activation reaction giving a range of end products from ethane and ethylene to liquid aromatic products [11][4]. From the experimental studies on transition meatal catalysts for methane activation and conversion to benzene products, the activity of the catalysts were found to be in the decreasing order of Mo > W > Fe > V > Cr on ZSM-5 Zeolites support. Also the increasing number of Bronsted acid sites depending on the silica to alumina ratio in the zeolite catalyst has positive effect in methane conversion[12]. 2.5% loading of tungsten metal catalyst on ZSM-5 support also showed fair performance when 1.5% Zn-H_2SO_4 promoter is applied under reaction condition of 1123 K and 0.1 MPa, a methane conversion of 23% has been reached with a 96% selectivity of benzene[13].

For dehydro-aromatization of methane, molybdenum as a single metal catalyst on ZSM-5, zeolite support has been found to perform the best though the highest conversion achieved is in the range of 18% to 20% [4],but the selectivity towards benzene and naphthalene is very high compared to that of aliphatic hydrocarbon when ZSM-5 is used as the support as ZSM-5, zeolites has the special microporous framework which enables ring formation after activation of methane to methyl radicals[12]. Also the Bronsted acidity of ZSM-5 plays a considerable role in the catalyst activity[8]. 3% loading of molybdenum on ZSM-5, zeolite support contributes in better conversion of methane and less coke formation compared to the other supports like Al_2O_3, SiO_2, mordenite etc. But at high reaction temperature like 900 to 1000 K the conversion of methane is still pretty low in the range of 8 to 10% and for higher operating temperature methane conversion increases but the catalyst stability is very poor and the conversion rate deteriorates with

10 to 15 hours of operations[14][8]. To overcome these challenges, finding out a more efficient bi-functional catalyst has remained to be a very potential field of research.

As the transition metal catalysts like molybdenum, tungsten, iron, vanadium, chromium, nickel, zinc have been studied extensively for catalyzing methane activation reaction and were found to demonstrate low performance in terms of methane conversion, other metals like ruthenium and platinum also have drawn interests of the researchers. Platinum being a very expensive metal is not an attractive option for industrial application but the price of bulk ruthenium is one tenth of that of platinum and a small metal loading of 2% to 6% will be economically feasible. Studies have been done on ruthenium catalyst on silica support for oxygen-free conversion of methane. A two-step conversion is done where at the first step activation of methane is done at the temperature range of 400 to 800 K which produce surface carbonaceous species like methylidene and vinylidine intermediates. At the second step re-hydrogenation of the carbonaceous species is performed at lower temperature at the range of 360 to 380 K to generate ethane and the yield of ethane was found to be 13% to 15% [15]. In another study it is mentioned that for ruthenium catalyst on silica support methane undergoes dissociative adsorption on the catalyst surface and produces three different types of carbonaceous species and this process requires activation energy of 22 kcal/mol. Similarly after hydrogenation aliphatic hydrocarbons like ethane and propane are formed and the yield is a function of carbon coverage of the catalyst surface and also hydrogenation temperature[16]. Studies on two step conversion of methane was pioneered by two different research groups since 1991 and both the groups studied the kinetic and thermo-dynamical constraints for the direct conversion of methane to higher hydrocarbons and found that compared to Ni, Mo, W and other transition metals, Ru, Co and Pt perform better by lowering the activation energy of the exothermic chemisorption

process on the catalyst surface and thus contributes in increased methane activation and formation of intermediates at moderate operating conditions [17],[18],[19].

Though two step conversion of methane has been studied on ruthenium catalyst, there is no significant research work found on single step conversion over ruthenium metal catalyst on ZSM-5 zeolite support. Industrial research has been done on conversion of synthesis gas (CO and H_2) to higher hydrocarbon with above 80% selectivity towards the products in the range of C_{12} to C_{20}[20]. For non-oxidative direct conversion of methane, ruthenium has been added with the Mo/HZSM-5 catalyst as a promoter in another study where it showed better performance in conversion and benzene yield than only molybdenum on HZSM-5 catalyzed processes[21]. This study showed that the number of strong acid sites decreased with the increase of ruthenium loading but at the same time the intermediate and weak acid sites of the Mo/HZM-5 catalyst increased [21]. Another study of oxygen-free methane conversion showed the effect of varying the molybdenum metal loading (1 to 3 wt%) on HZSM-5 support keeping the ruthenium loading constant (0.15 wt.%). The catalysts were prepared by ion exchange and vapor deposition method and showed lower rate coke formation and better stability of catalyst at operating temperature of 600°C but the methane conversion rate was found to be still pretty low [22]. Further study is required in this field to increase the conversion of methane and yield of higher hydrocarbon at the same time having better catalyst stability.

In this work activity of ruthenium single metal catalyst supported by ZSM-5 zeolites of Si/Al ratio of 23:1 has been studied for a range of operating temperature and also variable metal loading for conversion of methane to higher hydrocarbons in a single step process. Also to understand the contribution of ZSM-5-zeolites in the conversion

135

process, the same ruthenium metal loading on SiO_2 support has been studied as well to compare the quality of product and conversion of methane.

Over other transition metal catalysts ruthenium has specific advantages which are supposed to contribute in more efficient conversion of methane. Ruthenium possess' optimum metal carbon bond strength which is not too low so that after formation of the Ru-C bond, it gets time to be converted to surface carbonaceous species or intermediates. Again the bond strength is not too high so that the intermediate species can undergo coupling or aromatization processes[15]. Also contributing in lowering the activation energy of the methane chemisorption exothermic process on the catalyst surface, ruthenium metal catalyst may show better stability as operating conditions will be moderate[17].

5.2 Objectives

The objective of this work is catalytic conversion of methane derived from bio resources to higher hydrocarbon in an oxygen-free route.

- (I) Preparing suitable bi-functional catalyst for methane activation and conversion to higher hydrocarbon molecules and characterization of the catalysts.
- (II) Improving the conversion efficiency of methane using ruthenium metal as a catalyst on ZSM-5 zeolite support in a one-step conversion process.
- (III) Studying catalyst activity of different loadings of ruthenium metal on ZSM-5 and SiO_2 support.
- (IV) Optimizing the operating temperature of methane conversion on ruthenium catalyst bed.
- (V) Studying catalyst activity of series bed of Ru/SiO_2 followed by ZSM-5 to increase the selectivity of aromatic products.

136

5.3 Experimental

5.3.1 Catalyst Preparation

The metal precursor used for preparing the catalyst was ruthenium(III) nitrosyl nitrate solution in dilute nitric acid (linear formula $Ru(NO)(NO_3)_x(OH)_y$, x+y=3) with a composition of 1.5% Ru, was purchased from Sigma-Aldrich. The density of the solution was 1.07 g/ml at 25°C and molecular weight 318.10. A nitrate precursor was chosen over chloride salt solution of ruthenium as chloride ions are difficult to remove fully by reduction process [15].   As support material ZSM-5, zeolite and silica have been used separately. Zeolite ZSM-5, ammonium was purchased from Alfa Aesar with a $SiO_2:Al_2O_3$ ratio of 23:1, stock no. 45879. Manufacturer provided surface area 425 m^2/g. The silica support used was a 99.8% pure amorphous silicon dioxide powder purchased from Sigma-Aldrich.

For preparation of catalyst, the well-established wet impregnation method has been followed. Two different amounts of metal loading were done on ZSM-5 zeolite support. The required amount of ruthenium nitrosyl nitrate solution has been calculated to prepare two different batches of catalysts having 1.5 wt.% Ru and 3.0wt% Ru loading on 6 g of ZSM-5. The ruthenium salt solution was manually added to the ZSM-5 support using a pipette following the incipient wetness technique in several steps. Number of steps of loading the precursor was calculated considering the pore volume of the ZSM-5 support and total volume of solution required to get a 1.5 or 3.0 wt.% loading of ruthenium metal. In between the impregnation steps the catalyst has been dried at 110°C overnight in a 'Thermolyne' furnace. After the impregnation, the catalyst was calcined in presence of air at 500°C for 5 hours. Similar steps are followed for preparing 3 wt% Ru on amorphous silica support. The calcined catalysts are shown in Figure 5.3. Prior to starting an experiment a fixed amount of catalyst has been mixed

with silica sand as a filler material and loaded in the reactor for in situ reduction. Pure H_2 gas was flown on the packed bed of catalyst for 5 hours at 500°C temperature and the flow rate was maintained at 15 ml/min.

(a)   (b)   (c)
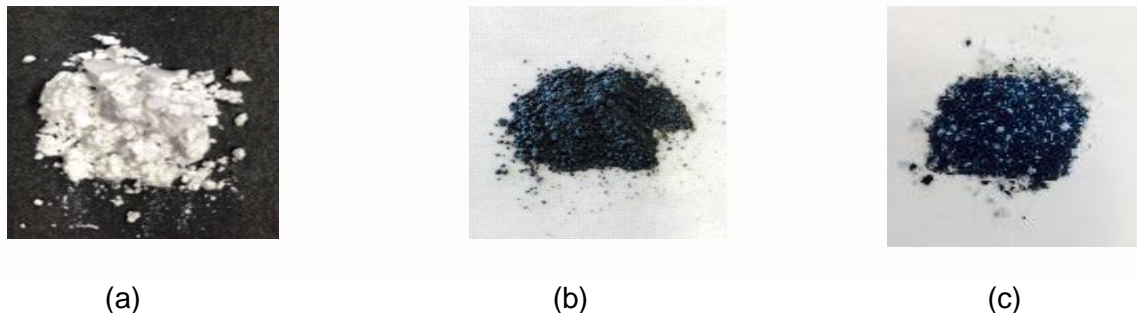
Figure 5.3: (a) pure ZSM-5 catalyst (b) 3 wt.% Ru/ZSM-5 after calcination (c)

3wt%Ru/SIO$_2$ after calcination

5.3.2 Experimental setup and procedure

A schematic of the apparatus is shown in Figure 5.4 and the lab experimental setup is shown with the reactor in a tubular furnace in Figure 5.5. Chemically pure grade methane was flown to the reactor directly from a compressed gas cylinder passing through two digital flow meters in series, one for showing the pressure reading in 'psia' and the other one for volumetric flow rate in 'ml/min'. A stainless steel tubular reactor (High Pressure Equipment Company, Erie, PA) with 0.8 cm internal diameter (i.d.) and 20.4 mL internal volume has been placed inside an electric furnace. Operating temperature in the reactor was monitored by a thermocouple (Omega Engineering). The reactor was packed with either 11 g mixture of Ru/ZSM-5 (4.5 g) and silica sand of a particle size in between 10 to 20 mesh (6.5 g) for both 1.5 wt.% and 3 wt.% ruthenium loadings or with 6.4 g mixture of 3 wt.% Ru/SiO$_2$ (2.0 g) and silica sand (4.4 g). Again for series bed experiments, a catalyst bed of 3 wt.% Ru/ZSM-5 (2 g) followed by pure ZSM-5 (2 g) was used in a series, both mixed with 3 g of silica sand separately. The product outlet line from the reactor is 1/16" 316 stainless steel tubing which passed through an

ice water bath and then water cooled using a double tube heat exchanger of which the outer tube was made of copper. After passing through the heat exchanger, the product gas mixture was fed to a 'phase separator' consisting of a 30 ml Jerguson gage with sight glass. The product mixture entered at the middle of the flash separator and the separated gas exited from the top. At the outlet of the separator, a pressure gauge of maximum capacity of 60 psig has been placed to measure the pressure of the product gas. The gas product then passed through a tubular steel vessel packed with anhydrous calcium sulfate to remove the moisture if any was present before entering gas chromatograph.
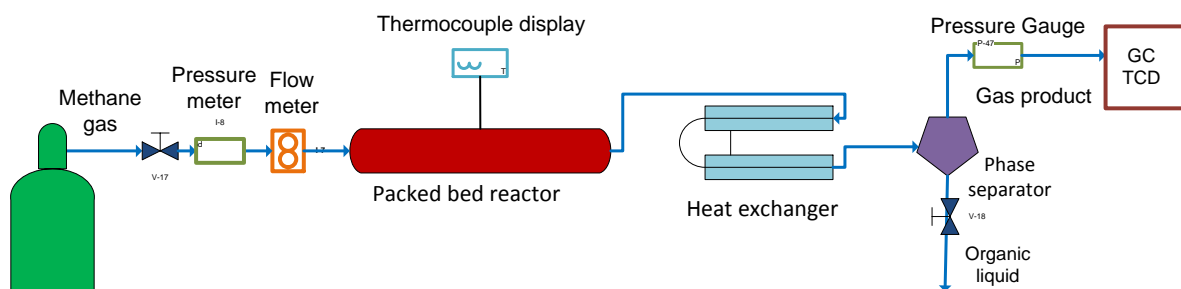
Figure 5.4: Schematic diagram of experimental setup for direct non-oxidative catalytic upgrading of methane
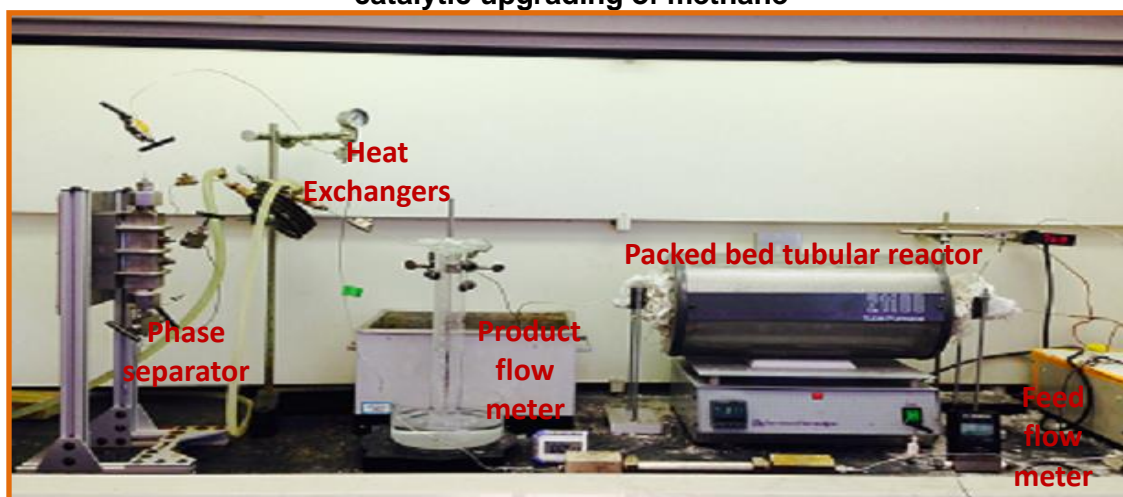
Figure 5.5: Lab scale experimental setup for direct non-oxidative catalytic upgrading of methane

A very minute amount of organic liquid product has been formed after 5 hours of continuous operation which was difficult to measure as it did not flow out of liquid –gas phase separator when the valve at the bottom outlet was opened. The liquid product has been washed out form the separator using cyclohexane as a solvent.

After every two experimental runs, nitrogen gas has been flown through the reactor at the same operating temperature of that of the last experiment to remove any chemical residue or coke deposit.

Operating temperature has been varied from 500°C to 800°C with a 100°C increase to examine the kinetics of methane conversion for different catalyst and support combinations and also for the series catalyst beds with pure ZSM-5. Pressure drop varied a little with changing the catalyst bed and changing temperature but the flow rate of feed methane was controlled to keep constant for ease of comparing the product quality for a definite weight hourly space velocity. The pressure drop across the bed varied from 15 psia to 17 psia depending on the packing of the catalyst bed and operating temperatures.

5.3.3 Product Characterization

5.3.3.1 GC Chromatography

An online SRI 8610C gas chromatograph (GC) with a thermal conductivity detector (TCD) has been used to determine the composition of the gas product. The inlet of the GC was directly connected with the product outlet line from the experimental setup. Sample injection to the GC was done online by means of a six-port injection valve attached through a 10 µL sample loop. A Hayesep DB packed column (Agilent Technologies) 9.14 m in length and 2 mm i.d. and 3.2 mm o.d. was used for the gas

chromatographic analysis. This column has been selected as it can separate and C_1-C_{10} hydrocarbons and hydrogen gas as H_2 is one of the major components of the product gas mixture. Helium was used as the carrier gas.

5.3.3.2 Fourier Transform Infrared (FTIR) Spectroscopy

The IR analysis of the gas mixture was done using a Nicolet IR100 FTIR instrument and Spectra Tech Econo gas cell of 50 mm path length and NaCl windows. Product gas has been collected by connecting the top outlet tubing from the phase separator to a 500 ml flex film gas sampling bag (SKC, Inc., PA). A gas tight syringe of 5 ml capacity (SGE, Austin, TX) was used to transfer gas from the sample bag to the gas cell. The cell was flushed with gas several times to ensure that no air or previous gases are left inside. The background taken for subtraction was the IR spectrum of the empty cell containing air. The IR analysis has been performed especially to detect the type of bonds in the gaseous products which could not be detected in the GC analysis.

5.3.3.3 UV-Vis Spectroscopy

The very small amount of liquid phase of the product mixture was diluted in the wash solvent i.e. cyclohexane or ethanol and analyzed in a Genesys 10S UV-Vis Spectrophotomter by Thermo Scientific. 10 mm path quartz cells from Fisher brand are used for sample analysis in the UV and visible light range of 200 to 500 nm wavelength. Pure cyclohexane has been used as the background as it is the main solvent or wash liquid for the product mixture.

5.3.3.4 Gas Chromatography-Mass Spectrometry (GC-MS)

The organic liquid product phase consisting of solvent cyclohexane has been analyzed using a GC-MS instrument. The GC-MS was equipped with a DB-1701 column (30m, 0.25mm, 0.25um) from Agilent Technologies to separate the hydrocarbons and cyclic

compounds in liquid product phase dissolved in cyclohexane solvent. After a series of experimental runs at same operating temperature, the catalyst was washed with solvent cyclohexane and also that liquid sample has been analyzed using the GC-MS. The GC was also from Agilent (Model 7890) contains a flame ionization detector (FID) and can detect hydrocarbons from C_2 to C_{20}. The injection volume taken of each product sample is 1 µL.

5.3.4 Catalyst Characterization

Five different types of catalysts were prepared for comparing the effect of ruthenium metal loading and different support materials in non-oxidative methane conversion reaction. The different types were:

a. 3 wt% Ru/ZSM-5

b. 1.5 wt% Ru/ZSM-5

c. 3 wt% Ru/SiO$_2$

d. Pure ZSM-5

e. 3 wt% Ru/ZSM-5 followed by pure ZSM-5 series bed (50/50 wt ratio)

The catalysts have been characterized with several techniques and the properties of fresh catalyst and used catalyst were compared.

5.3.4.1 Powder X-ray Diffraction

The Powder X-Ray diffraction patterns of the 3 wt% Ru/ZSM-5 catalyst and pure ZSM-5 catalyst were acquired by analyzing the powder catalyst samples with a 'Bruker D8 Advance Diffractometer' equipped with a Co Kα radiation source. Diffraction patterns have been collected in the 2θ range of 5° to 90° using a step of 0.05°.

5.3.4.2 Scanning Electron Microscopy

After calcination of the catalysts, images were taken at the micron level with a Scanning Electron Microscope (Zeiss, EVO 50, UK) at different points of each catalyst sample to ensure even distribution of ruthenium metal on the support ZSM-5 or SiO_2.

5.3.4.3 Fourier Transform Infrared Spectroscopy

The FT-IR analysis has been performed with a Nicolet IR 100 FT-IR instrument from Thermo Scientific. Catalyst samples were crushed and mixed with KBr to fine powder and made into a thin translucent disk by pressing in a pelletizer which acted as the sample holder as well and directly out inside the chamber of the FT-IR instrument which has been continuously purged with 20 cc/min flow of N_2 gas. Infrared ray passed through the sample and by applying Fourier transformation the instrument directly showed the spectra of transmittance (%) vs wavenumber (cm^{-1}) for the sample. KBr has been used as background for analysis.

5.3.4.4 BET Surface Area and Pore Size Analysis

Brunauer, Emmett and Teller (BET) surface area and pore size analyzer of NOVA 2200e series from Quantachrome Instruments has been used to measure the surface area, pore volume and pore size of different catalysts both freshly made and spent and results were compared to explain the catalyst performance and stability. 0.2 to 0.3 g of catalysts were taken for analysis and prior to nitrogen adsorption for pore volume and surface area analysis the samples have been degasified under vacuum for 12 hours at 250°C temperature. The samples then again have been weighed and put into the adsorption chamber in the dewar filled with liquid nitrogen and nitrogen gas was flown into the sample cells to get the Langmuir adsorption isotherm and from that the surface area and pore volume and pore size are calculated.

5.3.4.5 Temperature Programmed Reduction

In situ reduction has been performed for the calcined metal impregnated catalyst prior to each experiment. The reduction temperature for 3wt%Ru/ZSM-5 catalyst was measured with a Micromeritics Chemsorb 2750 instrument. 0.13g of 3 wt%Ru/ZSM-5 calcined catalyst was taken in a quartz tube in a temperature-controlled furnace containing a thermal conductivity detector (TCD). The sample was first purged with 50 ml/min of N_2 flow at 100 °C for 1 hour and cooled down to room temperature. Then, the carrier gas was switched to a reducing gas mixture (10% H_2 in Ar) with a flow rate of 50 mL/min and the temperature is increased to 900 °C with a constant rate of 5°C/min. The H_2 consumption (TCD signal) was recorded automatically by a computer.

5.3.4.6 Thermogravimetric analysis (TGA)

Deterioration of catalyst surface properties were evaluated by measuring solid carbon deposition on the surface. The amount of carbon deposited on a sample of 3 wt% Ru/ZSM-5 spent catalyst was measured by TA Instruments (New Castle, DE) Q500 thermal gravimetric analyzer (TGA). The sample was dried overnight. The sample chamber of the TGA instrument was purged with 60 cm^3/min of compressed air. The method set for the analysis started at the initial temperature of 22 °C, ramped at 10°C/min and held at 120°C to further remove residual water. Then again ramped at the same rate up to 900 °C and held at the final temperature for 45 minutes.

5.4 Results and Discussion

5.4.1 Catalyst properties

With the impregnation of ruthenium nitrosyl nitrate solution on the ZSM-5, zeolite support and calcination at 500°C, new bonds were created in between ruthenium metal ion with

Al$_2$O$_3$ and SiO$_2$ in zeolite. Also presence of ruthenium oxide could be ensured by comparing the peaks of Powder X-ray diffraction patterns of 3wt%Ru/ZSM-5 with Ru$_2$O$_3$ XRD spectrum from literature. In Figure 5.6, a comparison of X-ray diffraction patterns is shown between pure ZSM-5 zeolite and ruthenium loaded on ZSM-5 support. The presence of ruthenium oxide can be proven on the catalyst by the characterized peaks at 2θ values of 35° and 54.3° in the spectrum of 3 wt% Ru/ZSM-5 which are not present in the pattern of pure ZSM-5
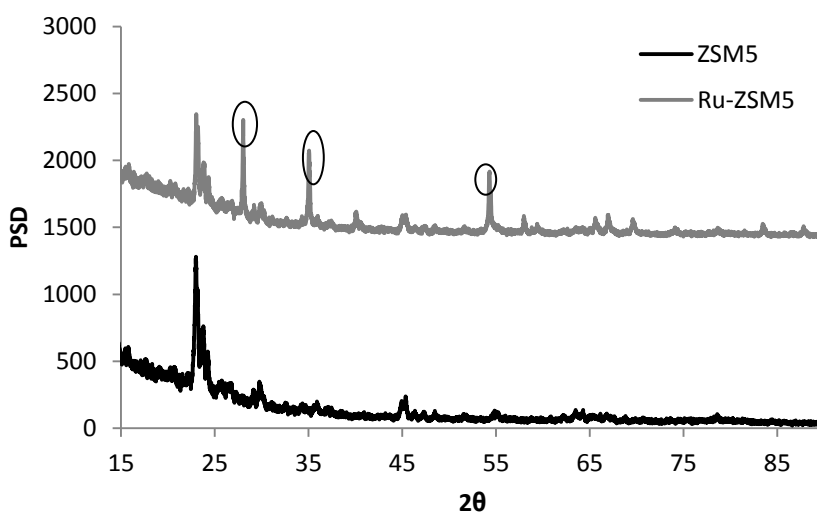
Figure 5.6: Comparison of X-ray diffraction spectra of pure ZSM-5 and 3wt% Ru/ZSM-5

Images of the prepared catalysts at micron level have been taken using a Scanning Electron Microscope (SEM). Energy dispersive X-ray spectroscopy is used along with SEM imaging to measure the composition of metals and oxygen in the catalyst.

Element	Weight%	Atomic%
O	63.58	76.68
Si	32.99	22.67
Ru	3.43	0.66
Totals	100.00	
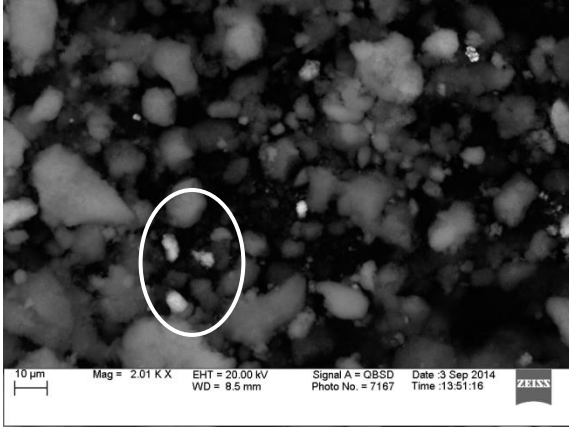
(a)

Element	Weight%	Atomic%
O	56.14	70.22
Al	2.85	2.12
Si	37.98	27.06
Ru	3.03	0.60
Totals	100.00	
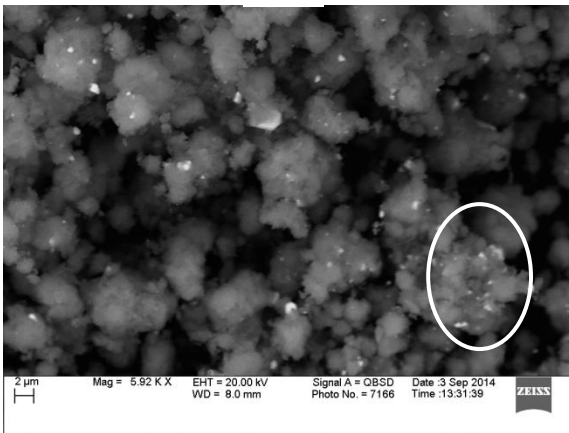
(b)
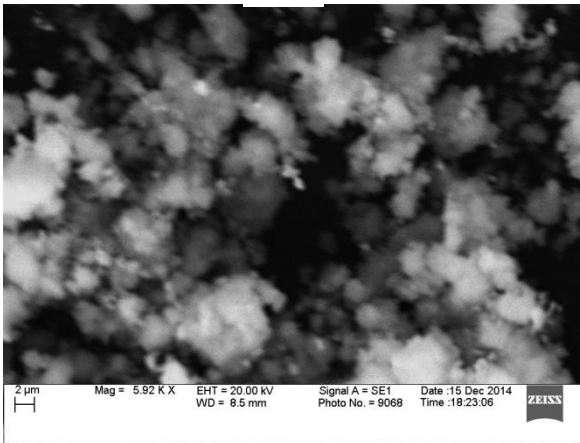
Element	Weight%	Atomic%
O	57.64	71.05
Al	2.89	2.12
Si	37.75	26.50
Ru	1.71	0.33
Totals	100.00	

(c)
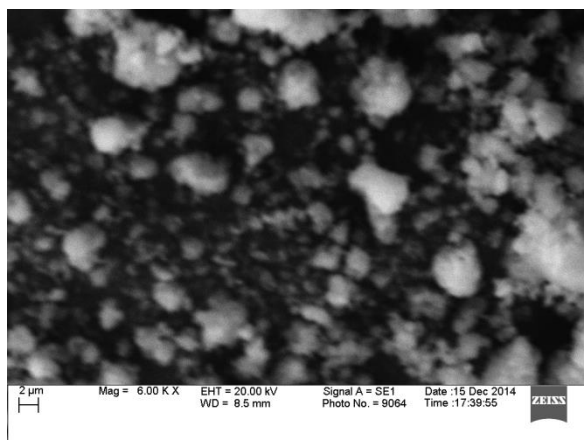
Element	Weight%	Atomic%
O K	63.93	75.62
Al K	2.74	1.93
Si K	33.33	22.46
Totals	100.00	

(d)

Figure 5.7: SEM images with EDS analysis of a) 3wt% Ru/SiO2 fresh catalyst b) 3 wt% Ru/ZSM-5 fresh catalyst c) 3 wt% Ru-ZSM-5

Comparing Figure 5.7 (a) and (b) it can be seen, the particle sizes of the two different support materials are different. Particle size of SiO_2 support is in the range of 15 to 20 μm whereas the ZSM-5 particle size is in the range of 2 to 8 μm. The dispersed visible white dots on the surface of the support materials in Figure 5.7 (a) and 5.7 (b) and the corresponding values from EDS analysis show that ruthenium is well dispersed on the support material. In Figure 5.7 (C) the spent catalyst of 3wt% Ru/ZSM-5 seems very similar to that of fresh catalyst but the dispersed ruthenium metals are less distinctive. Again comparing with pure ZSM-5 catalyst in Figure 5.7 (d) the presence of ruthenium in 5.7 (b) and (c) become more evident and the particle size of ZSM-5 found to be in the same range both as a support material and as pure catalyst.

Bonds formed in the catalysts containing ruthenium is principally of ruthenium metal or metal oxide with the Al or Si from ZSM-5 catalyst and only Si when SiO_2 is used as the support material. Comparison of these bonds formed are done by comparing the peaks in the spectra generated using Fourier Transform Infrared spectroscopy for fresh and spent metal catalysts on support material and also for pure ZSM-5 in Figure 5.8.
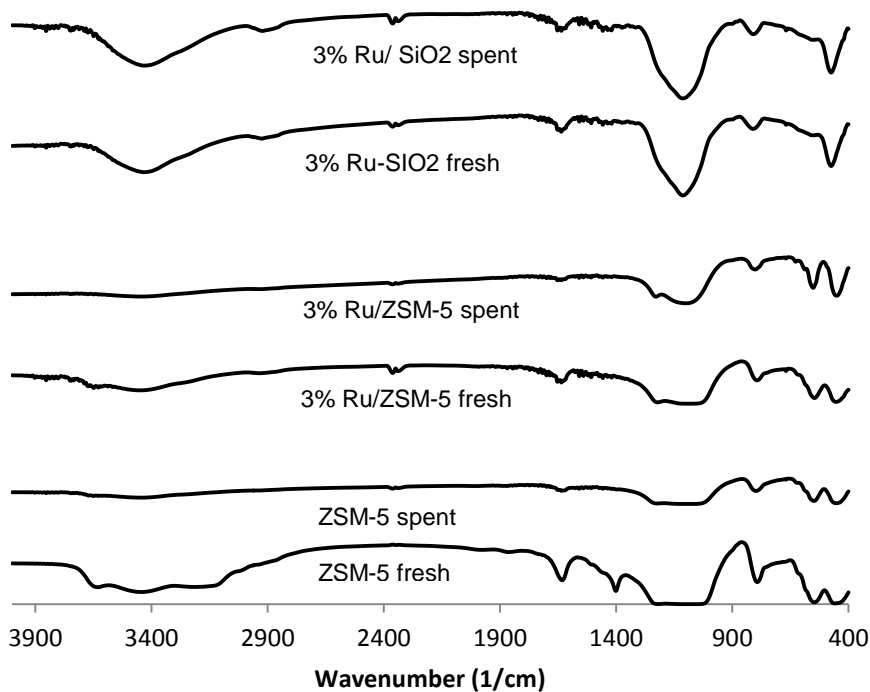
Figure 5.8: Comparison of FT-IR spectra of fresh and spent catalysts

Significant differences can be noticed for the area under the peaks for fresh and spent catalyst. ZSM-5 supported catalysts showed higher peak height and greater area under the peaks for fresh catalysts comparing with the IR spectrum of the spent catalysts. The change in peak height and peak area implies the deterioration in catalyst activity in the spent catalyst. No new chemical bond has been formed in the catalyst with the reactant or product molecules as no new peak was seen to elute that was not present in the spectra of the fresh catalysts. For the SiO_2 based ruthenium metal catalyst, not much change in the peak heights and peak area were observed which can be due to low surface activity and thus almost no change in the IR spectra taken after 20 hours of operation.

Surface area and pore volume are major characteristic properties of a catalyst. With reaction time if surface area and pore volume changes especially decreases at a fast rate it can be assumed that the catalyst is not stable. Again, no change in catalyst surface area may refer to, no significant conversion or reaction taking place on the catalyst bed. Fresh and spent catalysts for methane conversion process were analyzed with BET surface area and pore volume analyzer and compared in Table 5.2.

Table 5.2: BET surface area and pore size data for different catalysts

Catalyst	Surface area (m^2/g)	Pore volume (cc/g)	Pore size (nm)
Pure ZSM-5	292	0.21	1.43
3 wt% Ru/ZSM-5 (fresh)	329	0.21	1.29
3 wt% Ru/ZSM-5 (spent)	235	0.37	3.12
3 wt% Ru/SiO$_2$ (fresh)	177	2.28	25.65
3 wt% Ru/SiO$_2$ (spent)	171	1.21	14.16
1.5 wt% Ru/ZSM-5 (fresh)	334	0.31	1.88
1.5 wt% Ru/ZSM-5 (spent)	315	0.20	1.29

In Table 5.2 comparing the surface area of pure ZSM-5 1.5 wt% Ru/ZSM-5 and 3wt% Ru/ZSM-5 fresh catalyst, it can be seen that the surface area increases with increasing loading of impregnated metal on ZSM-5 surface but the pore volume and pore size are quite similar. This implies that the loaded metal did not occupy much volume inside the pores as the metal loading is low and it has been distributed both on the surface of the support particles and inside the pores of ZSM-5 support. Again SiO$_2$ has a larger particle size that is evident from SEM image (Figure 5.4(a)); hence it showed smaller surface

area compared to that of ZSM-5 supported catalysts in Table 5.2. Significant change in surface area can be observed in case of fresh and spent 3wt% Ru/ZSM-5 catalysts indicating a conversion of methane and coke deposition over the time of operation (60 hours).

To find out the optimum reduction temperature for the metal impregnated catalyst, 3 wt% Ru/ZSM-5 fresh catalyst after calcination was taken as a sample and temperature programmed reduction (TPR) analysis has been performed. From the plot of TCD signal intensity with increasing temperature, in Figure 5.9 it can be seen that a very sharp peak was observed at 101°C reduction temperature which implies that most of the ruthenium oxide in the sample of the catalyst has been reduced at that temperature.
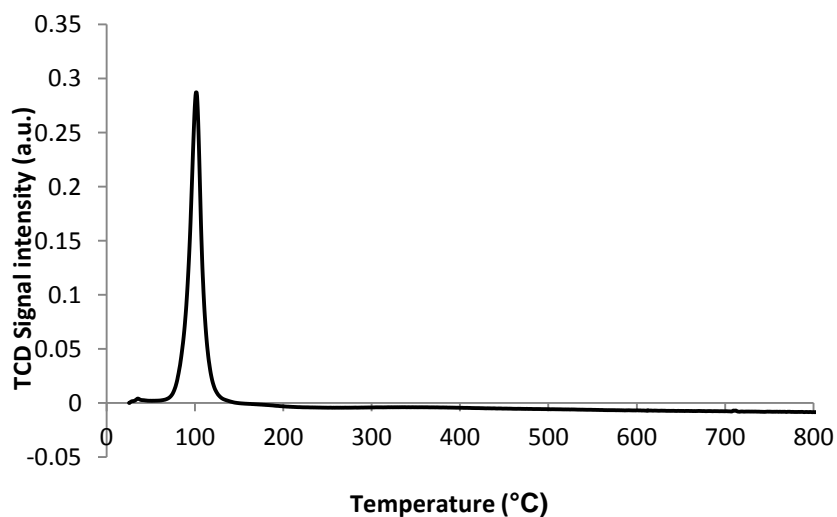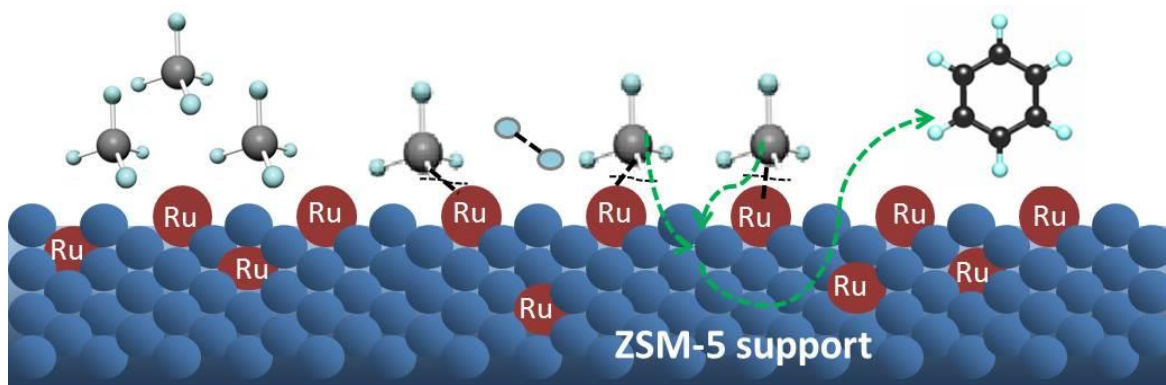

Figure 5.9: TCD signal strength for the reduction process with increasing temperature

The in situ reduction was done at much higher temperature in the reactor as previous studies mentioned that higher reduction temperature contributes in increasing the active metal surface area by removing anion part of the metal salt properly [23].

5.4.2 Reactions involved

Conversion of methane has been compared on different catalysts based on ruthenium metal ZSM-5 and silica support. Metal loading and metal-support combination were varied to find the effect on methane conversion and also the contribution of these factors in the reaction mechanism. The probable reactions taking place when a bi-functional catalyst like ruthenium metal on ZSM-5 zeolite support has been used in a continuous flow packed bed reactor at operating temperatures higher than 500 or 600°C is as follows.

$$CH_4 + [Ru] \xrightarrow{\Delta} CH_3 - [Ru] + \frac{1}{2}H_2 \quad \ldots\ldots (5.1)$$

$$CH_4 + [Ru] \xrightarrow{\Delta} C - [Ru] + 2H_2 \quad \ldots\ldots (5.2)$$

$$6CH_3 - Ru \xrightarrow{ZSM-5} C_6H_6 + 6H_2 \quad \ldots\ldots (5.3)$$
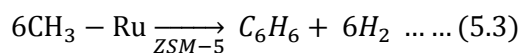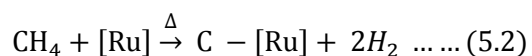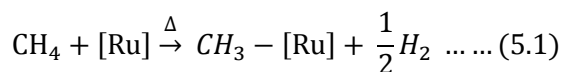
(a)
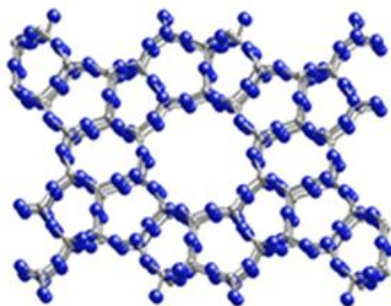
(b)

Figure 5.10: (a) methane activation and bond formation on Ru/ZSM-5 catalyst surface (b) ZSM-5 zeolite molecular framework

5.4.3 Effect of temperature

Catalyst performance in conversion of methane to higher hydrocarbon products and hydrogen were evaluated by varying operating temperature keeping the feed flow rate and catalyst bed pressure in a constant range of 5 to 15 ml/min and 15 to 18 psia respectively. Catalyst performance has been measured based on two major criteria, quality of product i.e., presence of higher hydrocarbon molecules in the product mixture and percent conversion of methane based on change in area under GC chromatogram.

Product gas collected at the top outlet is analyzed with FT-IR spectrophotometer and the spectra at different operating temperatures for different catalysts were compared to find the structural differences and the bonds present in product hydrocarbon gas mixture.

(a)

(b)
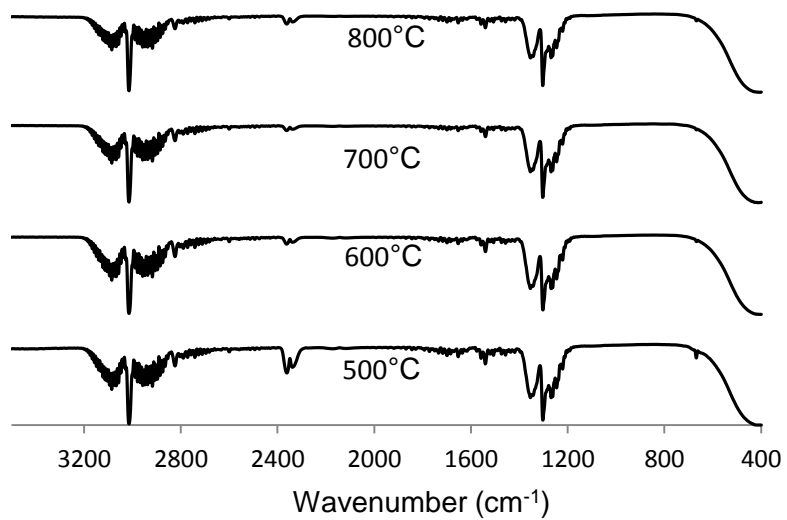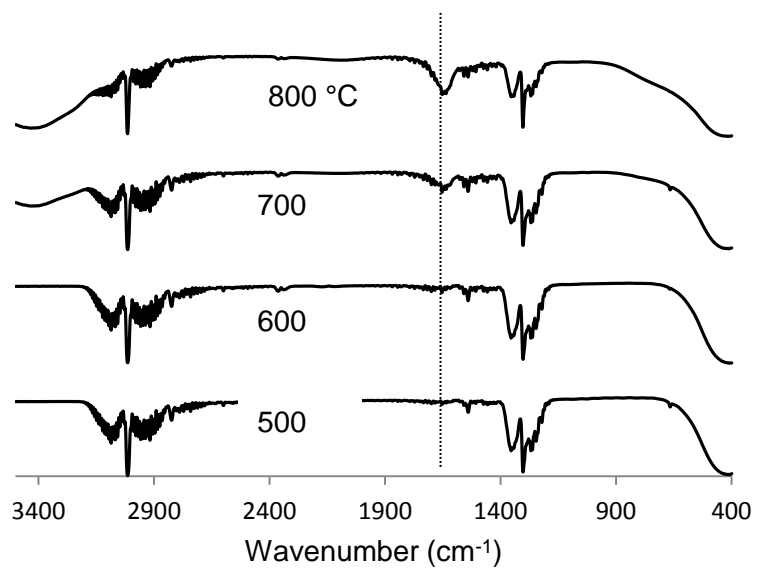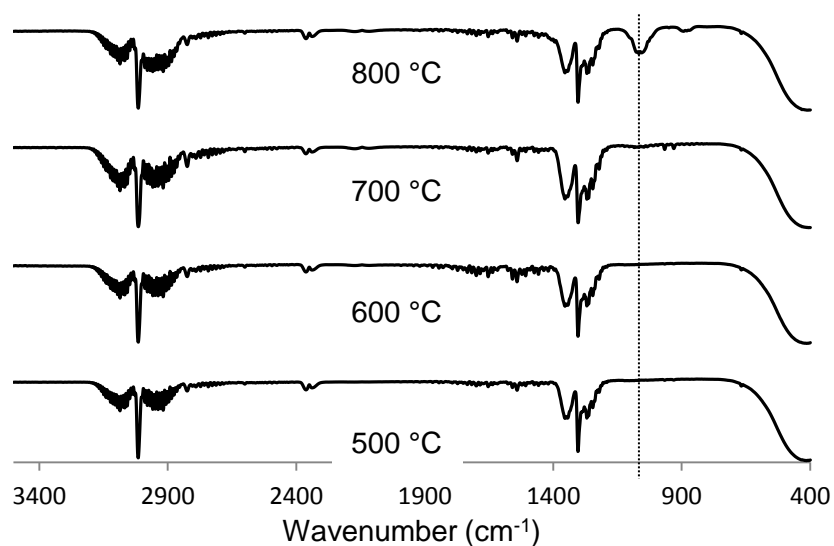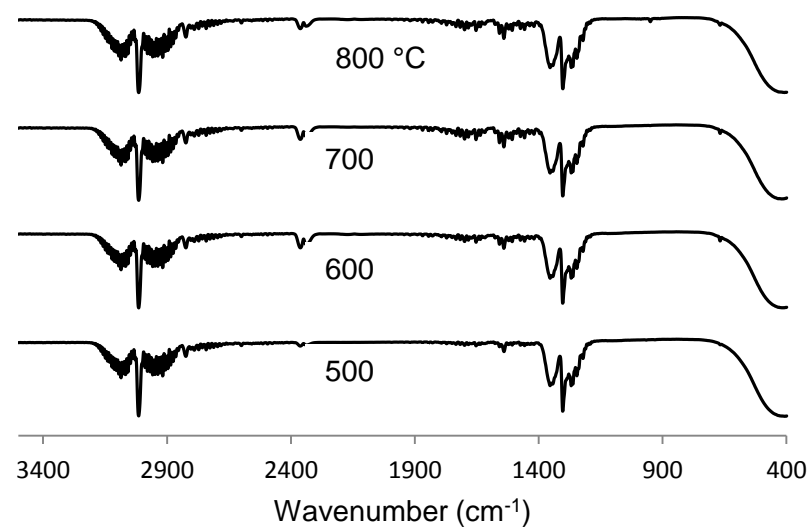
Figure 5.11: Comparison of FT-IR spectra of product gas mixture at different operating temperatures on (a) 1.5 wt% Ru/ZSM-5 catalyst bed (b) 3 wt% Ru/ZSM-5 catalyst bed (c) 3 wt% Ru/SiO2 catalyst bed (d) 3wt% Ru/SIO2 followed by ZSM-5 in a series catalyst bed.

In Figure 5.11 (a), no significant change in the bond structure was observed in the product gas for 1.5 wt% Ru/ZSM-5 catalyst which implies that no alkenes, alkynes or aromatic hydrocarbon products were present in the product gas mixture even at higher operating temperature. Almost similar results were observed by comparing the IR spectra derived by analyzing the product gas on 3wt% Ru/SiO$_2$ catalyst bed in Figure 5.11 (c) But in figure 5.11 (b), the IR spectra derived from analyzing product gas at 700 and 800°C operating temperatures showed a new peak eluted at wavenumber 1615 cm^{-1} which represents unsaturated hydrocarbon or benzene ring in the product gas mixture. This peak was found only in case of 3 wt% Ru/ZSM-5 catalyst bed but not for lower metal loading or for SiO$_2$ based support. For the series catalyst bed of 3wt% Ru/SiO$_2$ followed by pure ZSM-5, the IR spectra derived from analysis of the product gas at operating temperatures 700 and 800°C new peaks have been observed that were not present for the lower temperature product gas mixtures. In Figure 5.11 (d) , the peak at wavenumber 1035 cm^{-1} also showed the presence of unsaturated carbon-carbon bond structure in the product gas mixture which can be attributed to catalytic activity of ZSM-5 at the later end of the series bed as these peaks were not present when only 3 wt% Ru/SiO$_2$ has been used as the catalyst bed. Comparing the IR spectra of the product gas mixtures on different catalyst bed and operating temperatures, it has been observed that at higher operating temperatures 700 to 800°C, 3wt% Ru/ZSM-5 catalyst bed showed activity towards direct conversion of methane to aromatic or cyclic hydrocarbons also the series bed of catalyst showed conversion of methane to unsaturated higher hydrocarbon in the gas phase, though a single bed of 3 wt% Ru/SiO$_2$ did not show any activity to produce unsaturated hydrocarbon gases from methane. As the conversion to higher hydrocarbon and aromatics are taking place only at the operating temperature range of 700 to 800°C, the small amount of liquid product has been collected at those operating temperatures by washing the phase separator using a solvent cyclohexane. This wash

liquid has been analyzed using UV-Vis spectroscopy. In Figure 5.12 the wash liquid consisting of the solvent cyclohexane and the liquid product from CH_4 conversion on 3 wt% Ru/ZSM-5 catalyst bed was analyzed and compared to the UV-Vis spectrum of pure cyclohexane. It has been observed that the product liquid in cyclohexane showed new peaks in the range of wavelength 220 to 260 nm. Also the liquid product was independently analyzed in the UV-Vis, and the result is shown in Figure 5.13 where it showed the peaks in the wavelength range where pure benzene peaks are seen. From literature, it is established that benzene shows absorbance peaks in UV-Vis spectroscopy in the wavelength range of 220 to 260 nm which is the same range where the peaks were observed for the product liquid.
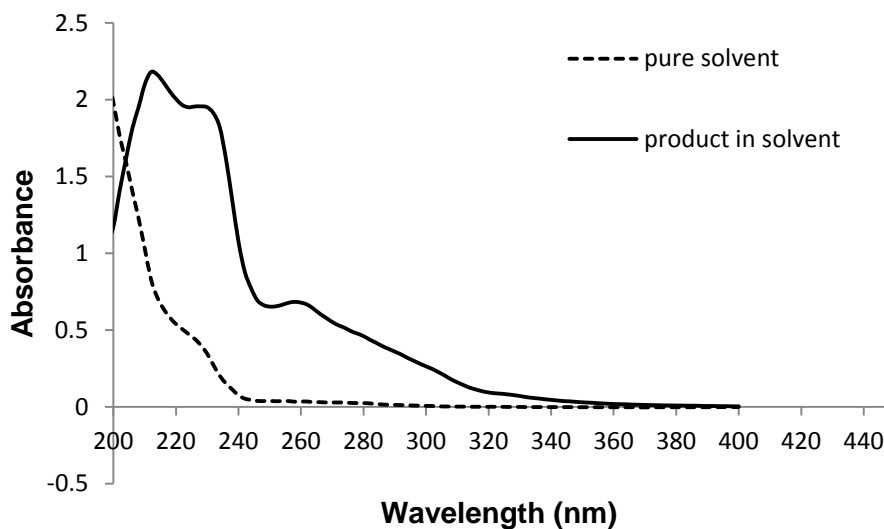
Figure 5.12: Comparison of UV-Vis spectra of liquid product from conversion of CH$_4$ on 3 wt% Ru/ZSM-5 catalyst bed at 800°C with pure solvent cyclohexane
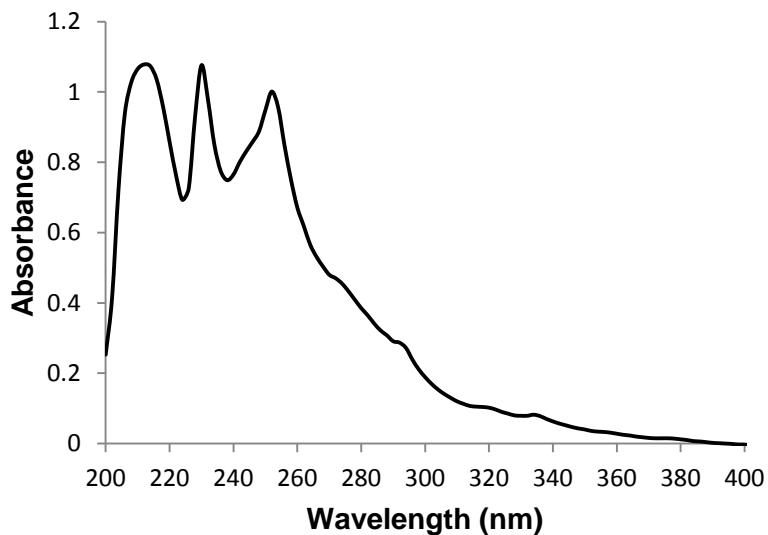
Figure 5.13: UV-Vis spectrum of product liquid of conversion of CH$_4$ on 3 wt%

Ru/ZSM-5 catalyst bed at 800°C

Again for the series bed of 3wt% Ru/SiO$_2$ followed by ZSM-5 new peaks were observed at wavelength 255 nm which is not present in the solvent spectrum i.e. ethanol in this case (Figure 5.14).
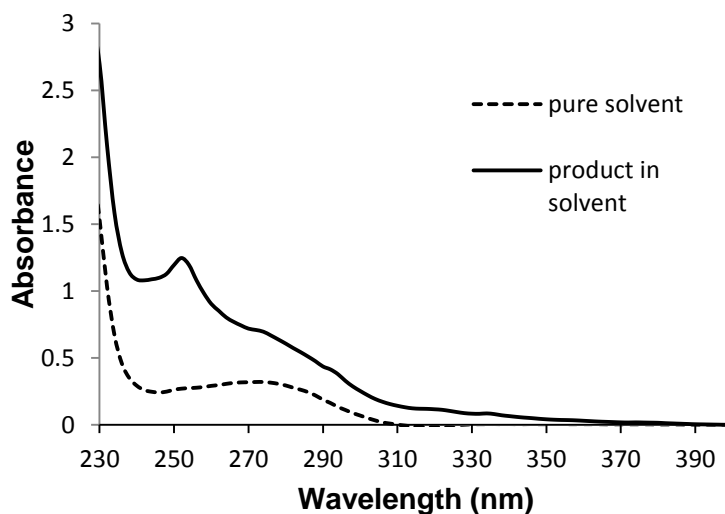
Figure 5.14: Comparison of UV-Vis spectra of liquid product from CH$_4$ conversion

on series catalyst bed at 800°C and pure solvent ethanol

From both the IR spectra and UV-Vis spectrocscopic analysis it was evident that at higher operating temperature range of 700 to 800°C CH_4 conversion to aromatic hydrocarbon has taken place on 3 wt% Ru/ZSM-5 catalyst bed and unsaturated hydrocarbon has been produced in case of the series bed of 3wt% Ru/SiO$_2$ followed by pure ZSM-5 catalyst bed.

5.4.4 GC peak area based conversion of CH$_4$

Percentage of conversion of CH_4 on each of the catalyst bed mentioned at different operating temperatures were measured based on change in area of online GC chromatograms. The GC-TCD was first calibrated with 99.9 mol% CH_4 and with a calibration gas with known composition of CH_4 of 10 mol%. Based on this two point calibration line the composition of unconverted methane in the product gas mixture has been determined and thus the conversion of methane was calculated with the following equation.

CH_4 % conversion:

$$\left\{ \frac{\left[feed\ flow\ rate \left(\frac{ml}{\min}\right) * area\ under\ the\ curve\ for\ pure\ CH_4 * \left(\frac{p}{14.7}\right) \right] - \left[product\ flow\ rate \left(\frac{ml}{\min}\right) * area\ under\ the\ curve\ for\ unconverted\ CH_4\ in\ product\ gas * \left(\frac{p'}{14.7}\right) \right]}{\left[feed\ flow\ rate \left(\frac{ml}{\min}\right) * area\ under\ the\ curve\ for\ pure\ CH_4 * \left(\frac{p}{14.7}\right) \right]} \right\} * 100\%$$
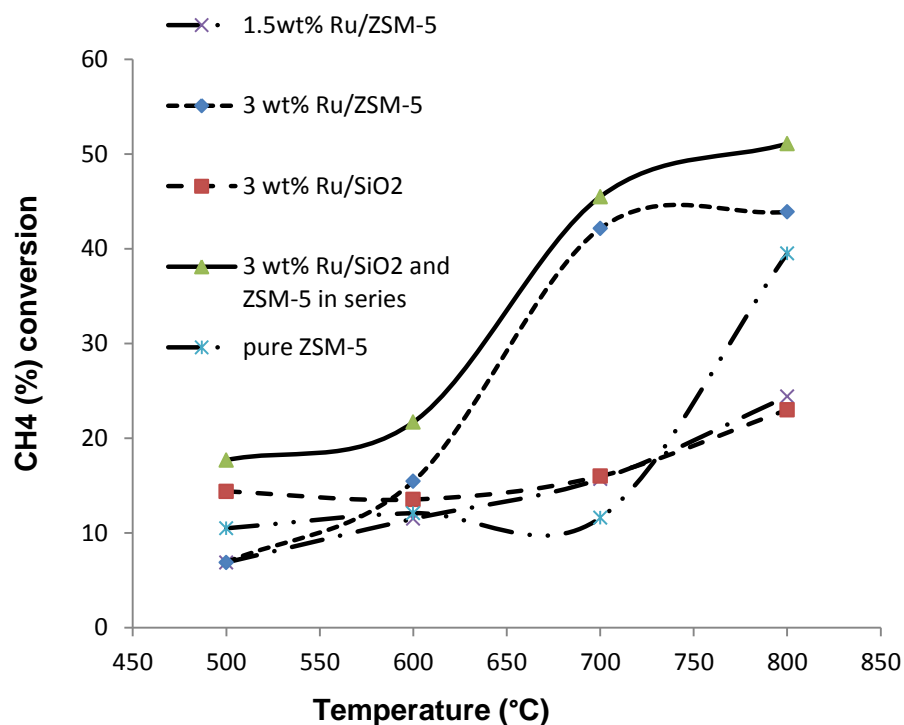
Figure 5.15: Conversion of CH$_4$ with operating temperature on different catalysts

In Figure 5.15 it has been observed that temperature played a very significant role in methane conversion. At 500 and 600°C, conversion were lower than 20% for all the catalysts but a sharp rise in conversion was noticed at 700°C operating temperature for the catalysts 3 wt% Ru/ZSM-5 and the series bed of 3 wt% Ru/SiO$_2$ followed by ZSM-5. Based on conversion performance, the series bed of Ru/SiO$_2$ and ZSM-5 showed best results, a conversion as high as 51% at 800°C and 3wt% Ru/ZSM-5 single catalyst bed showed a conversion of 44% at the same operating temperature. Single catalyst of rutenium metal on silica support gave lower converion but using ZSM-5 in a series after 3wt% Ru/SiO$_2$ the conversion rose higher and even better than single catalyst bed of 3wt% Ru/ZSM-5. This can be explained by the catalyst activity of both 3 wt% Ru/ZSM-5 which has been supposedly contributing in activating the CH$_4$ to methyl free radical and

159

then special channel structure and sheets consisting of chains of five membered rings making the framework structure of ZSM-5 aids in producing benzene like structure form the methyl radicals[24],[25]. In this way the methyl radicals did not undergo further dissociation to carbon black. Almost similar mechanism probably has taken place on 3 wt%Ru/ZSM-5 catalyst bed. In this case, methane has been activated catalyzed by ruthenium metal and high temeprature and then combined with other free radicals to produce higher hydrocarbons specially cyclic structures like methyl cyclohexane, isopropyl cyclobutane, di-methyl cyclopentane and similar product molecules inside the support structure which have been detected by GC-MS analysis of the wash liquid solvent containing the liquid product. Beacause of solvent dilution, the concentration of the product hydrocarbons were found to be very low but it can be noticed that the product molecules detected by the GC-MS were in a big range starting from seven carbons to twenty carbon atoms taken from data library of the GC-MS according to the retention time of the product molecules. Being the yield of the higher hydrocarbon molecules very low, it has been very difficult to detect and separate them from the noise peaks in the GC chromatogram. In the continuation of this work, a proper calibration will be done with high hydrocarbon molecules to ensure the detection and quantitative measurement of the heavy hydrocarbon products.

The presence of higher hydrocarbon in the gas phase of product has also been ensured by the chromatograms collected from online GC with the reactor. For both 3 wt% Ru/ZSM-5 catalyst packed bed and the series bed of 3 wt% Ru/SiO$_2$ followed by pure ZSM-5 the product gas mixtures analyzed by online GC-TCD showed chrromatograms with significant area under the peaks for hydrocarbons chains or cyclic structures containing higher than four carbons. As the column has been calibrated with calibration gases consisting of C$_1$ to C$_4$ hydrocarbon gases and it was observed that the product

gas mixture chromatograms for these two catalyst beds contained peaks eluted after the retention time of C_4 hydrocarbon, it can be assumed that the higher hydrocarbon product molecues were consisting of five or more carbon atoms.

In Table 5.3, the area under the chromatogram peaks for the product gas mixture on different catalyst beds at 800°C operating temperature shown and compared.

Table 5.3: GC peak area for product gas components at 800 °C on different catalysts

Catalyst	GC area under the peaks		
	CH_4	H_2	C_5 and higher
Pure ZSM-5	254	321	--
1.5 wt% Ru/ZSM-5	318	215	--
3 wt% Ru/ZSM-5	236	204	82
3 wt% Ru/SiO$_2$	324	66	--
3 wt% Ru/SiO$_2$ followed by ZSM-5 in series bed	201	181	56

From GC chromatogram results in Table 5.3 it is observed that except for 3wt% Ru/ZSM-5 and the series bed of 3wt% Ru/SiO$_2$ followed by ZSM-5, the other catalyst beds did not produce higher hydrocarbons in the gas phase. Higher hydrocarbon molecules were produced only when ZSM-5 has been used as a catalyst or at the of a series catalyst bed.

5.4.5 Percent yield of hydrogen

From online GC-TCD analysis, along with methane conversion measurement, hydrogen yield has been calculated based on the same process by calibrating the area under the peak in the chromatogram with known amount of hydrogen injection. In figure 5.16 it is observed that the yield of hydrogen also matched with methane conversion rate on each of the catalyst beds. Hydrogen yield was found to be low for silica supported ruthenium

metal catalyst at all operating temperatures but ZSM-5 supported ruthenium metal catalysts showed higher percent of yield of hydrogen and it increased with increasing operating temperature.
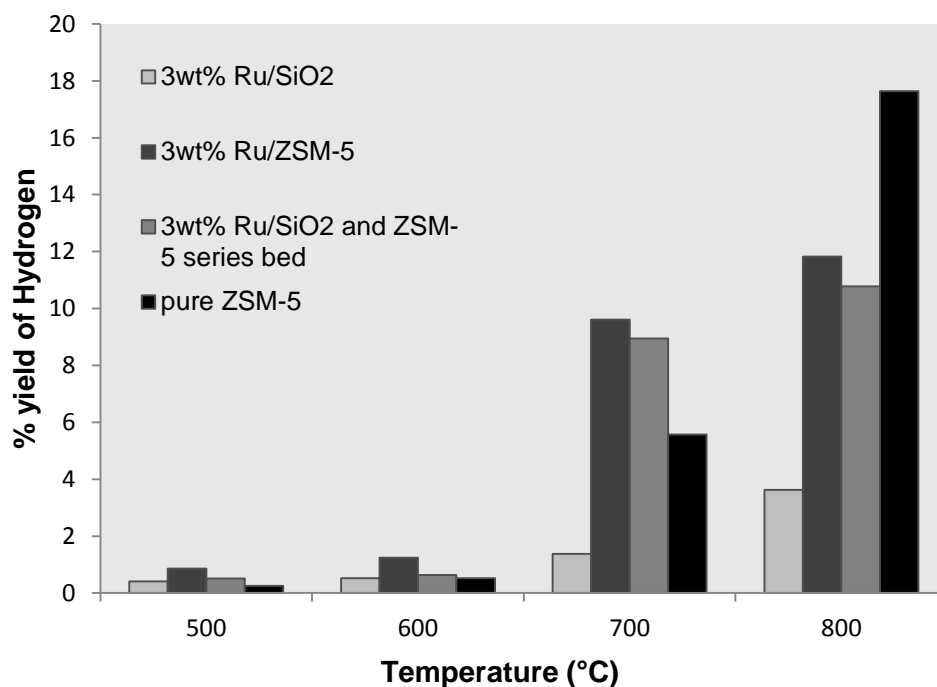
Figure 5.16: Percent yield of hydrogen from methane conversion reaction on different catalyst beds at different operating temperatures

Though 3wt% Ru/SiO_2 catalyst bed showed low percent yield of hydrogen, the series bed of 3wt% Ru/SiO_2 followed by pure ZSM- 5 gave much higher percent yield of hydrogen at 700 and 800°C as the conversion of methane were also high. The percent hydrogen yield from 3wt% Ru/SiO_2 catalyst bed was comparable to that of percent yield from 3 wt% Ru/ZSM-5 catalyst bed as the conversion of methane was analogous for these two catalyst beds. In Table 5.3 and in Figure 5.16, it can be observed that pure ZSM-5 single catalyst bed contributed in higher yield of hydrogen at 800°C operating

temperature compared to the other catalyst at the same temperature. From Table 5.3 and Figure 5.16, it was evident that at 800°C single catalyst bed of pure ZSM-5 gave high conversion of methane but it was also producing more hydrogen and that implies, only pure ZSM-5 was not producing much higher hydrocarbon. The series catalyst bed and 3wt% Ru/ZSM-5 contributed in higher conversion of methane but lower percent yield of hydrogen and that is why heavier hydrocarbon molecules were observed in the product stream as the rest of the hydrogen were contributing to build the higher hydrocarbon chain.

5.4.6 Effect of operating time

To find out the effect of operating time on the conversion rate as well as on catalyst life 60 hours of continuous reaction has been conducted and product samples were analyzed every two hours with the online GC-TCD. Methane conversion has been calculated based on change in area under the peak in GC chromatogram every two hours and it is observed in Figure 5.17 that methane conversion increased with hours of operation and reached up to 55% at 46 hours of operation. It went down slightly after 46 hours and till 60 hours of operation the conversion was found to be 50% which was still higher than conversion achieved in 1st 30 hours. Continuous operation has been done only on 3wt% Ru/ZSM-5 catalyst bed as it has shown best performance in conversion of methane producing higher hydrocarbon products.
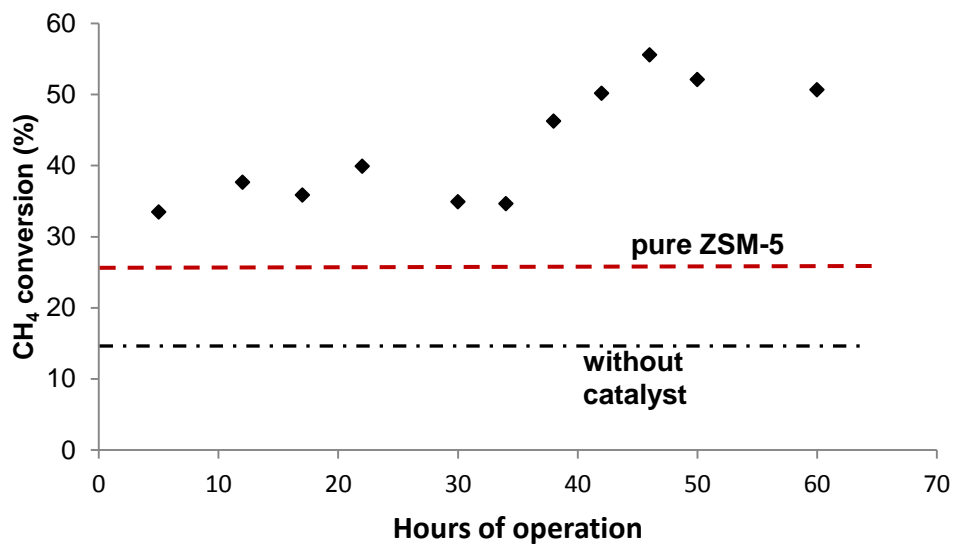
Figure 5.17: Conversion of methane based on GC-chromatogram peak area

change with hours of operation on 3 wt% Ru/ZSM-5 catalyst packed bed
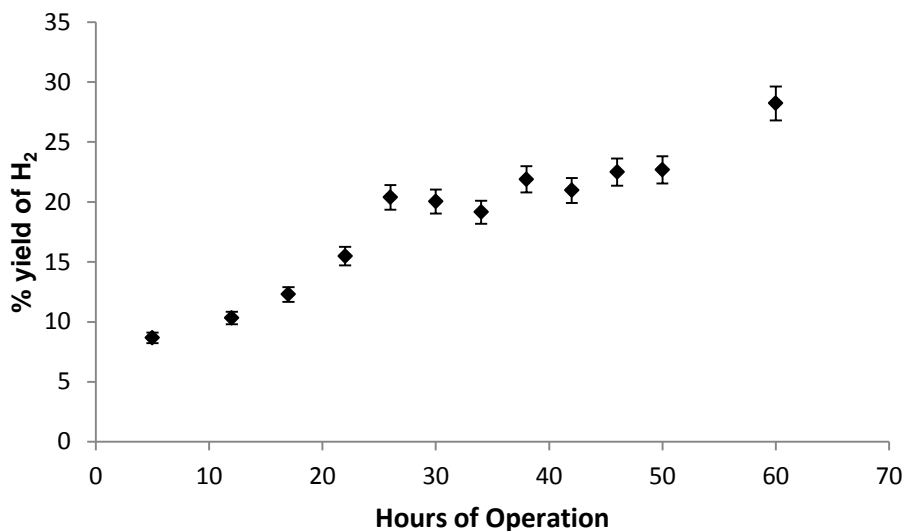
Figure 5.18: Percent yield of hydrogen with hours of operation on single catalyst

bed of 3 wt% Ru/ZSM-5

Though conversion was high, after 40 hours operation, in figure 5.18 it is seen that %yield of hydrogen was also high and stable in the range of 20% to 25% during 26 to 50 hours of reaction time. At 60 hours of continuous operation, conversion of methane

went down slightly but percent yield of hydrogen rose as high as 28% which was probably due to at this stage, methane molecules were just breaking down producing hydrogen gas molecules and carbon black. When this phenomenon became predominant, catalyst activity started deteriorating. Considering both methane conversion and percent yield of hydrogen during the continuous reaction for 60 hours on 3wt% Ru/ZSM-5, it can be seen that during 5 hours to 50 hours of operation, the catalyst performance and product quality has been stable and consistent which showed improvement of catalyst life compared to other transition metal catalyst on zeolite or silica support[12],[11].
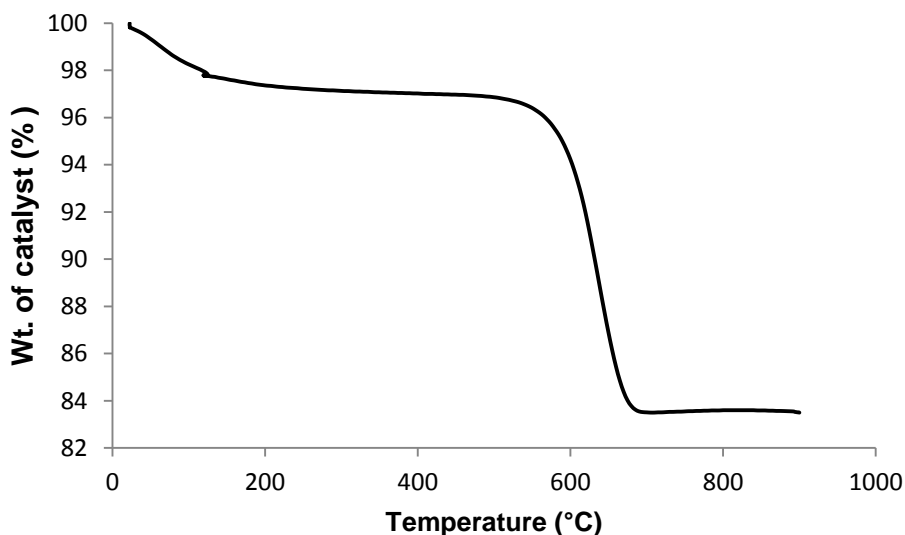
Figure 5.19: Thermo gravimetric analysis results on spent catalyst of 3 wt% Ru/ ZSM-5 after 60 hours of operation

Amount of coke deposition was measured on 3 wt% Ru/ZSM-5 after 60 hours of operation by thermo gravimetric analysis (TGA) of the spent catalyst. A weight loss of 16.5 wt% has been observed from the spent catalyst as the temperature of the spent catalyst sample rose from 22 °C to 900°C in 135 minutes. As a coke deposition of 16.5 wt% of the catalyst has been taken place after 60 hours of continuous methane flow on

the catalyst bed that also explains the slow deterioration rate of the catalyst as coke deposition was not very high in amount.

5.5 Conclusion

In this work direct methane conversion to higher hydrocarbon products have been studied in a oxygen free route to avoid the sharp change in energy density observed in the oxidative routes like steam or CO_2 reforming process. To improve the conversion of methane a conventional bi-functional metal catalyst has been prepared with ruthenium metal on ZSM-5 or SiO_2 support materials as the conventional transition metal catalysts show poor conversion results and less stability of catalysts at high operating temperature. Among the four catalysts tested for methane conversion, 3wt% Ru/ZSM-5 performed the best, both in conversion rate and product quality. Above 40% of methane conversion has been achieved at 700°C operating temperature and C_5 to C_8 cyclic hydrocarbon were produced along with hydrogen. Lower ruthenium loading i.e. 1.5wt% have not contributed in producing higher hydrocarbon products. Also 3wt% Ru/SiO_2 catalyst showed low conversion even at high temperature and no higher hydrocarbon product was observed. On the other hand, series bed of 3wt% Ru/SiO_2 followed by pure ZSM-5 showed significantly improved conversion of methane and product quality compared to single catalyst bed of both 3wt% Ru/SiO_2 and pure ZSM-5 catalyst separately. Catalyst stability has been investigated by measuring the methane conversion and hydrogen yield for a continuous 60 hours experimental run on 3wt% Ru/ZSM-5 catalyst bed. After reaching equilibrium, conversion and hydrogen yield were observed to be consistent till 50 hours of operation. Catalyst performance started deteriorating as more hydrogen was being produced and negligible yield of high hydrocarbon products were observed after 50 hours of continuous reaction. Compared to other transition metal catalysts, this bi-functional catalyst with ruthenium metal and

166

ZSM-5 zeolite have certainly shown potential improvement in catalyst performance in terms of conversion of methane and stable catalyst life at high operating temperature.

References

[1]   D. P. Chynoweth, J. M. Owens, and R. Legrand, "Renewable methane from anaerobic digestion of biomass," *Renew. Energy*, vol. 22, no. 1–3, pp. 1–8, Jan. 2001.

[2]   U. E. P. Agency, "Inventory of U.S. Greenhouse gas emissions and sinks: 1990-2012," *Federal Register*, vol. 79, no. 36. Office of the Federal Register, pp. 10143–10144, 2014.

[3]   The White House, "Climate Action Plan: Strategy to Reduce Methane Emissions," 2014.

[4]   J. H. Lunsford, "Catalytic conversion of methane to more useful chemicals and fuels: a challenge for the 21st century," *Catal. Today*, vol. 63, no. 2–4, pp. 165–174, Dec. 2000.

[5]   A. Holmen, "Direct conversion of methane to fuels and chemicals," *Catal. Today*, vol. 142, no. 1–2, pp. 2–8, Apr. 2009.

[6]   M. C. Alvarez-Galvan, N. Mota, M. Ojeda, S. Rojas, R. M. Navarro, and J. L. G. Fierro, "Direct methane conversion routes to chemicals and fuels," *Catal. Today*, vol. 171, no. 1, pp. 15–23, Aug. 2011.

[7]   R. A. Periana, "Platinum Catalysts for the High-Yield Oxidation of Methane to a Methanol Derivative," *Science (80-.)*., vol. 280, no. 5363, pp. 560–564, Apr. 1998.

[8]   T. V. Choudhary, E. Aksoylu, and D. Wayne Goodman, "Nonoxidative Activation of Methane," *Catal. Rev.*, vol. 45, no. 1, pp. 151–203, Jan. 2003.

[9]   G. KELLER, "Synthesis of ethylene via oxidative coupling of methane I. Determination of active catalysts," *J. Catal.*, vol. 73, no. 1, pp. 9–19, Jan. 1982.

[10]   T. Serres, C. Aquino, C. Mirodatos, and Y. Schuurman, "Influence of the composition/texture of Mn–Na–W catalysts on the oxidative coupling of methane," *Appl. Catal. A Gen.*, Dec. 2014.

[11]   S. Majhi, P. Mohanty, H. Wang, and K. K. Pant, "Direct conversion of natural gas to higher hydrocarbons: A review," *J. Energy Chem.*, vol. 22, no. 4, pp. 543–554, Jul. 2013.

[12]   B. M. Weckhuysen, D. Wang, M. P. Rosynek, and J. H. Lunsford, "Conversion of Methane to Benzene over Transition Metal Ion ZSM-5 Zeolites," vol. 346, pp. 338–346, 1998.

[13]　J. Zeng, Z. Xiong, H. Zhang, G. Lin, and K. Tsai, "Nonoxidative dehydrogenation and aromatization of methane over W/HZSM-5-based catalysts," *Catal. Letters*, vol. 53, pp. 119–124, 1998.

[14]　D. Wang, J. H. Lunsford, and M. P. Rosynek, "Characterization of a Mo/ZSM-5 Catalyst for the Conversion of Methane to Benzene," *J. Catal.*, vol. 169, no. 1, pp. 347–358, Jul. 1997.

[15]　M. M. Koranne, D. W. Goodman, and G. W. Zajac, "Direct conversion of methane to higher hydrocarbons via an oxygen free, low-temperature route," *Catal. Letters*, vol. 30, pp. 219–234, 1994.

[16]　J. Carstens and A. Bell, "Methane activation and conversion to higher hydrocarbons on supported ruthenium," *J. Catal.*, vol. 429, no. 0200, pp. 423–429, 1996.

[17]　H. Amariglio, J. Saint-Just, and A. Amariglio, "Homologation of methane under non-oxidative conditions," *Fuel Process. Technol.*, vol. 42, pp. 291–323, 1995.

[18]　M. Belgued, A. Amariglio, L. Lefort, P. Par, and H. Amariglio, "Oxygen-Free Conversion of Methane to Higher Alkanes through an Isothermal Two-Step Reaction on Ruthenium," vol. 291, no. 0186, pp. 282–291, 1996.

[19]　M. Belgued, A. Amariglio, P. Par, and H. Amariglio, "Oxygen-Free Conversion of Methane to Higher Alkanes through an Isothermal Two-Step Reaction on Platinum (EUROPT-1)," vol. 448, no. 0108, pp. 441–448, 1996.

[20]　J. Kandaswamy, C. L. Kibby, and R. J. (Chevron U. I. . Saxton, "Zeolite supported ruthenium catalysts for the conversion of synthesis gas to hydrocarbons, and method for preparation and method of use thereof," 15-Dec-2011.

[21]　Y. Shu, Y. Xu, S. Wong, L. Wang, and X. Guo, "Promotional Effect of Ru on the Dehydrogenation and Aromatization of Methane in the Absence of Oxygen over Mo / HZSM-5 Catalysts," *J. Catal.*, vol. 19, pp. 11–19, 1997.

[22]　A. Hassan and A. Sayari, "Highly active, selective and stable Mo/Ru-HZSM-5 catalysts for oxygen-free methane aromatization," *Appl. Catal. A Gen.*, vol. 297, pp. 159–164, 2006.

[23]　P. KOOPMAN, "Characterization of ruthenium catalysts as studied by temperature programmed reduction," *J. Catal.*, vol. 69, no. 1, pp. 172–179, May 1981.

[24]　G. T. Kokotailo, S. L. Lawton, D. H. Olson, and W. M. Meier, "Structure of synthetic zeolite ZSM-5," *Nature*, vol. 272. pp. 437–438, 1978.

[25]　D. H. Olson, G. T. Kokotailo, S. L. Lawton, and W. M. Meier, "Crystal structure and structure-related properties of ZSM-5," *J. Phys. Chem.*, vol. 85, no. 3, pp. 2238–2243, 1981.

Chapter 6

Conclusions

In this work upgrading of biomass fermentation products and renewable natural gas to energy dense higher hydrocarbon molecules have been performed by thermochemical catalytic conversion. Upgrading of ABE fermentation products that are acetone, n-butanol and ethanol mixture was optimized by varying operating temperatures, weight hourly space velocity on two different packed beds of catalysts. High energy content organic liquid product has been formed by dehydration of ABE mixture on γ-Al_2O_3 catalyst bed. The higher heating value of the organic product phase was 40 kJ/g, that is comparable to that of gasoline and jet fuel. The actual yield value of heavy hydrocarbon products (in the range of C_5 to C_{13}) was 35 wt% of feed at 400°C and 0.22 h^{-1} weight hourly space time (WHST). The highest actual yield of gaseous product phase containing mostly 1-butene and its isomers was 30.2 wt% of feed and this gas stream has been proposed to be redirected to the separation unit of ABE fermentation broth located before the catalytic upgrading unit in the integrated process flow. Separation efficiency of ABE components separately and as a mixture were measured from dilute aqueous solution using liquid butene in a pressurized extraction vessel. A mole based distribution coefficient of 1.71 has been attained for n-butanol single component extraction. For acetone, ethanol and butyric acid extraction separately from aqueous solvent, the distribution coefficients are lower. To compare the separation efficiency, a

two-step approach of adsorption on activated charcoal followed by liquid-solid extraction using 1-butene and percent recovery of each of the components, mole and mass based distribution coefficients were calculated, and it has been observed that percent recovery and distribution coefficients increased for acetone and significantly for ethanol than that of the direct liquid-liquid extraction process. For extraction of ABE as a mixture, a preferential extraction of n-butanol was observed over the other components in the mixture due to its least polar characteristic among the components and thus higher solubility in the organic phase.

For deoxygenation of butyric acid solely, three different acid catalyst performances were observed and among γ-Al_2O_3, ZSM-5 and ZrO_2, ZrO_2 performed the best in removing oxygen from butyric acid molecule and producing 4-hptanone with a yield of 70wt% of feed at 400 °C operating temperature. The energy content of the organic liquid phase was 36 kJ/g. At higher temperature aromatic hydrocarbons like toluene, para xylene and phenol compounds are produced in smaller amount. Higher conversion of butyric acid directly to aromatics has been achieved by a series packed bed of ZrO_2 followed by ZSM-5.

In non-oxidative conversion of methane, four different catalyst and support combinations were prepared, characterized and their performances were optimized with temperature. Operating temperature has been varied from 400° to 800°C. From online GC analysis and FT-IR analysis of the product gas, it has been observed that a sudden rise in methane conversion took place at 700°C operating temperature on 3 wt% Ru/ZSM-5 catalyst bed and heavy hydrocarbon molecules of C_4 to C_{10} range were produced but with a very low yield. For 1.5 wt% Ru/ZSM-5 and 3 wt% Ru/SiO_2 catalyst beds , methane conversion were found to be low even at high temperature and no significant production of higher hydrocarbon molecules were observed. A catalyst bed of 3 wt% Ru/SiO_2

followed by pure ZSM-5 in series has also been studied and the products were found to be comparable with that of 3wt% Ru/ZSM-5 catalyst bed with higher methane conversion. For calculating the yield of heavy hydrocarbon and conversion of methane more accurately continuation of this work has been proposed with an online GC-FID connected to the product line.

Chapter 7

Future Directions

7.1 Developing metal impregnated bi-functional catalyst for upgrading biomass fermentation products

In this study ABE fermentation products and butyric acid have been catalytically dehydrated and deoxygenated to produce energy dense higher hydrocarbon molecules. Commercial catalysts like γ-Al_2O_3, ZSM-5, ZrO_2 were used for the deoxygenation purpose. This study can be further taken forward by preparing bi-functional catalyst by wetness impregnation or fusion of metals like Ni, Cr, Cu, Zn, Fe on γ-Al_2O_3, ZSM-5, ZrO_2 supports to increase the catalyst activity by reducing bond breaking energy required for 'C-O' or 'C=O' bonds in alcohol, ketones and acids in fermentation products.

Also only a single type of ZSM-5 catalyst with a Si: Al ratio of 23:1 has been studied for the dehydration purpose and it was observed that cracking activity of the catalyst was predominant producing small hydrocarbon molecules in the gas phase due to very strong Bronsted acid sites of the catalyst. From literature, it has been shown that with increasing Si: Al ratio the strength of acid sites decreases for ZSM-5 catalyst also the pore size in the framework structure of ZSM-5 increases [1],[2]. These two factors may contribute in producing higher hydrocarbon molecules compared to the ZSM-5 catalyst that has been studied. The effect of Si:Al ratio and thus acid strength and pore size of the active sites of different ZSM-5 catalyst can be studied with the same experimental setup and operating conditions.

7.2 Catalytic oligomerization of butenes and unsaturated hydrocarbon gas mixtures derived from ABE deoxygenation process

Upgrading the ABE mixture to produce heavy hydrocarbon liquid product and unsaturated hydrocarbon gas containing mostly butene and its isomers was a successful step for producing higher energy content hydrocarbon products. Since the final goal of the project is to get liquid transportation fuel, the large amount of butene getting produced in the deoxygenation/dehydration process need to be further process to convert the gaseous hydrocarbon to liquid fuel and the best chemical process to perform that job will be oligomerization of the gas mixture as unsaturation is present there. Oligomerization of butenes and other unsaturated hydrocarbon gases produced in the deoxygenation process can be done using inorganic heterogeneous catalyst.
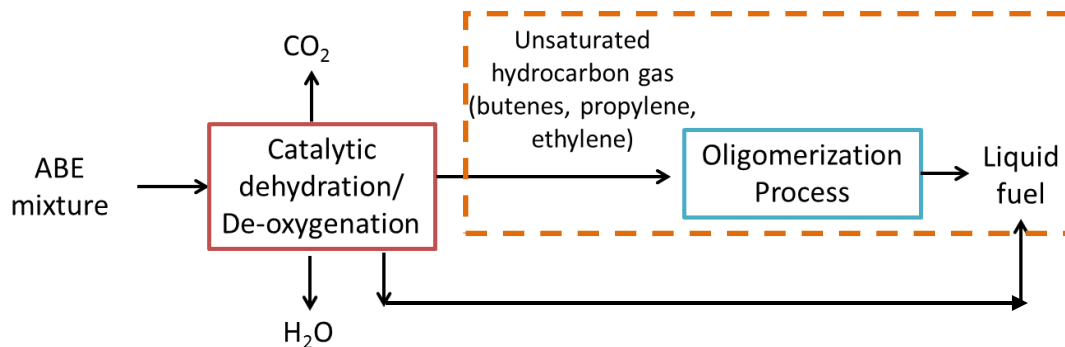
Figure 7.1: Process scheme for producing liquid fuel from ABE deoxygenation and oligomerization in a two-step process

In Figure 7.1 the process scheme is described starting from ABE mixture to liquid drop-in fuel. In this work the oligomerization process will be described which is highlighted in the dashed rectangular area. Oligomerization of unsaturated hydrocarbon gases have been studied in several research works. US navy has started working on conversion of 1-butene to jet fuels applying zirconium-catalyzed batch conversion process in the

presence of methyl aluminoxane (MAO). In this study the catalyst was prepared Al/Zr ratio of 100 (mol/mol). Oligomerization has been done by condensation of 1-butene on CaH_2 and then transferring it to the high pressure reaction vessel on the course of dry ice bath. The products from 16 hours' batch process at ambient temperature were analyzed by gas chromatography-mass spectrometry (GC-MS) and it showed complete consumption of 1-butene. From GC –MS analysis it was found that, after oligomerization the product composition was approximately 27 mol% C_8, 26 mol% C_{12}, 18 mol% C_{16}, 12 mol% C_{20}, 8 mol% C_{24}, 5 mol% C_{28}, 4 mol% C_{32} showed in Figure 7.2.
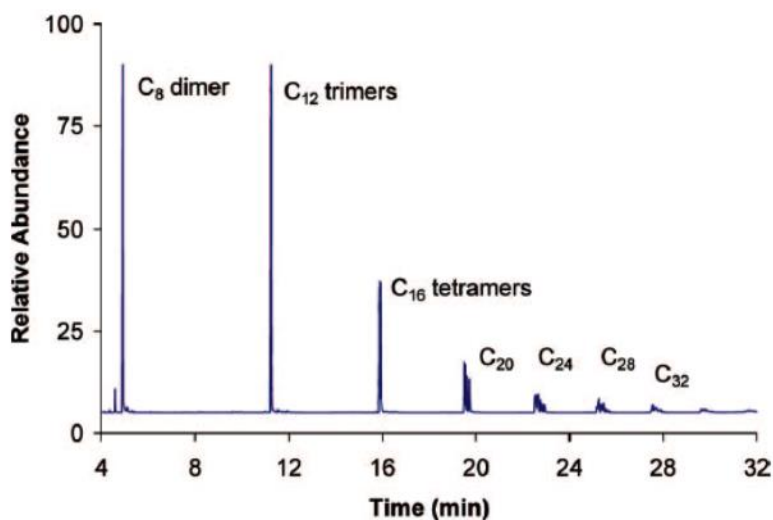

Figure 7.2: Experimental results of the product GC-MS analysis of oligomerization of butene over AL/Zr catalyst [3]

Other studies on olefin oligomerization could be seen using solid acid catalysts like Zeolites, solid phosphoric acid or transition metal acids. Oligomerization of the primary Fischer-Tropsch products from the refineries containing good amount of butene can be done by solid phosphoric acid (SPA) for converting it to hydrogenated motor gasoline. The hydration of the catalyst and temperature play significant role in production of gasoline from butene oligomerization. With lower temperature and higher hydration rate

better grade of motor gasoline can be produced. Also the aromatic content of the liquid product from oligomerization of butenes over liquid phosphoric acid increases with increase in temperature and catalyst concentration [4].

Using silica-alumina catalysts for olefin oligomerization at 120°C and a WHSV of $8h^{-1}$ the conversion of isobutene, 1-butene and 2-butene had been 95%, 85% and 35% and conversion was found to be not much affected by changing the space velocity. At operating temperature lower than 160°C, the oligomerization of 1 butene was found to be the preferred reaction over the double bond isomerization [5]

(a)   (b)
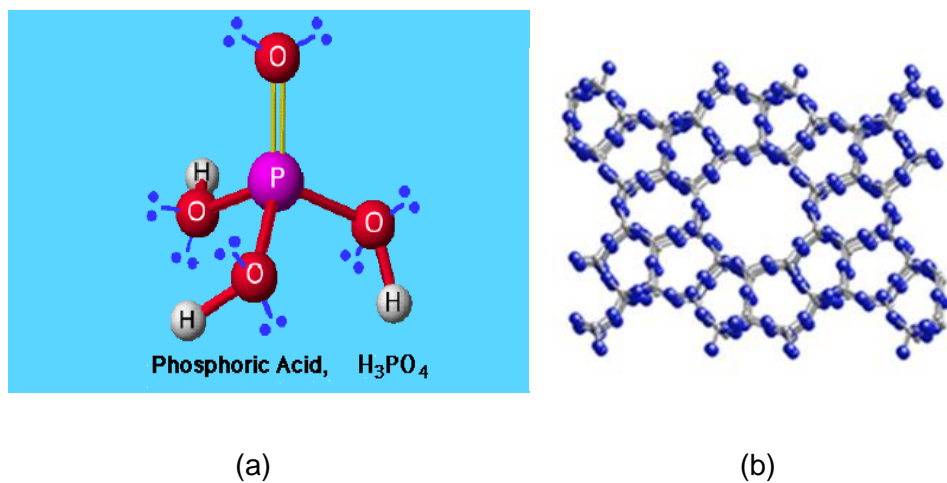
Figure 7.3: Structures of (a) phosphoric acid catalyst and (b) ZSM- 5 lattice structure

Except for transition metal catalysts and solid acid catalysts and zeolites, applicability of Ziegler-Natta catalysts has also been studied in oligomerization of butene. Methylaluminoxane activated metallocenes have shown better selectivity in producing jet fuels and diesel fuels. ZSM-5 ,-12 and -23 zeolites produce short chain oligomers with modest number of branching which can be used as diesel fuel cut as it has very high cetane number. Again large pore zeolites, amorphous silico-aluminas and

polyphosphoric acids can produce significant number of branching and thus low cetane numbers which can be compared to the gasoline and jet fuel range hydrocarbons [6].

Though ZSM-5 is well known for its activity in cracking of hydrocarbons, using zeolites in oligomerization or polymerization purpose can be studied extensively based on the research work mentioned above. Also comparison of catalytic activity of other solid acid catalyst like SPA in oligomerization of butene and its isomers can contribute immensely in the synthetic fuel industry. These two catalysts have been selected as they are commercially available and comparatively cheaper but they found to have high activity in olefin oligomerization. As a continuation of biomass catalytic upgrading process performed in this study, oligomerization of butene and other unsaturated hydrocarbon gases over solid acid catalysts to produce liquid transportation fuel using SPA and ZSM-5 can be a promising future direction. Studying the effect of operating parameters to optimize the oligomerization process and also controlling the distribution of oligomers by catalyst pretreatments are important aspects of the study to look in to.

The principal reaction involved in this process is:

SPA, ZSM-5

C_4H_8 C_8H_{18} $C_{12}H_{26}$ $C_{16}H_{32}$
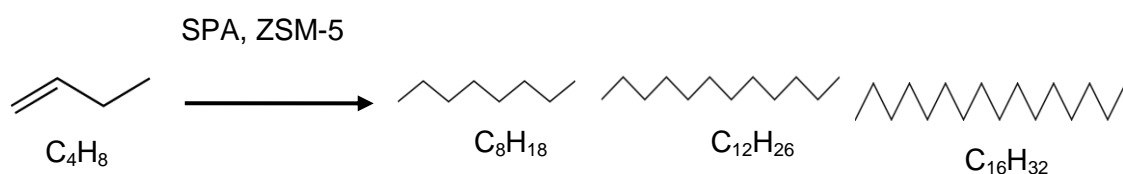
This is the last and finishing step for producing liquid transportation fuel from ABE mixture derived from Biomass. So successful completion of this step will be able to contribute in determining the total cost involved in the process of producing Biomass to liquid fuel via the 3 step approach of ABE fermentation, deoxygenation and oligomerization.

7.3 Two-step separation of fermentation products from dilute aqueous solution with a consecutive adsorption and extraction column with recycle stream

In this study it has been observed that the separation efficiency of ABE components from aqueous solution on by adsorption on activated charcoal was very high but the main challenge was retrieving the adsorbed components by extraction using liquid butene. It showed significant improvement in increasing distribution coefficient in the liquid butene phase for acetone and ethanol extraction from activated charcoal phase compared to the liquid-liquid direct extraction from the dilute aqueous solution of ABE. Also experimental data showed that multiple stage separation helped in improving extraction efficiency. So for more practical and industrial approach, a process design development can be done where ABE fermentation broth from the fermentation reactor will be directly fed to the separation unit where it'll be pumped in a separation column containing a packed bed of activated charcoal. It will be operated as a semi-batch process where after an optimum adsorption time liquefied butene will be passed through the adsorption bed and extract phase will be collected from the of the column and the raffinate phase will be recycled again to the separation unit inlet. The proposed design of the separation process is shown in Figure 7.4
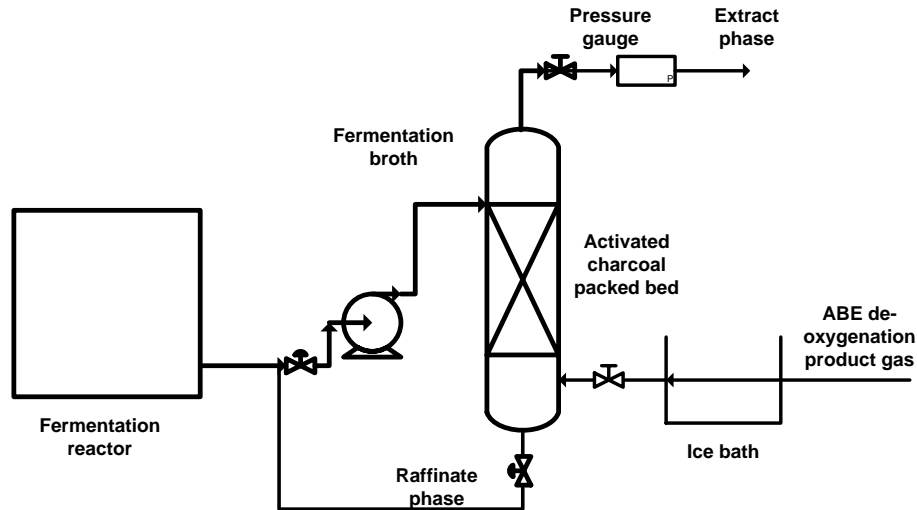
Figure 7.4: Semi-batch adsorption and liquid solid extraction process for separation of ABE components from the fermentation bro

References

[1]   J. C. Serrano-ruiz and J. A. Dumesic, "Catalysis for Alternative Energy Generation," pp. 29–57, 2012.

[2]   B. Xu, C. Sievers, S. B. Hong, R. Prins, and J. A. van Bokhoven, "Catalytic activity of Bronsted acid sites in zeolites: Intrinsic activity, rate-limiting step, and influence of the local structure of the acid sites," *J. Catal.*, vol. 244, no. 2, pp. 163–168, 2006.

[3]   M. E. Wright, B. G. Harvey, and R. L. Quintana, "Highly Efficient Zirconium-Catalyzed Batch Conversion of 1-Butene : A New Route to Jet Fuels," *Energy & Fuels*, vol. 10, no. 12, pp. 3299–3302, 2008.

[4]   A. de Klerk, D. O. Leckel, and N. M. Prinsloo, "Butene Oligomerization by Phosphoric Acid Catalysis: Separating the Effects of Temperature and Catalyst Hydration on Product Selectivity," *Ind. Eng. Chem. Res.*, vol. 45, no. 18, pp. 6127–6136, Aug. 2006.

[5]   A. de Klerk, D. J. Engelbrecht, and H. Boikanyo, "Oligomerization of Fischer−Tropsch Olefins: Effect of Feed and Operating Conditions on Hydrogenated Motor-Gasoline Quality," *Ind. Eng. Chem. Res.*, vol. 43, no. 23, pp. 7449–7455, Nov. 2004.

[6]   B. G. Harvey and H. a. Meylemans, "The role of butanol in the development of sustainable fuel technologies," *J. Chem. Technol. Biotechnol.*, vol. 86, no. 1, pp. 2–9, Jan. 2011.
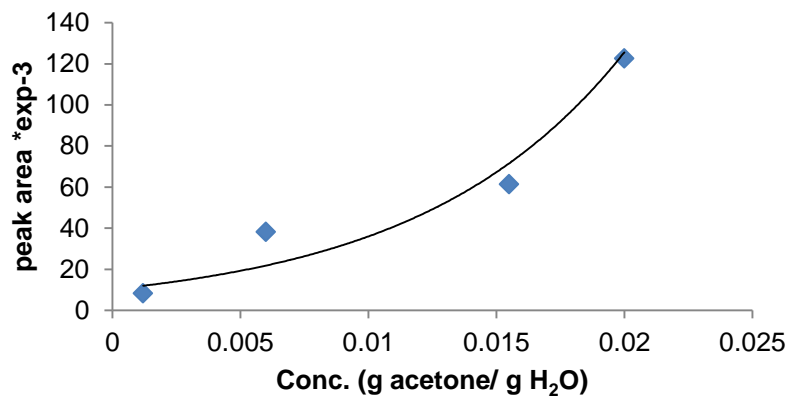
Appendix A

Calibration curves for measuring the concentration of ABE components in the raffinate phase directly from the peak area while analyzing with high performance liquid chromatography (HPLC)
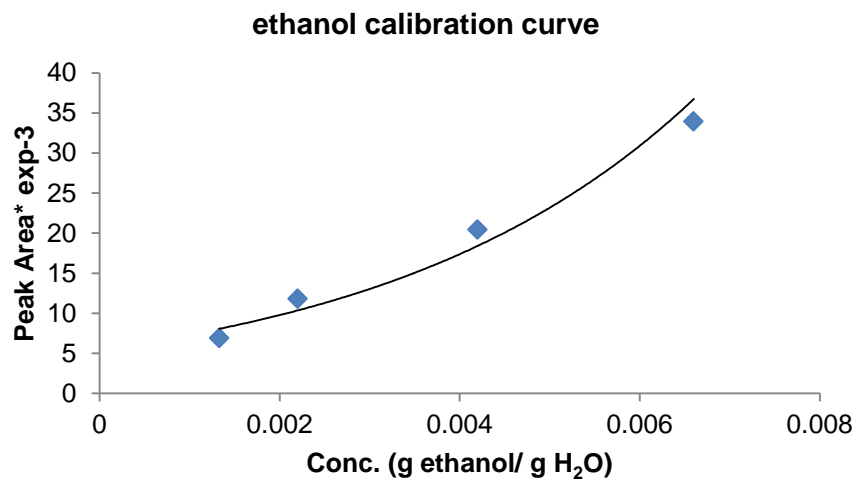
n-butanol calibration curve
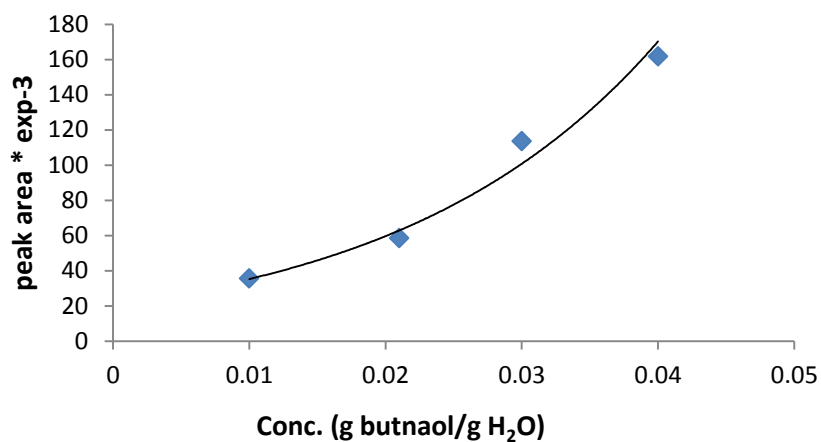
(a)

acetone calibration curve

(b)

ethanol calibration curve

(c)

Figure A.1: Calibration curves for individual components of ABE mixture: (a) n-butanol, (b) acetone and (c) ethanol for co-relating concentration with peak area in HPLC analysis

Appendix B

Table A.1 Results for conversion of methane on a 6wt% Ru loading on ZSM-5 support with varying operating pressure and temperature

Temperature	Feed Pressure	Product flow rate	GC peak area		% conversion (calculated)
(°C)	(psia)	(ml/min)	H2	CH4	
400	20	3.6	31.31	888.23	21.58
400	30	10.56	27.48	888.23	21.58
400	60	45.05	52.5	877.6	22.30
400	128	172.25	0	991.38	14.63
500	20	3.17	40.52	730.52	32.20
500	30	11.5	125.24	974.95	15.74
500	60	40.93	42.95	730.83	32.18
500	128	146.8	16.8	933.66	18.52
600	20	3.13	39.43	976.2	15.66
600	30	10.46	273	972.44	15.91
600	40	15.71	130.22	696	34.52
600	50	27.17	32.5	937.5	18.26
600	60	34.5	49.1	975.3	15.72
700	30	10.25	715.55	673.9	36.01
700	30	10.2	932.4	661.1	36.87

)